Integrated Microfluidic Devices for Cell Culture and Assay

Thesis by

Mike C. Liu

In Partial Fulfillment of the Requirements
for the Degree of

Doctor of Philosophy

California Institute of Technology

Pasadena, California

2010

(Defended September 17, 2009)

Acknowledgements

Foremost, I would like to express my deep and sincere gratitude to my advisor, Dr. Yu-Chong Tai for providing me the opportunity to conduct research in his lab and giving me endless support in the past five years. His insights, wisdoms, advices and enthusiasm for research have greatly influenced me and made the completion of my dissertation possible. I have been very fortunate to have him as my mentor.

I would like to acknowledge the former and current members of the Caltech Micromachining Lab for providing me support and helpful discussions. They have also made my stay in this lab a very enjoyable experience. Trevor Roper has been superb at solving equipment problems and keeping our lab running. Agnes Tong and Christine Garske have provided the administrative supports and organized many group activities. My gratitude goes to Siyang Zheng, who gave me numerous helps when I started in this lab. I would like to thank my fellow colleagues, Victor Shih, Matthieu Liger, Angela Tooker, Scott Miserendino, Damien Rodger, Changlin Pang, PJ Chen, Brandon Quoc Quach, Wen Li, Nick Lo, Jason Shih, Luca Giacchino, Ray Huang, Jeffrey Lin, Monty Nandra, Justin Kim, Bo Lu, Wendian (Leo) Shi, Yok Satsanarukkit, Jay Chang, Joy Zhao and Charles DeBoer.

I am appreciative of my undergraduate mentor, Professor Luke Lee, who gave me tremendous support at UC Berkeley and inspired me to pursue a graduate study in Bioengineering. I would also like to thank my candidacy and thesis defense committee members, Dr. Anand Asthagiri, Dr. Joel Burdick, Dr. John Dabiri, and Dr. Changhuei Yang. I have worked with many people outside of Caltech. I would like to thank Dr.

Chih-Ming Ho and Leyla Sabet from UCLA, Dr. Dean Ho from Northwestern University and Dr. David Caron, Dr. Astrid Schnetzer, Beth Stauffer, and Erica Seubert from USC.

I would like to thank my parents, Ching-Rong Liu and Kuei-Eing Chaw and my sister, Lisa Liu. They have given me unconditional support and provided me with encouragements throughout my life. I am sincerely grateful for all the things they have done for me. Everything I am, I owe to my family. Finally, I would like to thank my girlfriend, Stephanie Peng, who has always brightened my day and shared many wonderful moments since the day we met.

Abstract

This thesis presents the development of three-dimensional (3-D) microfluidic devices for cellular studies, with focus on applications for high-throughput cell culture and cell-based assay. Microfluidic devices provide potential inexpensive platforms for high-throughput screening with the advantages of precise liquid handling, ability to control cell culture microenvironment, and reduced reagents and cells.

Because a mixture of drugs or chemical compounds can often treat diseases more effectively or act synergistically in certain cellular pathways, a device capable of screening the combinatorial effects of multiple compound exposures on cells is highly desirable. To this end, a novel method to monolithically fabricate 3-D microfluidic networks was developed, and based on this fabrication technology, the first cell culture device with an integrated combinatorial mixer was constructed. The proof-of-concept chip having a three-input combinatorial mixer and eight individually isolated micro culture chambers was fabricated on silicon utilizing the surface micromachining of Parylene C (poly(chloro-p-xylylene)). Unlike other 3-D microfluidic fabrications, multilayer bonding process was favorably obviated. By incorporating several microfluidic overpass structures to allow one microfluidic channel to cross over other microfluidic channels, the combinatorial mixer generated all the combinations of the input fluidic streams. Cell culturing on-chip was successful, and the ability to simultaneously treat arrays of cells with different combinations of compounds was demonstrated.

To facilitate cell-based assay, another combinatorial cell array device was fabricated on glass with incorporated membrane. Characterization of the combined

compound concentration profile at each chamber with a fluorescence method was developed. We demonstrated functionality of the quantitative cell-based assay by screening three different compounds' ability to reduce cytotoxicity of hydrogen peroxide on neuron cells and also assaying combinatorial exposures of three chemotherapeutic agents on breast cancer cells. The 3-D microfluidic fabrication process was extended to construct multilayer microfluidic device with integrated membrane. Applications of microfluidic devices for marine microbiology were demonstrated. Based on the capabilities demonstrated in this work, devices with high-density cell array and integrated high-input combinatorial mixer can be constructed. At the same time, the technology has general applicability for building complex 3-D microfluidic devices, which can broaden the applications for current lab-on-a-chip systems.

Table of Contents

List of Figures

Chapter 1: Cell Culture and Cell-Based Assays

1.1 Introduction to Cell Culture and Platforms

Cell culture is the technique to maintain and grow cells *in vitro* outside of their original environments. Cell culture has been used extensively as a model system for biology, disease, and therapeutics. It is applied across the disciplines of genetics, immunology, cancer, medicine, vaccine production, tissue engineering, and countless other applications.

The cell culture technique was developed over a century ago by Dr. Ross Granville Harrison in 1907 [1]. Harrison was working in experimental embryology and devised a method to culture and observe frog embryo nerve fiber growth *in vitro*. This influential technique was gradually refined, and used in primary explants for the next 50 years. Several developments in the 1950s popularized the cell culture technique. The use of trypsin allowed adherent cells to be dissociated from surface so subculturing of cell lines can be done conveniently. The use of cells to grow virus and use the virus for vaccine production has driven advancement in cell culture technology. Development of antibiotics made it easier to prevent the cell culture from contamination. One major breakthrough occurred in 1952 with the establishment of the first human cell line, HeLa. George Otto Gey used cervical cancer tissues from patient, Henrietta Lacks (hence the name HeLa), to create an immortal cell line. This laid the foundation for research in this field as HeLa rapidly became adopted in numerous labs for cancer studies and polio vaccine testing and development. The ability to grow human cells also stimulated interest in the use of cells as biological models and the use of human tissue for

developing cell lines. More cell lines were established and researchers were able to develop growing media suitable for different cell lines. Cell culture for researchers became a more accessible technique as many of the cell lines, reagents and culture vessels were reliably manufactured and became available commercially. For example, the American Type Culture Collection (ATCC) currently has over 4,000 cell lines.

In general, cells for culturing can be divided into three categories: primary, secondary, and continuous cell lines. Primary cells are directly extracted from tissues, isolated by either mechanical methods such as dissection and filtration or chemical methods with use of enzymes such as trypsin, collagenase, or DNase. These cells can survive outside of their original environment for some time but do not have the capacity to proliferate and will eventually die. While primary cells can be laborious to obtain and maintain, primary cells often represent the best biological model because they closely resemble the properties of their parent tissue. Secondary cells, like primary cells, are derived from tissues, but secondary cell lines have the capability to divide a limited number of times before senescence, the cell's loss of ability to divide by genetically determined events. MRC-5 is a type of secondary cell that is derived from tissues of human lungs. It has capability to double approximately 50 times before dying and has been used in studies such virus infection [2]. Continuous cell lines are able to grow continuously. Continuous cell lines are usually derived from tumor cells that have an unstable chromosome number and have undergone transformation such as loss of function of the p53 tumor suppressor gene. Cells can also be induced to become immortalized by transfection with genes such as SV40 large T antigen, which affects retinoblastoma (Rb) and p53 tumor suppressor proteins [3]. Another method to establish

a continuous cell line is by inducing cells to express telomerase. This prevents the progressive shortening of telomeres which normally leads to cell apoptosis after several generations [4]. While continuous cell lines can lose some of the cell properties (such as loss of contact inhibition) *in vivo*, or even gain certain functions (such as continuous proliferation), continuous cell lines are generally easier and less expensive to maintain than primary and secondary cells and offer an unlimited source of identical of cells. A wide selection of continuous cell lines has been developed and researchers can choose a particular type suitable for their specific study.

Cell lines are generally maintained inside a cell incubator with a defined temperature and gas mixture (commonly 37^{o}C and 5% CO_2). Culture vessels are flasks, petri dishes or well plates made up of glass or disposable plastics. Polystyrene is the most common plastic in the cell culture lab today. Polystyrene is hydrophobic and therefore requires a surface treatment, such as gas plasma, to provide a suitable substrate for cell attachment. Cultured cells are either grown in suspension or adherent cultures. Most of the cells derived from tissue require adherence to a surface, while some cells such as lymphocytes or sperm cells can be grown in suspension. Some anchorage-dependent cells can readily attach to glass or treated plastics, while others require attachment factors such as collagen, fibronectin, laminin and poly-L lysine. Each cell line is grown in a unique media consisting of the necessary growth factors, a regulated pH, a specific balanced salt concentration, and nutrients such as glucose, amino acids, vitamins and carbohydrates. Serum is commonly used to supply cell culture with growth factors, adhesion factors, lipids and hormones. Most sera are derived from fetal bovine,

calf, adult horse and human. Serum-free media is available but is more expensive and requires a different formulation for different cell lines.

Cells should be handled carefully to avoid contaminants. When taken outside of the incubator, cells should be handled in a laminar flow hood, where a constant flow of filtered air prevents contamination. The laminar flow hood can have two flow configurations. Horizontal flow hoods have filtered air directly blowing at the worker. Vertical flow hoods blow filtered air from the top of the hood down to the work surface. When working with cell cultures, reagents, containers and any other tools such as pipette and pipette tips need to be sterile to prevent contamination. Other aseptic techniques such as cleaning the work surface with biocide before use and preventing cross-contamination between bottles should be followed closely. During the culture process the media has to be changed to replenish the nutrients for cells. For adherent cells, this can be done by aspirating the existing media and replacing it with new media. For suspension cells, the cells are centrifuged to sediment the cells and the media is replaced. Some cells lines continuously grow and can fill the culture vessels to reach confluency so subculturing to split cells and transfer cells to new vessel is necessary. For suspension cells, pipetting is used. For adherent cells, cells are washed to remove medium or serum and incubated with a trypsin solution to cleave the bonding between the cells and substrate so cells can be collected in suspension. Depending on cell types, some cells can also be suspended by using cell scrapers. Cells can then be diluted and reseeded. Cells can be stored for years using cryopreservation. This creates a “back-up” of cells to protect against genetic drift, contamination, or an unexpected discontinuity of cell line such as senescence or equipment failure. Cryogenic storing can be achieved by placing

cells in a container with media and cryoprotectant, typically dimethyl sulfoxide (DMSO) or glycerol. The containers are stored at cryogenic temperatures (below -130^{o}C) by placing them in liquid nitrogen or liquid nitrogen vapor.

Using cells as a model system has several advantages. Cells are maintained in a controlled environment with defined pH, temperature, osmotic pressure and gas mixture. Variations that occur *in vivo* are avoided, making cell culture suitable for systematic studies. Cells can be exposed to media with specific nutrient, protein and hormone concentrations. The duration of this exposure can be controlled. As opposed to use of animals as models, the use of cells is more humane and efficient. Unlike using tissue or animal model, cell lines are a homogeneous group of cells and offer the ability to study cell responses with reduced variations due to inhomogeneity inside a tissue. Experiments using cell culture can be replicated as the same cell lines can be used across different labs. Cells can be directly exposed to tested compounds such as drugs. As a result, lower amounts of precious compounds are needed than *in vivo* where the majority of the compounds are lost or delivered to body parts not under investigation.

On the other hand, using cell culture has some drawbacks. Great care must be taken to avoid contamination by bacteria, yeast or other cell lines and expertise is needed to perform cell culture experiments under aseptic conditions. Also, great attention must be paid to assess the biological relevance of cell culture experiments. While primary cells are taken directly from tissues, they have been extracted out of their original environment and continuous cell lines have undergone transformation. Some cell-cell interactions that occur between different types of cells may be lost and effects by endocrine and nervous systems are absent. Also, unlike cells *in vivo*, cellular metabolism

in cultured cells is dominated by glycolysis and the citric acid cycle only has a minor role. Cultured cells may also have genetic and phenotypic instability as some cells may differentiate and produce heterogeneity in a population. Therefore, the overall health and fidelity of the cell line needs to be constantly monitored. Straightforward methods include observing the cell morphology and counting to determine growth rate. Expression of specialized functions by cells can be checked by running polymerase chain reaction (PCR) or immunological assays. In addition, most of the cells are maintained in serum, which is poorly defined and can vary from batch to batch. Despite these limitations, cultured cells still express certain specialized functions that are representative of the *in vivo* model and with proper design of experiment, they can be used effectively.

The use of cell culture has numerous applications. It provides a good model for studying basic biology and biochemistry. In these areas, cells have been used to study replication and transcription of DNA, protein synthesis, cell metabolism, RNA processing, differentiation, apoptosis, intracellular signal transduction, membrane trafficking and many other processes. Virology proved to be one of the initial applications of cell culture because of the stringently controlled growing conditions and standardization of cell lines for culture and assay of viruses [1]. Cell culture has been used for virus detection in the clinical setting and for basic science research of viral infections. Furthermore, cell cultures have been used to produce antiviral vaccines including polio, rabies, and hepatitis. In addition to vaccine production, cell culture can be used to produce other products in large scale. Cells can be engineered to produce monoclonal antibodies, insulin and hormones for medical use. Research is continually underway to grow cells into tissue for tissue grafts or organ replacement. Embryonic and

adult stem cells have been investigated to control the differentiation and development of these cells. Cultured cells can also be used to test the toxicity of compounds such as cosmetics. In addition, they can be used to study how those compounds affect the growth and health status of certain cells such as liver cells. Because cancer cells can be cultured or normal cells can be transformed to become cancerous, cell culture has been used extensively in cancer research. Culture cells can be used to screen for potential cancer drugs and to study drug mechanisms and interactions. Cell-based screening is important in drug development for the pharmaceutical industry.

1.2 Need for High-Throughput Cell Culture, Cell-Based Assay and Combinatorial Screening

Cell-based assay has been applied to various fields. It has been integral to drug discovery and development. Various drugs for treating different diseases all require extensive screening to be done. Biochemical/molecular assays and cell-based assays have both been used for screening. Biochemical assays often require specific targets for screening, and chemicals are tested for their ability to modify the targets. This is often done by testing for ligand binding. For example, the compounds are evaluated for their ability to stimulate or inhibit certain kinases or receptors, such as G protein-coupled receptors (GPCRs). It is also important to test for the selectivity of the potential compound because a compound that acts on an undesirable target can induce harmful results. For example, fluorescence resonance energy transfer (FRET) can be used to test for protease activity. In such method, an acceptor fluorescence molecule is bound to one side of a substrate while a donor that can transfer energy to the acceptor molecule is

bound to the other side. Upon protease cleavage of the substrate, the distance between the donor and acceptor molecules increases and the fluorescence from the donor becomes detectable. This method can also be used for screening protein-protein interactions. Cell-based assay has received increased attention and has several advantages over ligand binding assay on specific targets. Cell-based screening can be miniaturized to reduce cost and provide "information rich" data [5]. Advances have produced assays that are user-friendly while still providing sophisticated results. While biochemical assay requires a specific target, cell-based assay allows the potential compound to interact with several targets. Living cells are the ultimate targets of all drugs and using them as models can be more efficient than focusing on isolated genes or proteins. Cell-based assay can test for multiple targets and reveal the effect of a whole transduction pathway. Novel target sites and signal pathways can also be discovered during the assay. The development of different cell lines from specific tissues makes it convenient to screen drugs for multiple types of cancer [6]. Cell-based screening can be performed in a high-throughput manner, which is difficult and costly to achieve with animal models.

The number of new chemical entities that can be potential drugs and number of possible drug targets have increased, and this requires more screening to be done. Development in combinatorial chemistry has generated a huge library of potential drug candidates that need to be tested and it has been predicted that combinatorial chemistry will generate as many as 10^{30}–10^{50} small molecules to be screened [7]. Advancements in genomic, proteomic and metabolomics have resulted in an increase in new chemical entities. Human antibodies, which have been used as drugs, can be screened and optimized from a huge library of antibodies produced from phage, mouse antibodies

recombined with human antibody genes, and human antibodies raised in mouse grafted with human immune cells. Drug targets are usually enzymes and receptors and current drugs only address a total of about 500 molecular targets [8]. Although most of the targeted receptors are in the G protein-coupled receptor family, other drug targets include DNA, ion channels, nuclear receptors and hormones. The number of possible targets that drugs can act on is increasing as new genes and their associated functions are discovered. DNA sequencing projects have revealed novel genes with characteristics similar to G protein-coupled receptors. There are at least 1,000 of these, and many research programs are underway to reveal the functions of these new receptors as well as analyze their potential to become drug targets. In a drug screening, panels of compounds are screened using various *in vitro* and cell-based assays to identify compounds that produce positive results, or "hits." Those compounds are either subject to more complex characterization or are modified to produce more specific compounds for screening. In the beginning of 1990s, a large screening program would generate 200,000 data points, which rose to 5–6 million in mid 1990s, 50 million in 2000, and is still rising [8]. The pharmaceutical companies are also driven by the desire to lower cost while increasing efficiency. A potential drug is costly to develop from the hit discovery stage to the clinical trials, and many compounds fail at the clinical trial stage. Therefore, better screening techniques are needed to lower late stage failure of drugs.

Besides compound screening for drug discovery and development, high-throughput cell-based assays have applications in other fields. One obvious field is basic cellular biology research. Some areas requiring screening for different factors include identifying inhibitors or promoters of cell adhesion, signaling molecules in inflammatory

responses, transcription factors, growth factors and molecules causing cell stress. An emerging field, systems biology, which attempts to characterize the interaction of cellular pathways and molecular components and to predict the behavior of biological systems, requires an enormous amount of data. Since this type of research is generally carried out in academia, it is important that screening be done in high-throughput manner to save labor and time while reducing cost. Also, many start-up pharmaceutical companies would like to run high-throughput screenings, but do not have access to high-end equipments that large pharmaceutical companies are able to use. Most high-throughput screening instrumentations are costly and can be difficult for many labs and small companies to purchase and maintain. Therefore, inexpensive platforms for high-throughput screening are highly desirable.

Another aspect of biology that adds to the total number of screening experiments to be done is that multiple factors can interact with each other to produce synergetic, additive or antagonistic results. Cells are sustained in complex environments and cell fates are dictated by the integration of numerous extracellular signals. Many cellular pathways in various biological phenomena are governed by the combinatorial effects of several factors. The regulation of gene expression is governed by activators, repressors, general transcription factors, protein-protein interactions, and protein-DNA interactions [9, 10]. For example, stem cell differentiation is controlled by multiple factors including activators to Notch-related receptor GLP-1, epidermal growth factors (EGF), fibroblast growth factors, transforming growth factor β (TGFβ), Macrophage inhibitory protein 1α, and numerous others that are currently being identified and studied [11].

In addition, a mixture of drugs can display synergistic interactions and become more effective than single agent at treating diseases. Cancer cells can also develop resistance to certain drugs and using a combination of drugs can circumvent this problem [12, 13]. For example, treatment of acute lymphoblastic leukemia (ALL) often consists of a panel of drugs including vincristine, prednisone, and anthracycline [14]. Initial treatment of adult Hodgkin's lymphoma often includes adriamycin, bleomycin, vinblastine, and dacarbazine. In treating other diseases such as HIV, combination therapy has been standard [15]. As a result, drug screenings often include multiple combinations of different compounds. This raises the demand of high-throughput screening as the number of potential compounds and all the possible combinations to be tested grows significantly.

1.3 Technology for High Throughput Screening

Currently there are several types of instruments as well as cell-based assays that have been used to run in high-throughput manner. Some of the assay types and the technology to handle high-throughput screening will be reviewed.

The cell proliferation assay to test cell's growth in response to external stimuli has been implemented for high-throughput screening. Proliferation assay can be done by counting cells after staining with vital and dead cell dyes. Throughput can be increased by running a MTT (3-(4,5-Dimethylthiazol-2-yl)-2,5-diphenyltetrazolium bromide) assay. In such method, yellow MTT is added to the cells which is then reduced to purple formazan in the mitochondria of living cells [1]. The change in color can be measured by spectrometer. Cytotoxicity is another type of assay that can be run in similar procedure.

Dead cells with compromised membrane can be stained with trypan blue or red fluorescent propidium iodide. Another category of cell-based assay is quantification of cellular messengers. Calcium, Ca^{2+}, a key cellular messenger, can be detected using Ca^{2+} sensitive dyes such as Fluo-3. Membrane potential can be measured using potential indicator dyes such as bis-(1,2-dibutylbarbituric acid) trimethine oxonol ($DiBAC_4$) and such detection is important for screening drug targeting ion channels [5]. Gene expression is critical to many biological events and it can be measured in living cells, providing invaluable tool to study of cell regulation and control. Most of the methods involve transfecting the cells with the genes of reporting enzymes or green fluorescent proteins. Activation of the target gene results in the production of the reporter products, which can be detected by a fluorescent, colorimetric or luminescent method. For example, the luciferase gene can be inserted and the subsequent activation results in production of an enzyme that converts luciferin into a luminescent form which is then detected [16]. When green fluorescent protein is used as the reporter, real-time characterization can be done to yield an information-rich readout of the dynamic of cellular responses. Many other assays such as measurement of pH or cAMP also exist. More assay systems that act on new targets or pathways and that increase current sensitivity are being developed. Such developments will continue to assist high-throughput cell-based assay research.

Numerous strategies have been developed to run many experiments in parallel for high-throughput screening. Test volumes have continuously been shrinking, with the 96 well microplate replacing 1 mL assays, followed by the development of 384 well and 1,536 well microplate. The individual well sizes are about 0.2 mL, 50 μL, and 2 μL for

the 96, 384 and 1,536 well plates, respectively [17]. The reduction in size reduces reagents and allows experiments to be run in a high density manner. Processes are also being automated to handle various tasks such as pipetting, assay reading and sample storage. Robots have been developed to handle those tasks and make the process less labor intensive and less expensive. Other instruments such as data processing and detectors are integrated with the robots to complete the whole high-throughput screening systems. Robotic systems for automatically handling the whole cell culturing processes have been implemented. Current high-throughput screening robots can run as many as 100,000 assays per day, which is more than one assay per second [17]. Companies such as Aurora Biosciences and Automation Partnership are making robotic systems and partnering with pharmaceutical companies to set up high-throughput screening labs.

However, while the current robotic systems can handle numerous experiments simultaneously in an impressive manner, those methods are limited by some problems. Robotic systems are expensive to purchase and maintain, and many academic and small companies do not have the resources to use them. As the wells are miniaturized, the liquid handling ability of the dispenser becomes important as small variation can result in a relative large impact. As the volume becomes smaller, evaporation becomes a significant problem. Surface tension can cause the surface of small wells in well plates to become uneven, making it difficult to image. In addition, while the wells for assay are miniaturized, the whole robotic systems are still huge and operate in a factory-like setting. Automation Partnership's system is about 150 feet long by 30 feet high and 200 tons in weight [17]. Furthermore, it is unlikely that a well plate with higher density than 1,536 wells per plate can be produced. However, it is still desirable to further miniaturize the

assay size to save cost and reagents. For all theses reasons, a technology that can perform cell-based screening of multiple combinations of compounds in an inexpensive and high-throughput manner will significantly impact a wide spectrum of fields including systems biology, drug discovery and stem cell research.

Chapter 2: Lab-on-a-Chip and Microfluidic Systems

2.1 Introduction

Microfluidics is the field that deals with technology and phenomena of fluid behavior and control in the submillimeter length scale. The term microfluidic device is often used interchangeably with lab-on-a-chip (LOC) and micro-total-analysis-system (μTAS). This area has been growing rapidly as a result of advances in biology and microelectromechanical systems (MEMS). Many believe the development of microfluidic devices has the potential to revolutionize modern biology and chemistry laboratory processes. The field of microfluidic is interdisciplinary, combining different studies in physics, biology, engineering, chemistry and microtechnology.

The development of microfluidic system stems from the field of microelectromechanical systems (MEMS), which itself is originated from the semiconductor industry. In the 1970s, researchers started to develop microfabrication technology and began using silicon to build MEMS devices. In 1979, Terry el al. developed a gas chromatography device on silicon, marking the invention of the first microfluidic device [18]. More miniaturized devices based on silicon were developed in the 1980s. Devices such as miniaturized pumps, valves, mixers and sensors were invented [19-21]. The successful invention of these new technologies spurred the understanding and exploration of novel microfluidic effects. In 1990, Manz et al. proposed that MEMS technologies could be applied to biological and chemical processes, and that a single device could incorporate many aspects of laboratory processes including sample preparation, separation, sample transport and detection [22]. Such devices have

been termed lab-on-a-chip or micro-total-analysis system and have sparked the development of microfluidic devices. These miniaturized devices possess superior analytical performance while reducing the amount of reagents required. This concept has been the motivation of the research in this field even today. One of the most prominent microfluidic devices was the electroosmotic pump, which utilized voltage applied on the electrical double layer of a channel to drive a fluid. Such devices did not rely on mechanical moving parts for pumps and valves, instead flow at different sections of the chip was controlled by adjusting voltage [23]. Electrophoresis devices, which used applied voltage to separate charged particles, were also very popular, and were used to separate various biological entities [24]. The majority of research during this time involved miniaturization of analytical processes and equipments. In the mid 1990s, the field of microfluidic started to bloom, and the growth can be shown in the dramatic increase in number of patents related to microfluidics from 1994 and 2004 [25]. Another important development was the use of novel materials other than silicon. Polymers such as PMMA (poly-(methyl methacrylate)), Parylene C ((poly(chloro-p-xylylene)), SU8 and PDMS (polydimethylsiloxane) were all used to construct microfluidic devices. Recently, microfluidic devices have been integrated into novel applications such as gene sequencing, flow cytometer, fuel cells, and disease diagnostics.

However, the field of microfluidics has many obstacles to overcome before widespread acceptance. For example, the adoption of microfluidic devices by researchers outside of this community has been slow because the devices are often complicated to use. External fluid delivery systems have to be carefully coupled with the microfluidic chip to provide proper sealing and true reduced reagent volumes. Unlike larger instrumentation,

small bubbles in the microchannel can cause devastating device failures. Furthermore, while the microfluidic device itself is small, the external detectors, sample injection, and pumping systems are often bulky. Finally, researchers have found that simply miniaturizing existing instrumentation does not always improve functionality over the existing mature technology. Looking into the future, microfluidic devices need to become simpler to use to gain adoption. In addition, microfluidic devices need to be used in high demand applications and provide valuable and novel utilities instead of merely miniaturizing existing technologies.

Despite current challenges for widespread acceptance, microfluidic devices provide various advantages over macro devices. One obvious advantage that was recognized very early was the small scale of the devices. As the length scale is reduced, processes such as diffusion and thermal energy transfer are significantly faster and devices can operate with faster analysis and response time. The small size also makes microfluidic devices portable for clinical or field use in point-of-care diagnostics. In addition, microfluidic devices are small enough to make them implantable devices such as drug-delivery devices or continuous blood-monitoring devices. Because the device is compact, more experiments can be run in parallel or on one single chip to increase throughput. Microfluidic devices have the capability to handle liquid precisely in the nanoliter range and reduce cost of running experiments by requiring less reagents. In addition, each device requires minimal material cost for construction, and using microfabrication steps, devices can be mass produced. Mass manufactured low cost sensors can be deployed in large quantities for applications such as defense against terrorist biological warfare attacks. Devices can be made disposable, providing user-

friendly operating process and sterile experimental conditions for each experiment. Different components of analytical or biological experimental processes can be integrated on a single microfluidic chip to provide a platform with multiple functionalities.

2.2 Fabrication Technologies for Microfluidics

Many different methods have been developed for fabricating microfluidic devices. The first microfluidic devices in the 1980s utilized fabrication technology borrowed from MEMS (microelectromechanical systems) and the semiconductor industry. Most of these devices were fabricated with bulk micromachining, which involved etching of substrates such as silicon or glass and bonding of the different layers. Other methods that were developed eventually included surface micromachining, the deposition and patterning of various thin film layers. Recent development of soft lithography, the process of micro-molding soft elastomers, has gained wide reception because of its simplicity. Other processes such as injection molding, hot embossing and laser ablation have all been applied to microfluidic fabrication. The details of the different fabrication techniques will be presented in the following sections.

One common technique that is used in many microfluidic fabrications is photolithography. Photolithography involves coating (usually by spin-coating) a photosensitive photoresist on a substrate and baking of the photoresist to slightly harden it. A mask is made with a pattern that has areas that either block or allow light to pass through. Depending on the type of photoresist, exposed areas become soluble or insoluble in developer. The patterned photoresist remains after developing and can be

used as masking material during etching of the underlying substrate or as a structural or sacrificial material itself.

2.2.1 Bulk Micromachining

Bulk micromachining involves patterning a substrate, usually silicon or glass, by selectively etching the substrate and creating structures such as trenches or holes inside the substrate. This is a popular technique because various etchants have been extensively studied and developed. Furthermore, the etching profile (isotropic or anisotropic), selectivity and rate can be precisely controlled.

To wet etch silicon isotropically, or etching with the same rate in all direction, HNA (HF, HNO_3, and CH_3COOH) can be used [26]. The HNO_3 is used to oxidize the surface while HF can dissolve the oxidized product. CH_3COOH is used for the transport of products and reactants.

To create more complex shapes, chemicals for anisotropic etching can be used. The anisotropic property arises because the etchant etches one crystal orientation faster than the other. The etchant usually contains alkaline solution to dissolve silicon. Typical etchants include KOH, EDP (ethylene-diamine pyrocatechol), and TMAH ($(CH_3)_4NOH$). These etchants have a 10 to 400 times higher etching rate in the <1 0 0> plane than the <1 1 1> plane. EDP was the first etchant developed but suffers from high toxicity and less selectivity than the other two. KOH has the best selectivity among the three and is a good chemical to use for creating grooves. However, KOH also etches away material such as SiO_2 and aluminum. TMAH has lower selectivity than KOH but is compatible with CMOS fabrication processes. Glass, which is often a preferable substrate to silicon for biological imaging applications, can be etched using HF solutions. However, the

etching rate can be slow and masking material such as photoresist is etched too. Therefore, in many applications silicon is preferred to glass.

The dry etching process using plasma can be applied for bulk micromachining of silicon. Although wet etching is typically less expensive, easier to implement, and etches at a higher rate, plasma etching has certain advantages. Plasma etching produces smaller feature sizes than wet etching because the wet process can indiscriminately damage the other features on the substrate. Furthermore, dry etching does not cause undesirable results such as delamination of the bonded layers. Plasma etchers typically use a gas with fluorine such as SF_6 or CF_4. These gases are charged to become high energy plasma that produces fluorine free radicals. The fluorine free radicals react with the silicon to etch it. SF_6 is the most common gas used in dry etching and the reaction results in gaseous products of SiF_6. Depending on the plasma etcher configuration, etching profiles from isotropic to slightly anisotropic to totally vertical can be produced. Typical plasma etchers, which have a RF power electrode at the top of the chamber, away from the substrate, produce an isotropic etching profile. Reactive ion etching (RIE), utilizes a power electrode at the bottom in contact with the substrate. This causes the plasma particles to accelerate preferentially towards the substrate, producing a more anisotropic profile. Deep reactive ion etching (DRIE) produces the most vertical sidewalls by using a switching chemistry between SF_6 and C_4F_8. The C_4F_8 passivates the sidewalls of a trench, forming a protective layer from the subsequent SF_6 etching, which makes the trench deeper. The two gases are continuously switched and aspect ratio of 30:1 can be achieved.

The etched patterns are generally bonded with another substrate such as glass or silicon to complete the microchannels. Three common bonding methods have been developed and used extensively: Si-Si fusion bonding, anodic bonding and eutectic bonding. In fusion bonding, the Si surface is cleaned and hydrated to produce OH functional groups on the surface. The two surfaces are brought in contact at one point to start a "contact wave" that propagates through the whole surface. Then, the two surfaces in contact are thermally annealed at 800^{o}C to 1200^{o}C to create covalent Si-O-Si bond with the removal of H_2O group. The bond strength can be comparable to that of intrinsic silicon. Anodic bonding is used to join a silicon substrate with a Na^+ based material such as Pyrex glass. The two surfaces are cleaned and brought into close contact. The two surfaces are heated to temperature of 200^{o}C–500^{o}C, and a voltage of 200 V–1,000 V is applied with the more positive potential on the silicon. The applied voltage causes the positive Na^+ to be displaced from the bonding surface, leaving negative charges at the interface. The resulting electrostatic force and migrations of ions facilitate formation of chemical bonds which would otherwise require temperature of around 1,000^{o}C. This is a versatile technique as Pyrex can be sputtered as a thin film and used as a glue to bond Si to other surfaces. In eutectic bonding, eutectic alloys such as Au/Sn are coated on the substrate and used as glue. The surface coated with the eutectic layer is brought together with another surface and heated to the eutectic point inside a vacuum chamber to facilitate bonding.

2.2.2 Surface Micromachining

Surface micromachining involves deposition and selective patterning of layers of sacrificial and structural thin films on the substrate. Unlike bulk micromachining, the

substrate remains intact. The layers are patterned with photolithography. Sacrificial layers aid in defining the final shape of the device and are removed using specific solvent. Structural layers remain and form the final device. The process flow for the general surface micromachining process is shown in Figure 2-1.

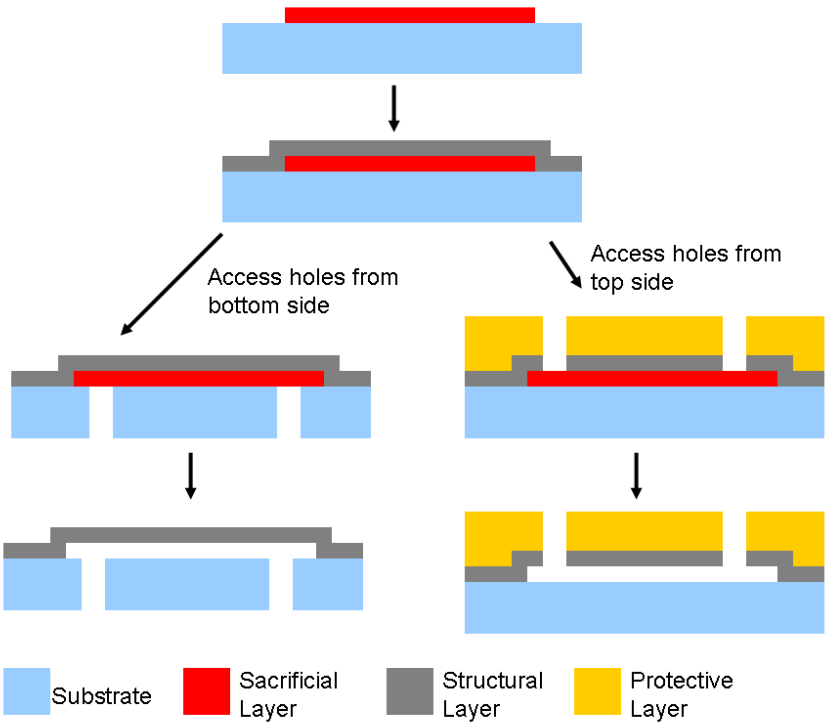

Figure 2-1. General process for fabrication of microchannel with surface micromachining. Access holes can be made from the top or bottom side of the substrate.

In surface micromachining, polysilicon is most commonly used as the structural material and silicon dioxide as the sacrificial material. Both polysilicon and silicon dioxide can be deposited using the chemical vapor deposition (CVD) process. Polysilicon can be etched using SF_6 plasma etching and silicon dioxide can be removed using HF solution.

Surface micromachining is not limited to glass and silicon substrates. A wide variety of materials can be used as long as the process used for the removal of sacrificial

layer does not damage the structural layer. When using alternate materials for surface micromachined devices, it is important to ensure that the adhesion between the different deposited layers is strong. It is especially important to choose the proper solvent and dissolution procedure to remove the sacrificial layer as improper choice can result in delamination of the deposited layers. Many combinations of materials have been used for surface micromachining and recently the use of polymers has drawn much attention. With polymers, photoresist can be used as the sacrificial layer and removed by dissolution in organic solvent such as acetone. Polymers such as PMMA, Parylene and SU8 can be deposited on the photoresist to form microfluidic channels. Access holes for making fluidic connection to the fluid delivery macro components can be made either at the bottom or the top of the device. Making access holes from bottom requires bulk micromachining to create holes through the entire substrate which is time consuming and expensive. Also, care must be taken to ensure that etching through the whole wafer does not affect the features on the top side. When access holes are made on the top of the device, channels need to be protected from the coupling pieces such as o-rings and gaskets to prevent channels from collapsing. In this case, a conformal coating of thick polymers such as SU8 can be applied and patterned as a protective layer.

2.2.3 Soft Lithography

Soft lithography refers to the micro-molding of soft elastomers, most commonly PDMS (polydimethylsiloxane). PDMS has the advantage that it is flexible, optically transparent and inexpensive. Soft lithography has gained popularity since 1995 because it does not require complex equipments and has a short fabrication time. Many labs that do not have in-house cleanroom facilities can have access to microfluidic devices using

soft lithography. The general PDMS fabrication procedure starts with the fabrication of the mold. This can be done by patterning silicon wafers using DRIE or other bulk micromachining processes or patterning SU8, a negative photoresist that can achieve thicknesses of 100 μm or more. PDMS prepolymer generally consists of two components of polymer base and curing agent. A typical PDMS, Sylgard 184, generally consists of polymer base and curing agent mixed at a ratio of 10:1. Next, the mixture is casted on the mold and cured by heat. Sylgard 184 can be cured in 80^{o}C oven in 30 minutes. After curing, the PDMS piece is removed from the mold. Access holes are punched through the PDMS with a blunt-end syringe needle. The PDMS piece is then bonded to another substrate such as glass or another piece of PDMS. To bond PDMS to glass, the two pieces can be treated with oxygen plasma and bonded together via hydrophilic interaction [27]. PDMS can also be bonded to another piece of PDMS to create monolithic structures [28]. This can be achieved by treating both PDMS surfaces with oxygen plasma and bonding them together. Another method is by partial curing: both pieces of PDMS are cured for a short period of time at lower temperatures (~60^{o}C) and become hardened enough to handle but not totally cured. The two pieces are then brought into contact and cured together. This method has been useful in constructing PDMS valves and pumps where two layers of PDMS channels sandwich a thin PDMS layer in between them. The top control channel is actuated pneumatically to push the thin PDMS piece down to seal the bottom fluidic channel.

While PDMS has been a popular material for microfluidics, it has several shortcomings. Complex structures can be difficult to achieve and the aspect ratio is limited from 0.2 to 2 [29]. Features with small dimensions can be hard to replicate

faithfully. PDMS devices are unable to withstand high pressure and the typical methods used to bond glass to PDMS have working pressures limited to a maximum of 80 psi [27]. PDMS is highly porous, and diffusion of water vapor can lead to undesirable drying of the sample or even osmolarity change [30]. Small molecules can diffuse into or out of the bulk of PDMS, and this can produce undesirable effects such as decreasing the concentration of the input compounds for exposure on cells or target molecules for detection [31]. Because PDMS is permeable to most organic solvents, it swells significantly after exposure to organic compounds. Although pretreatment of the PDMS surface is generally used to reduce permeability, it is often inadequate. This is a serious drawback and makes it impossible to use PDMS in many applications. Because of these limitations, polymers with similar properties to PDMS but more chemically resistant are currently being developed.

2.2.4 Other Fabrication Processes

Conventional processes for making polymer parts have been applied to make microfluidic devices. Processes such as hot embossing and injection molding have been applied [32]. In the hot embossing process, the mold and polymer are heated to the polymer's glass transition temperature inside vacuum, and the mold and polymer are then brought in contact with an applied force. This results in the pattern on the mold being stamped into the softened polymer. In injection molding, polymers in granular pellets are forced into a cylinder and start to melt. The molten polymer is injected into a cavity containing a mold at 60 to 100 MPa. While these processes are unable to achieve highly complex structures that photolithography technology is capable of, these technologies are more matured and require shorter fabrication time and lower cost. Another advantage is

the wide range of polymer materials that are available including polymethylmethacrylate (PMMA), polypropylene (PP), polystyrene (PS) and polycarbonate (PC). As a result, those processes are more commonly used in making commercial microfluidic products. Another method is to use laser ablation to directly create microfluidic channels on plastics or glass. In laser ablation, a laser is shined on the material, breaking chemical bonds inside the material. Laser ablation has been applied to materials including glass, ceramics, polymers and metals.

After the pattern for the microchannel is made, bonding has to be done to enclose the channels. Process such as lamination, gluing, and thermal bonding can be applied to bond polymer-based microfluidic devices. In the lamination method, a film coated with an adhesive layer is sandwiched in between the polymer chip and another substrate such as glass. The setup is rolled into two heated rollers and the adhesive film is melted, joining the two pieces together. Gluing can also be used to join two pieces together. For both the gluing and lamination processes, care should be taken to avoid blocking the channel with the adhesive layer. Another way to join polymer pieces is by heating the polymers and applying pressure to seal the device.

2.3 Parylene Microfluidics

Parylene has emerged as a popular choice of material for constructing microfluidic devices. Many of the fabrication processes presented in the following chapters are based on Parylene. Also, the type of Parylene mentioned in the rest of the thesis refers to Parylene C, unless otherwise specified. The background, properties,

deposition, and pattering of Parylene for microfluidic device fabrication will be discussed in this section.

2.3.1 Parylene Background and Properties

Parylene has several unique material properties that make it advantageous to use as a microfluidic material. Parylene is transparent, chemically inert, and biocompatible. Parylene is conformally coated onto a surface using chemical vapor deposition method and deposition thickness can range from 0.1 to 1,000 μm. Parylene deposition is performed at room temperature and is suitable for encapsulating delicate items such as electronics and medical devices. Researchers eventually discovered Parylene's compatibility with CMOS/MEMS fabrication process and its superior material property has made it the material of choice for constructing microfluidic devices.

Parylene was first discovered in 1947 by Professor Michael Szwarc at University of Manchester in the United Kingdom when he was studying the chemical bonds in molecules such as xylenes, which have a carbon attached to a benzene ring [33]. Because he was interested in studying the bond strength, he heated the chemicals to a high temperature. He eventually noted formation of a thin film in downstream cooler area zone, and was intrigued by the unique physical and chemical property of the film. The material was named "Szwarcite," which is today's equivalent of poly-p-xylylene or Parylene N. The discovery spurred commercial interests and William Franklin Gorman proposed a chemical vapor deposition method to create Parylene film with the dimer of the p-xylylene as starting material. The "Gorman" process is still used in many Parylene coaters today. However, the synthesis of stable dimer was not reliable until Donald Cram at UCLA developed a method to synthesize the dimers in 1951. This development made

the commercialization of the Parylene deposition process viable. Over 20 types of Parylene were subsequently commercialized, while three types, Parylene N, Parylene C and Parylene D have been most commonly used (Figure 2-2). The recent development of Parylene HT has introduced another Parylene with superior material properties such as increased thermal stability, improved electrical properties, increased ultraviolet stability, and a lower coefficient of friction.

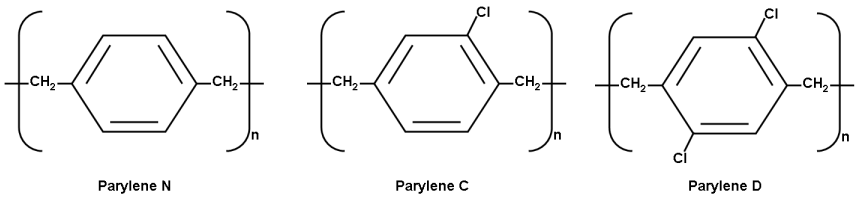

Figure 2-2. Chemical structures of the common Parylenes.

Parylene N, poly-p-xylylene, is the most basic form in the Parylene family. It is completely linear with no functional groups substituted. Parylene N has high dielectric strength and has constant dielectric across a large frequency range (2.65 from 60 Hz to 1 MHz) [34]. Parylene C has one aromatic hydrogen substituted with a chlorine group. Parylene D has two substituted chlorine groups and is able to maintain its mechanical and electrical properties at higher temperature. Parylene C is the most common Parylene for microfluidics. Parylene C has the highest mechanical strength among the three common Parylenes with Young's modulus of 400,000 psi. Because Parylene is deposited in a conformal and pinhole-free manner, it exhibits low permeability to moisture and gases and is stable toward many organic solvents [34]. Parylene C has been shown to be biocompatible and is certified with the stringent biocompatibility rating of both United States Pharmacopeia (USP) Class VI by the Food and Drug Administration (FDA) and

ISO 10993. It is resistant to corrosive body fluids and has been used to coat many chronic implantable devices [35, 36]. Parylene C is also preferred over the other two types of common Parylenes because it has the highest deposition rate of 2–3 μm/hr. In addition, Parylene C is transparent in the visible range which allows microfluidic devices for biological applications to be readily coupled with microscopy techniques.

2.3.2 Parylene Microfluidic Fabrication Process

Fabrication of Parylene-based microfluidic networks is based on surface micromachining techniques. The Parylene deposition and etching process will be described in this section.

Figure 2-3 shows the generalized Parylene deposition process using chemical vapor deposition (CVD). The simplified model of the Parylene deposition consists of three distinct stages: vaporization, pyrolysis and deposition [34]. The pressure difference in each of the three zones (1, 0.5 and 0.1 torr) drives the flow of the vapor. First, the Parylene dimers are loaded into a boat and are vaporized by heating to 150^{o}C. At this temperature, the dimers are sublimed and the vapor enters the pyrolysis zone. The pyrolysis zone is approximately 680^{o}C, and at such temperature, the cleavage of the methylene-methylene bond occurs. This yields the Parylene monomer, para-xylylene, a diradical monomer. Finally, the monomers enter the deposition chamber, where they adsorb and polymerize on the substrate at room temperature. When the monomers enter the deposition chamber, some adsorb to the substrate. Some of these monomers will desorp and leave the surface, while others come in contact with each other and begin the nucleation process [37]. The polymer propagates until all the monomers are used or until the process is stopped. It has been shown that the deposition rate can be increased by

decreasing the substrate temperature and it was suggested that the higher deposition rate is a result of the increased condensation of the monomers on the surface.

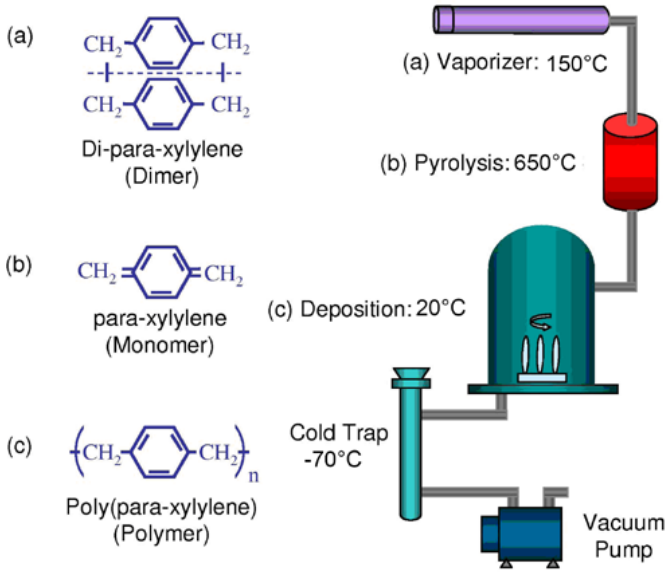

Figure 2-3. The Parylene deposition process. (a)–(c) show the chemical structures of Parylene at corresponding time points. Image adopted from [38].

One key advantage of this deposition process is the formation of a pinhole-free conformal coating on the substrate. Unconformal coatings lead to an inhomogeneous surface, and because of the large surface area to volume ratio in miniaturized devices, small inhomogeneities can be detrimental to the device. Another advantage of using CVD process is that the monomer gas is converted to polymer film directly, without catalysts or solvents. In addition, this coating process is substrate independent and almost all materials can be coated. The deposition occurs at room temperature and is compatible with existing MEMS/CMOS fabrication process and materials.

After Parylene is deposited, it can be selectively etched with many processes. Parylene can be removed using a solvent such as chloronaphthalene or benzolyl benzoate at 150^{o}C [39]. However, such process is not compatible with lithographic procedures.

UV laser ablation is also possible but is hampered by low throughput and high cost. Using plasma etching is the most practical and common method to pattern Parylene. Oxygen plasma can be used to etch Parylene with photoresist. As photoresist can be etched by oxygen plasma, a photoresist slightly thicker than the Parylene thickness has to be used. Metals such as gold or aluminum can also be used as the masking material. Plasma etching, reactive ion etching (RIE) and deep reaction ion etching (DRIE) can all be used to pattern Parylene [39]. RIE can achieve more vertical sidewall profile than plasma etching, while DRIE can achieve the most vertical sidewall profile. Typical etching rate is about 0.1 to 0.5 μm min^{-1}.

The deposited Parylene can be etched and followed up by other lithographic processes. Photoresist can be patterned on Parylene with good adhesion. Metals such as Cr/Au, Ti/Pt and Al can be deposited on Parylene using thermal or e-beam evaporation. Those metal layers can be patterned by the typical lithographic and etching processes as Parylene is inert to most solvents. Functionalized Parylene molecules with substituted groups such as aminomethyl or carboxylic acid have been synthesized and can be used to couple molecules such as proteins [40].

A typical process to construct Parylene microchannel utilizes the surface micromachining technique. Photoresist is first patterned on the substrate and Parylene is deposited. Parylene is patterned to make the access holes on the top side and the sacrificial photoresist can be eluted using acetone. Alternatively, access holes can be patterned from the bottom side by performing bulk micromachining.

To date, various integrated microfluidic devices and individual components have been made by extending the basic surface micromachining procedure. Some examples

include peristaltic pumps, electrolysis pumps, check valves, modular microfluidic systems and cytometers [41-44]. Parylene has also been applied to devices outside of microfluidic such as bioMEMS and implantable devices with examples including retinal implants and eye pressure sensing micro devices [45, 46].

2.4 Microfluidics for Cell Biology

In recent years, the applications of microfluidic devices in cell biology have grown, and many believe the development in microfluidics will greatly expedite advancements in cell biology. Microfluidics will enable cell biology experimentation to be done effectively in a high-throughput manner, with both multicellular and single-cellular studies. Reagents requirements for microfluidics devices are a couple of orders of magnitude smaller than macro scale devices. Many microfluidic devices also offer functionalities that are unachievable by traditional cell biology instrumentations or methods. Such functionalities are based on the devices' ability to control the microenvironment precisely in both spatial and temporal aspects. These capabilities have allowed microfluidics devices to make biomimetic physiological conditions possible for experimentation. In this section, various microfluidic devices applicable to cell biology will be introduced.

2.4.1 Controlling Microenvironment Using Microfluidic Flow

One major challenge in studying the cells is to understand the microenvironmental factors that regulate cells. The *in vivo* microenvironment is composed of complex interactions of neighboring cells, extracellular matrix molecules,

soluble factors, gas concentrations, physical effects by fluid flows, and temperature effects. Microfluidic flow has provided the ability to precisely control many microenvironmental cues for cellular studies.

The field of microfluidics has excelled in creating chemical gradients on a single chip. These devices are important because chemical gradients occur readily *in vivo* and their consequences have intrigued scientists for years. However, a reliable gradient generation is hard to achieve in traditional devices. Jeon et al. utilized the laminar flow and diffusion dominant properties of microfluidics to create a well-defined and precise chemical gradient on-chip [47]. The device has three inputs and a series of downstream dividers and serpentine mixers to continuously split the input streams and join and mix them into streams with different and defined concentrations. For example, by putting 0%, 50% and 100% of a solution into the inputs, a linear gradient was achieved at the output. More complex nonlinear gradient profiles were also achieved. Such devices have been adopted in studying wide array of phenomena caused by chemical gradient including chemotaxis of neutrophil and cancer cells and stem cell differentiation [48-50].

Microfluidic flow has also been used to expose a single cell to asymmetric signals by placing it at the interface of fluid streams. Because flow is laminar and two streams flowing alongside each other undergo minimal mixing, part of the cell receives the soluble factors directly while the other part does not. This has been used in studying mitochondrial movement within a single cell [51]. A similar mechanism has been applied to expose Drosophila embryo cells to temperature variation by placing a single cell at the interface of a warm and a cold stream [52]. Patterning of cells and proteins has been enabled by the use of microfluidic devices, and those studies are significant for

tissue engineering [53, 54]. Furthermore, the ability to control micro flow precisely has enabled the study of shear stress on cells in a convenient and systematic manner [55]. The microenvironment that cells reside in is composed of cell-cell interaction among different groups. Lee et al. developed a microfluidic device to precisely bring two cells in contact with each other for cell-cell interaction studies. Such devices can be implanted for performing studies in high-throughput manner [56]. All these instruments exploit unique properties of microfluidics to build devices and enable studies that are not possible with traditional macro devices.

2.4.2 Cellular Analysis Using Microfluidic Devices

Various processes in cellular analysis were miniaturized with the ultimate goal of building a complete system with multiple functionalities integrated on a single chip. Separation and sorting of cells is one of the routine process in cellular analysis and different cell sorting mechanisms on microfluidic platform have been developed. Some devices are miniaturizations of macro devices while others exploit unique features of microfluidics. One of the most successful methods is to use dielectrophoresis (DEP), in which particles (charged or neutral) are subjected to a non-uniform ac field. Cells are separated because the force on them differs depending on the cells' electrical properties, shapes, and sizes. Mammalian cells were sorted using this method [57]. Another method is to use "deterministic lateral displacement" in which an array of post is fabricated and particles are flowed through the posts. Small particles can follow the streamlines and stay in one lane, while large particles will continue to be displaced to another lane. This method has been applied for sorting cells such as blood cells in whole blood [58]. Cell cytometers, both using optical and impedance-based detection schemes have been created

as well [42, 59]. Cell lysis functionality has been made possible by either using barbs to mechanically lyse the cells or applying electric field to electrically lyse the cells [60, 61]. In addition, chips that are capable of analyzing cell lysates have been made. Systems such as on-chip PCR were fabricated and because of low thermal-mass of microsystems, fast cycling was possible [62]. Other components such as HPLC, capillary electrophoresis or isoelectric focusing have all been made [43, 63, 64]. Besides analyzing cell aggregates, single cells can also be analyzed in a high-throughput manner by taking advantage of the ability of microfluidic devices to position cells precisely. Carlo et al. created a device to efficiently position single cells in individual traps [65]. While these works focus on demonstrating the capability and advantages of using microfluidic systems, efforts must be put into improving compatibility with existing laboratory processes and integrating the various components for microfluidic devices to gain wider adoption.

2.4.3 Microfluidic Cell Culture and Cell-Based Assay Systems

As discussed in the previous chapter, cell culture and cell-based assay is a key process in various fields including pharmacology, cell biology and tissue engineering. High-throughput experimentation is desirable, but a reliable and cost-effective platform has been hard to achieve. Recently, many researchers have been developing microfluidic devices as potential inexpensive tools for high-throughput cell-based assays. The advancements in microfabrication and microfluidic technologies have enabled the development of various lab-on-a-chip devices with cell culturing functionalities. Using microfabrication techniques, chip-based devices with high-density arrays can be mass fabricated. Performing cell culture and assays with microfluidic devices also possesses

the advantages of increased throughput, precise liquid handling in the nanoliter range, and reduced sample volume. Fewer cells can be used for each experiment and this is beneficial for performing experiments on rare cells such as stem cells or primary cells. Furthermore, on-chip culture systems offer culture environments with characteristic lengths at the micro scale and the cell culture environment on-chip can be designed to better mimic the *in vivo* culture microenvironment than traditional cell culture systems.

Various on-chip culture systems with different functionalities have been developed. Prokop et al. developed a device to culture cells inside microfluidic channels and was able to culture cells for 5 days [66]. Hung et al. created a device with separate cell loading and media perfusion inlets to efficiently collect cells and perfuse them without cell loss [67]. The setup also enabled cell passaging by using trypsin, and cell culture over 2 weeks was achieved. To date, an abundant number of cell types have been successfully cultured on-chip, including human hepatocytes, fibroblasts, osteoblasts, stem cells, breast cancer cells and many others [68]. Devices that integrate other microfluidic capabilities have been created. Cell culture arrays were integrated with concentration gradient generators to expose them to a single compound at different concentrations [50, 69]. King et al. developed a chip with a high-density cell array and monitored gene expression in real time using reporter genes with green fluorescent proteins [70]. In a single experiment, multiple stimuli were applied to treat the cells at once and ~5,000 measurements were made. A creative device was made by Kim et al. that cultured cells under a logarithmic range of flow rates simultaneously and studied the cell responses at different flow rates [71]. Cell patterning and long-term studies of cellular differentiation using perfusion systems on-chip were demonstrated [72].

However, most of the current devices are not designed to screen for multiple compounds at once. Chip-based devices that have the capability to handle two or more inputs and assess the effects of multiple compound exposures on cells are valuable for numerous screening applications.

2.5 Microfluidic Phenomena Related to Cellular Studies

As the scale of the culture environment is reduced to micron scale, some of the dominant forces and physical phenomena in macro scale can become less important. On the other hand, other forces and physical phenomena that are generally ignored in macro device design can start to dominate. This provides the opportunity to exploit novel properties of microfluidics to achieve various functionalities unattainable by macro devices. Also, it is important to consider the dominant phenomena in microfluidic devices when designing devices for cellular studies. This section will briefly review some of the physics at micro scale pertinent to microfluidic for cellular studies.

2.5.1 Laminar Flow

In macro scale fluidic devices, flow is often turbulent, which is chaotic and unpredictable. However, in microfluidic devices, flow is generally laminar, in which the position of particle inside a fluid stream as a function of time can be predicted. In laminar flow, fluid can be treated as composition of several thin layers, or laminae, and the layers flow parallel to each other without disruption. One dimensionless number that gives an indication of the flow regime is the Reynolds number, Re, and is defined [73]

$$\mathrm{Re} = \frac{\rho v D_h}{\mu}, \tag{2.1}$$

where ρ is the density of the fluid, v is the velocity of the fluid, μ is the fluid viscosity and D_h is the hydraulic diameter, which is dependent on the channel's cross section geometry. Re < 2300 indicates the flow is in the laminar regime, and given the small size of microfluidic channels, most of the microfluidic flows have Reynolds number less than 1. As a result of this, two fluid streams flowing alongside each other inside a microchannel will mix only by diffusion.

Pressure driven incompressible flow is described by two equations, the Navier-Stokes equation [74]:

$$\rho\left(\frac{\partial \vec{v}}{\partial t} + \vec{v} \cdot \nabla \vec{v}\right) = -\nabla p + \mu \nabla^2 \vec{v}\,, \tag{2.2}$$

and the equation for conservation of mss:

$$\nabla \cdot \vec{v} = 0\,, \tag{2.3}$$

where $\vec{v}$ is the fluid velocity, p is the pressure, μ is the fluid viscosity, t is the time and ρ is the fluid density.

For microfluidic design consideration, the analytical solution for the Navier-Stokes equation can be solved assuming the no-slip boundary conditions. The exact solution depends on the cross sectional geometry of the microfluidic channel, but the flows always follow a parabolic profile. The steady state velocity profile for a rectangular channel can be approximated by the parallel plate Poiseuille flow [75]:

$$v_x(y) = \frac{\Delta P}{2\mu L}(h - y)y\,. \tag{2.4}$$

The velocity in the x direction, v_x, is a function of the position along the channel height, y, and h is the channel height, ΔP is the pressure difference of the two ends of the channel, L is the length of the channel, and μ is the viscosity of the fluid.

Flow profile can also be described conveniently using a fluidic resistance concept.

$$\Delta P = QR\,. \tag{2.5}$$

The pressure drop, ΔP, is equal to the product of volumetric flow rate through a channel, Q, and fluidic resistance of the channel, R. For a rectangular channel, the fluidic resistance is [73]

$$R = \frac{12\mu L}{wh^3}\left[1 - \frac{192h}{w\pi^5}\sum_{n=1,3,5}^{\infty}\frac{1}{n^5}\tanh\left(\frac{n\pi w}{h}\right)\right]^{-1}, \tag{2.6}$$

where w is the width of the channel, h is the height of the channel and L is the length of the channel. For channel with width much larger than height, the resistance can be approximated as

$$R = \frac{12\mu L}{wh^3}\,. \tag{2.7}$$

2.5.2 Diffusion

Diffusion can be the dominant transport process in microfluidic channels. Diffusion is the process by which particles move from higher concentration regions to lower concentration regions because of Brownian motion. In one dimension, diffusion can be modeled by the equation:

$$d^2 = 2Dt\,, \tag{2.8}$$

where d is the mean distance that a particle travels, D is the diffusion constant and t is the time. Diffusion becomes important when the time is long or the distance is short, so it is inconsequential in channel with centimeter or wider widths. Typical diffusion constant for some molecules in water are 2×10^3 $\mu m^2\, s^{-1}$ for solute ions, 100 $\mu m^2\, s^{-1}$ for small

proteins and 0.02 $\mu m^2\ s^{-1}$ for mammalian cells. A dimensionless number that indicates whether convection or diffusion is dominating is the Peclet number, *Pe*,

$$Pe = \frac{vl}{D}, \tag{2.9}$$

where *v* is the fluid velocity, *l* is the characteristic length and *D* is the diffusion constant. When the velocity is high, convective transport dominates, while when the length is small, diffusion dominates.

2.5.3 Shear Stress

Shear stress is the tangential force applied to the surface of an object. Inside a microfluidic channel, the shear stress at the wall is given by the equation,

$$\tau = -\mu \frac{dv}{dy}, \tag{2.10}$$

where τ is the shear stress, μ is the fluid viscosity *v* is the fluid velocity and *y* is the position along the height of the channel. For rectangular shape channel, the shear stress can be described using the parallel plate model [71]

$$\tau = \frac{6\mu Q}{h^2 w}, \tag{2.11}$$

where *Q* is the volumetric flow rate, *h* is the height of the channel and *w* is the width of the channel. As a result, shear stress is larger in smaller channels than larger channels. Depending on the cell type, the amount of shear stress that a cell can tolerate is different. In addition, fluid flow can lead to shear stress which can influence cellular behavior. For example, shear stress can cause endothelial cells to polarize in the direction of fluidic flow and can influence intracellular cAMP production in osteoblasts [76, 77].

2.5.4 Surface Effects

As the device size shrinks from macro to micro, the surface area to volume (SAV) ratio increases dramatically. The large SAV ratio would require attention to be paid to surface effects when designing microfluidic devices for cellular studies. A 35 mm culture dish with 2.5 mL of media has a SAV ratio of 4.2 cm^{-1} [73]. On the other hand, a cylindrical micro culture chamber with diameter of 100 μm and height of 100 μm has a SAV ratio of 600 cm^{-1}. With the increase in surface area to volume ratio, some parameters have to be taken into account. Proteins can be adsorbed to the surface and results in the depletion of proteins inside a microfluidic device. Also, with the increase in surface area, evaporation happens at faster rate.

Another force that becomes prevalent is surface tension, which is a result of the attractive forces between the molecules inside the liquid. Depending on the surface energy, liquid on solid/gas/liquid surface would result in different wetting behavior. For example, if a droplet of water is formed on a solid surface and the attraction between the liquid surface and solid is strong, this would result in strong wetting of surface. Such behavior is described as hydrophilic and the opposite effect, hydrophobicity can occur when the attraction between liquid and solid is not as strong as that in the liquid. The wetting behavior is affected by the properties of the liquid. For example, a more polar solvent such as water has stronger intermolecular bonding of the liquid molecules at the surface, and therefore, higher surface energy than ethanol. The wetting behavior can be quantified using the contact angle θ_c, the angle between the liquid and solid surface [74].

$$\gamma_{SL} + \gamma_{LG} \cos\theta_c = \gamma_{SG}, \tag{2.12}$$

where γ_{SL}, γ_{LG}, γ_{SG}, are the interfacial tensions of the solid/liquid, liquid/gas, and solid/gas interfaces, respectively.

As a result of surface tension, at the interface of liquid, solid, and gas, the surface of liquid is distorted, resulting in a pressure difference across the surface. Such pressure is described by the Young-Laplace equation [73]:

$$\Delta P = \gamma(\frac{1}{R_1} + \frac{1}{R_2}), \tag{2.13}$$

where ΔP is the pressure difference, γ is the surface tension of the liquid and R_1 and R_2 are the principal radii of curvature. A spherical drop of liquid would have $R_1 = R_2$, resulting in

$$\Delta P = \frac{2\gamma}{R}. \tag{2.14}$$

Chapter 3: 3-D Microfluidic Network Fabrication: Making Cell Culture Array on Silicon with Integrated Combinatorial Mixer

3.1 Introduction

The ability to assess the combinatorial effects of several compounds on cells is an important aspect in the field of quantitative biology and drug screening. As described in chapter 1, a mixture of drugs or chemical compounds can often treat diseases more effectively or act synergistically in certain cellular pathways, and many biological phenomena are governed by the combinatorial effects of several gene regulatory proteins or extracellular factors. This is one of the reasons for the increase in demand for high-throughput cell-based screening technology. The popular method of using multi-well plates with robotics is limited by the problems of poor small-volume liquid handling ability, large consumption of reagents, and high cost of operation. As discussed in previous chapters, microfluidic devices can overcome those problems and provide potentially inexpensive tools for high-throughput cell-based assays. Microfabrication enables inexpensive chip platforms with high-density arrays to be mass fabricated. Performing cell culture and assays with microfluidic devices also possesses the advantages of increased throughput, precise liquid handling in the nanoliter range, and reduced sample volume.

While various on-chip culture systems have been developed, most of the current devices are designed to expose cells to a single compound at once. The complexity of on-chip cell-based assay experiments can be greatly expanded by developing a cell

culture chip with an integrated combinatorial mixer to simultaneously deliver different combinatorial fluid streams to study cell cultures. Additionally, a chip-based combinatorial mixer can decrease the time and labor during the process of mixing and dispensing solutions. Creating a combinatorial mixer requires the fabrication of three-dimensional (3-D) microfluidic networks and different methods for creating 3-D microfluidic network will be described.

3.1.1 Background of Three-Dimensional (3-D) Microfluidic Devices

Previous methods of fabricating 3-D microfluidic devices often involved patterning and bonding of multiple layers. Kikutani et al. fabricated 3-D microfluidic chip by bonding several etched glass substrates [78]. Pyrex glass was first covered with Cr and Au to protect the substrate during etching and positive photoresist was photolithographically patterned on top of the metal layer. The Cr and Au were etched with I_2/NH_4I and $Ce(NH_4)_2(NO_3)_6$, and the glass was etched with 50% HF solution at a rate of 13 μm/min. Then, the photoresist was removed with acetone, and the metals were removed using the I_2/NH_4I and $Ce(NH_4)_2(NO_3)_6$ solution. Two glasses were patterned using this method for the top and bottom plates. For the middle glass plate, through holes were drilled using ultrasonic sandblasting. Finally, the glass plates were cleaned with ethanol and NaOH, and thermally bonded together inside a 650^{o}C furnace for 5 hours. Patterned polyethylene terephthalate (Mylar D, Dupont, Washington, DC) can be bonded together to make a 3-D microfluidic network as demonstrated by Neils et al. [79]. The sheets were patterned with CO_2 laser to create channels and windows. Some sheets had dry adhesive coating (501FL, 3M), and the cut Mylar sheets were aligned, bonded and pressed to create the final microfluidic structures. A total of 9 Mylar layers were stacked

together in this method. PDMS (polydimethylsiloxane), a popular material for constructing microfluidic devices, has been used in 3-D microfluidic. Jo et al. [80] presented a method to pattern and bond several 2-D PDMS layers to form complex 3-D channels. To create the 2-D layers, PDMS prepolymer mixture was cast onto a master created by patterned SU-8 on silicon wafer and a transparency film was lowered onto the PDMS prepolymer mixture. The stack was then clamped together with top and bottom flat aluminum plates, a Pyrex wafer and rubber sheet, and cured at 100^{o}C for three hours. The 2-D layers were peeled off from the master, and the surfaces were cleaned with diluted HCl solution. Finally, the layers were treated with oxygen plasma in reactive ion etching systems and aligned and bonded together.

3.1.2 Motivations for Monolithic 3-D Microfluidic Fabrication

While functional devices have been demonstrated, multilayer bonding process suffers several unavoidable drawbacks. Performing the bonding process can result in possible misalignment from layer to layer and such process can be challenging to batch fabricate for large-scale production. Furthermore, as the number of inputs for the 3-D microfluidic device increases, the number of layers can increase and result in an undesirably thick device. Possible delamination of the layers and device failure can result from contamination of the surface. In addition, many of the materials have not undergone extensive testing for biocompatibility and might not be suitable for cellular studies. Therefore, a monolithic fabrication process using biocompatible material to build the devices would be desirable. Such process should also have the capability to be scaled up to fabricate chip with large number of channels, inputs and outputs with only minor or no modification to the process.

This chapter will discuss the development of an integrated method to fabricate monolithic 3-D microfluidic networks and the fabrication of an on-chip cell culture device with an integrated combinatorial mixer based on such technology. As a first example, the device has a combinatorial mixer with three inputs and one control channel. The combinatorial mixer is capable of generating the eight combinatorial streams simultaneously for delivery to the eight culture chambers. Our fabrication method is based on the surface micromachining of Parylene C and can be scaled up to achieve high-throughput combinatorial cell-based assays. The packaging scheme to provide fluidic connection to the chip has been developed, and the capability to perform cell culture on this device has been demonstrated. Finally, the integrated combinatorial mixer has successfully been used to expose cells to different combinations of compounds.

3.2 Experimental

3.2.1 Chip Design

Figure 3-1 shows the device design layout. In essence, the device has an array of culture chambers, where cells will be grown, and an integrated combinatorial mixer, which delivers different solution combinations to the culture chambers. The array consists of 8 individually isolated micro culture chambers with cell loading inlets that enable cell introduction into the culture chambers. Each culture chamber also has an outlet so fluidic samples can be collected. The chamber dimensions are L 1500 μm × W 700 μm × H 32 μm. The chamber height of 32 μm is tall enough to accommodate a wide range of mammalian cells, as many of them have height around 10 μm. The device has a combinatorial mixer with three inputs, and the combinatorial mixer recombines those

inputs into the seven possible outputs. For example, compounds A, B, and C, will be recombined into A, B, C, A+B, A+C, B+C, and A+B+C. Note that one control channel that receives an unmixed input stream is also included as the 8th output. One key feature of the chip is the overpass structure that allows one microfluidic channel to cross over other microfluidic channels, and such fluidic network component makes the combinatorial mixer possible. Solutions containing different compounds will be injected into the chip via the fluid inlets of the combinatorial mixer, and the outputted combinatorial streams will flow into the culture chambers.

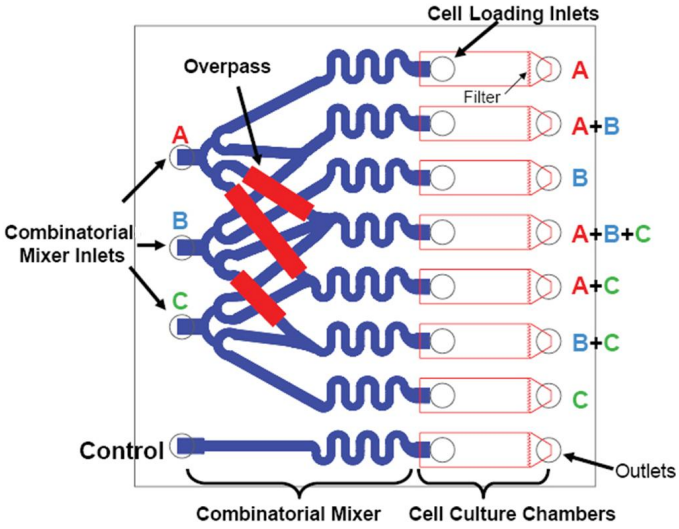

Figure 3-1. Layout of the device design showing the components of the 1 cm × 1 cm chip.

The device is realized by the surface micromachining of Parylene C (poly(chloro-p-xylylene)). Several of the beneficial properties of Parylene C make it an ideal material for both 3-D microfluidic fabrication and constructing a cell culture and cell-based assay device. Parylene C is compatible with lithographic CMOS/MEMS fabrication processes and our previous work has reported that multiple layers of Parylene C can be deposited and patterned to build complicated mechanical structures. This will allow our 3-D

microfluidic device to be monolithically fabricated, favorably avoiding the multilayer bonding process. Another aspect of this device is the ability to culture cells on-chip and Parylene C is suitable for this purpose. Because Parylene C has been shown to be biocompatible and resistant to corrosive body fluids, it was used in many implantable devices [35, 36]. Long-term cell culturing using Parylene C devices have been demonstrated [81]. Also, Parylene C is chemically inert and stable toward many organic solvents [34]. In addition, Parylene C is transparent in the visible range and this will allow cells to be easily observed with light microscopy. All these valuable properties of Parylene C make it the material of choice for fabricating our device.

3.2.2 3-D Microfluidic Fabrication

The device has two levels of microfluidic channels, and its five-mask fabrication process is shown in Figure 3-2. The 3-D rendition of the process flow is also included to aid visualization. The first-level channels were initially deposited, followed by the deposition of the overpasses and culture chambers. The device was fabricated using our developed Parylene surface micromachining technology: alternating layers of Parylene C and sacrificial photoresist are deposited, and the sacrificial photoresist between two layers of Parylene defines the channel. After the photoresist is removed, the remaining hollow Parylene structures become the fluidic networks of the chip.

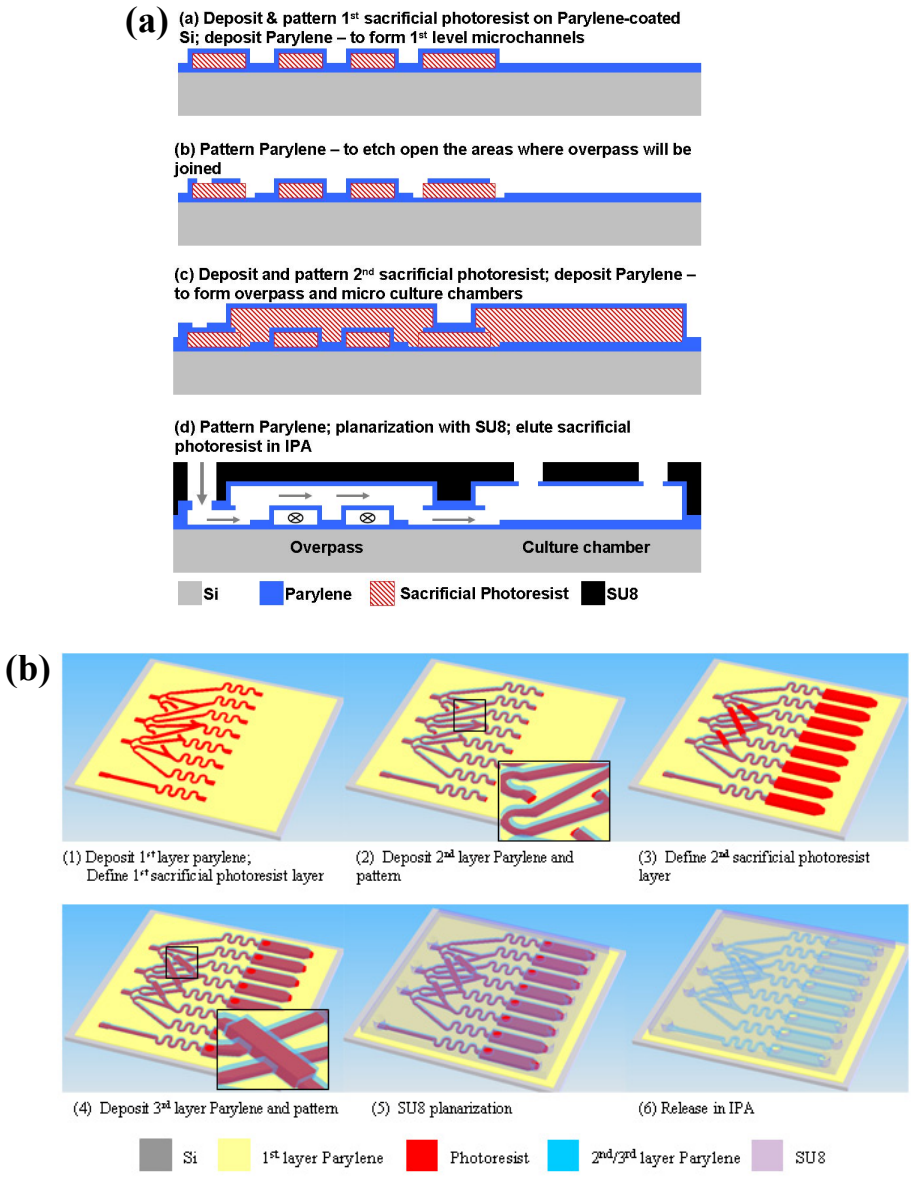

Figure 3-2. The monolithic fabrication process for making the three-dimensional microfluidic networks. (a) Cross sectional view of the fabrication process flow. (b) Three-dimensional rendition of the fabrication process flow. Inserts in (2) and (4) show how the overpass is made by first etching open the Parylene and joining the two etched regions with the 2nd sacrificial photoresist.

The detailed fabrication process can be broken down into the following steps.

First layer Parylene coating. Before any processing, the silicon wafer was cleaned with Piranha solution (H_2SO_4: H_2O_2, 3:1) at 120°C for 5 min. The wafer was then soaked in 0.5% silane A-174 (gamma-methacryloxy-propyltrimethoxysilane, Specialty Coating

Systems, Indianapolis, IN) solution (DI water: isopropyl alcohol: A-174, 100:100:1) for 15 minutes to promote the adhesion between the substrate and Parylene C. The Piranha treatment not only cleaned the surface, but also oxidized the substrate surface. The oxidized surface facilitated the binding of the adhesion promotion A-174 molecule onto the surface. The chemical structure of the A-174 silane coupling agent follows the general structure of silane-based coupling agents: RnSiX(4-n). R is the nonhydrolyzable organic moiety that binds to the coating polymer, which is Parylene C in our case. The X represents alkoxy moieties, and is methoxy in A-174. During the treatment, the methoxy group is hydrolyzed to methanol, forming hydroxyl group that can form hydrogen bonding with hydroxyl group on the substrate. Eventually, covalent Si-O bonding is formed in between the substrate and the coupling agent [82]. The other side of the silane molecule serves to grab onto the Parylene molecules to promote the adhesion onto the surface. After the treatment, a first thin adhesion layer of Parylene C was deposited (3 μm) to cover the entire wafer with a Cookson Electronics PDS 2010 system (Specialty Coating Systems, Indianapolis, IN). The subsequent deposited Parylene layers in the following processes are attached to this first Parylene layer instead of the silicon substrate and this is important because Parylene adhesion to silicon without proper treatment can be very weak. A-174 adhesion promoter cannot be applied for the subsequent Parylene depositions because when there are photoresist patterns on the substrate, isopropyl alcohol inside the treatment solution will quickly dissolve the photoresist.

First layer channel. The first sacrificial photoresist layer (AZ4620 from Clariant, Charlotte, NC) was spin-coated (15 μm) and patterned with photolithography to define the first-level channels. The sacrificial photoresist was hard baked at 120^{o}C for 6 hours.

To promote adhesion of the next Parylene layer to the first Parylene layer, the surface was roughened using oxygen plasma and cleaned with 5% HF for 30 seconds. A second layer of Parylene C (10 μm) was then deposited to cover the sacrificial photoresist to form the first-level channels.

Parylene patterning. Parylene C was patterned using oxygen plasma so the areas where the overpass structures would be joined were exposed. This Parylene patterning also opened the area where the mixer and the culture chamber would be connected. To pattern the Parylene, metal mask was used because oxygen plasma can also etch photoresist at a rate comparable to Parylene etching, so a very thick photoresist would have to be used. Also, when striping the masking photoresist, the sacrificial photoresist can be partially dissolved and this can lead to debris clogging the channel or trapped air expanding and destroying the channel during subsequent thermal processes. Cr/Au (200/2500Å) layer was deposited using an e-beam evaporator. To pattern the metal, a 15 μm AZ4620 photoresist was patterned on top of the metal, and the metals were etched using Au etchant type TFA (potassium iodide (KI) + iodine (I_2)) (Transene, Danvers, MA) and CR-7 Cr etchant (9% ceric ammonium nitrate + 6% perchloric acid in water) (Cynateck, Freemont, CA) . The photoresist was stripped using acetone. The Cr/Au metal layer was then used as an etch mask for Parylene patterning in oxygen plasma. The metals were stripped after Parylene patterning.

Second layer channel. A second sacrificial photoresist was spin-coated (32 μm) and patterned to define the overpass structures and the culture chambers. This second sacrificial photoresist covered the etched open areas, and the overpasses spanned several of the first-level microfluidic channels. A third layer of Parylene C (10 μm) was

deposited after the same adhesion promotion treatment procedure as described in previous steps. This Parylene was patterned using metal as mask and oxygen plasma etching.

SU8 planarization and chip release. The whole chip was strengthened and planarized with patterned 100 μm SU8 (MicroChem, Newton, MA) to facilitate the following packaging of the chip. The wafer was diced to yield chips with dimensions of 1 cm × 1 cm. Finally, the chips were soaked in 65^{o}C IPA (isopropyl alcohol) to dissolve the sacrificial photoresist in about one week.

3.2.3 Device Packaging and Fluidic Testing

A packaging scheme was developed to make the fluidic connections with the chip as shown in Figure 3-3. A slab of cured PDMS (4 mm thick) (Sylgard 184, Dow Corning, Midland, MI) with punched holes was aligned onto the chip. The PDMS and the chip were clamped together by two pieces of transparent acrylic that were milled with a computer-numerical-controlled (CNC) machine. The PDMS acted both as a gasket layer to provide proper sealing and as an adapter to connect the tubes. Syringes were connected with Teflon tubes, which had metal hollow tube (0.025 inch OD × 0.013 inch ID × 0.250 inch length) (New England Small Tube, Litchfield, NH) inserted at one end, and plugged into the ports of the piece of PDMS. Depending on different fluidic operations on the same device, the holes of the PDMS piece can be adjusted as open or blocked at different places to either open or close certain access holes on the chip.

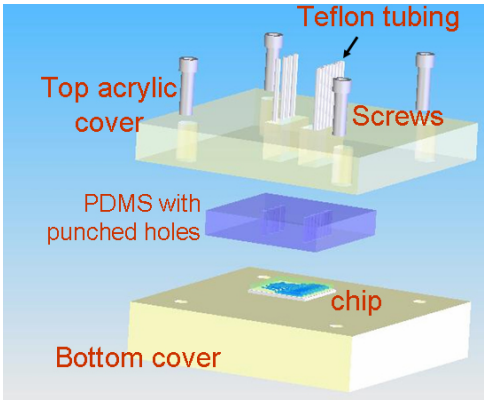

Figure 3-3. Schematic representation of the packaging method for making fluidic connection.

To solely test the combinatorial mixer on the fabricated device, the chip was packaged with holes open at the combinatorial mixer inlets and outlets, while the cell loading inlets were closed as illustrated in Figure 3-4. Green, red, and blue food coloring solutions were injected into the three inputs of the combinatorial mixer, and yellow food coloring was delivered into the control channel. Arrows in Figure 3-4 show that two fluid streams are separated spatially at the overpass region and flow in two different directions (→ and ⊗). The food coloring solutions were loaded into syringes and the flow rate was controlled by programmable syringe pumps (Harvard Apparatus, Holliston, MA). Pictures of the experiment were taken with a stereoscope equipped with a CCD camera (Diagnostic Instrument, Sterling Heights, MI).

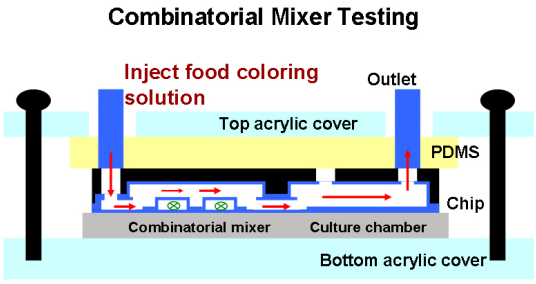

Figure 3-4. Chip packaged for testing the combinatorial mixer.

3.2.4 Testing Parylene C as Suitable Substrate for Cell Culture

Tests were first performed to verify that Parylene C is a biocompatible substrate for our specific cell culture. Three culture substrates were used in this experiment: (1) unmodified standard polystyrene petri dish (VWR Scientific, West Chester, PA), (2) petri dish coated with Parylene C, (3) petri dish coated with Parylene C and pretreated with 0.05% polyethyleneimine (PEI) in borate buffer solution. For samples (2) and (3), 5 μm Parylene C was deposited on 60 mm polystyrene petri dishes. Some petri dishes were further treated with 0.05% PEI solution for 24 hours, followed by rinsing with PBS three times before culturing. PEI solution has been shown to enhance cell adhesion to culture substrates [83]. B35 rat neuroblastoma cells were purchased from ATCC (Manassas, VA), and cultured in Dulbecco's Modified Eagle's Medium (Invitrogen, Carlsbad, CA) with 10% fetal bovine serum and 1% penicillin/streptomycin/amphotericin B. To assess the growth rate of cells on the different substrates, B35 cells were seeded onto the 60 mm petri dishes at an initial concentration of 6×10^4 cells mL^{-1} and the cell concentrations were recorded again 24 hours after cell seeding. The cell growth rate was modeled using the exponential model: $N(t) = N_o \times \exp(\mu t)$, where N is the cell concentration, N_o is the initial cell concentration, t is the culturing time and μ ($hour^{-1}$) is the specific growth rate. By culturing the cells through certain duration, t_f, and measuring the starting and final cell concentration, N_o and N_f, the specific growth rate, μ ($hour^{-1}$), can be derived as $\mu = \ln(N_f/ N_o)/ t_f$.

3.2.5 Microfluidic Cell Culture

Cell culture was done on-chip to test if the Parylene-based culture chamber can sustain cell growth. B35 rat neuroblastoma cells were cultured in 100 mm × 15 mm

polystyrene petri dishes and passaged every two to three days. The cells were maintained in Dulbecco's Modified Eagle's Medium with 10% fetal bovine serum and 1% penicillin/streptomycin/amphotericin B, and incubated in 5% CO_2 at 37°C. Cells were cultured on the chip using the following method. To culture the cells inside micro culture chambers, we assembled the device packaging with the cell loading inlets and outlets open, as shown in Figure 3-5. Before loading the cells onto the chip, the chip was sterilized by UV irradiation in addition to treatment of all the fluidic channels and culture chambers with 70% ethanol solution. After the ethanol solution was rinsed out with phosphate buffered saline (PBS) solution, the culture chambers were treated with 0.05 % polyethyleneimine (PEI) in borate buffer solution for 24 hours to enhance cell adhesion to the culture chamber. The PEI solution was subsequently rinsed out with PBS. Cells were suspended from petri dishes and delivered into the culture chambers with a syringe. The cells were allowed to settle and attach to the culture chamber surface for four hours. With the flow rate controlled by syringe pumps, cells were cultured with continuous perfusion of culture media at the flow rate of 33 nL min^{-1}. During the culture experiment, the device was kept inside an incubator that was set at 37°C and 5% CO_2. Cell growth was monitored periodically with a Nikon E800 upright microscope.

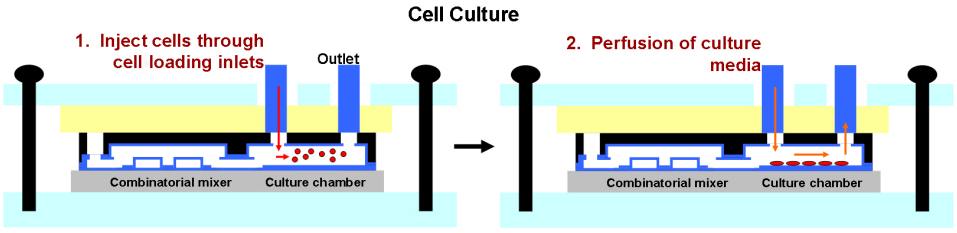

Figure 3-5. Schematics showing the device operation procedure for the on-chip cell culture experiment.

3.2.6 Integrated Combinatorial Mixer for Cell Treatment

A straightforward experiment was performed using the integrated combinatorial mixer for cell treatment. The device was assembled with all the inlets and outlets open, as shown in Figure 3-6. Cells were injected into the culture chamber following the same procedure as in cell culturing. After the loaded cells attached to the chamber surface, we injected three different cell staining solutions: 0.005% w/v crystal violet, 0.016% w/v neutral red and 0.01% w/v methylene blue through the combinatorial mixer channels. Crystal violet solution (0.5% w/v crystal violet with 10% ethanol and 0.8% ammonium oxalate) and methylene blue solution (1% w/v in water) were purchased from The Science Company (Denver, CO) and neutral red solution (neutral red 1.0 g/L, acetic acid 2 mL/L in water) was purchased from Sigma-Aldrich (St. Louis, MO). The cell staining solutions were diluted to the indicated concentration with phosphate buffered saline (PBS) solution. No fluid was injected into the control channel. The stain loading was controlled by syringe pumps and was set at 30 μL min^{-1} for a duration of 10 minutes. Pictures of each culture chamber were taken 30 minutes after the flow was stopped. With the above operation, cells in different culture chamber received different combination of stains, and the cells in the control chamber did not receive any staining solutions.

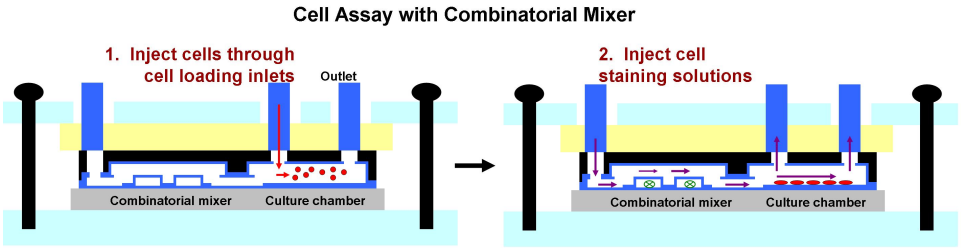

Figure 3-6. Schematics showing the device operation procedure for cell assay with combinatorial mixer.

3.3 Results and Discussion

3.3.1 Device Fabrication and Combinatorial Mixer Testing

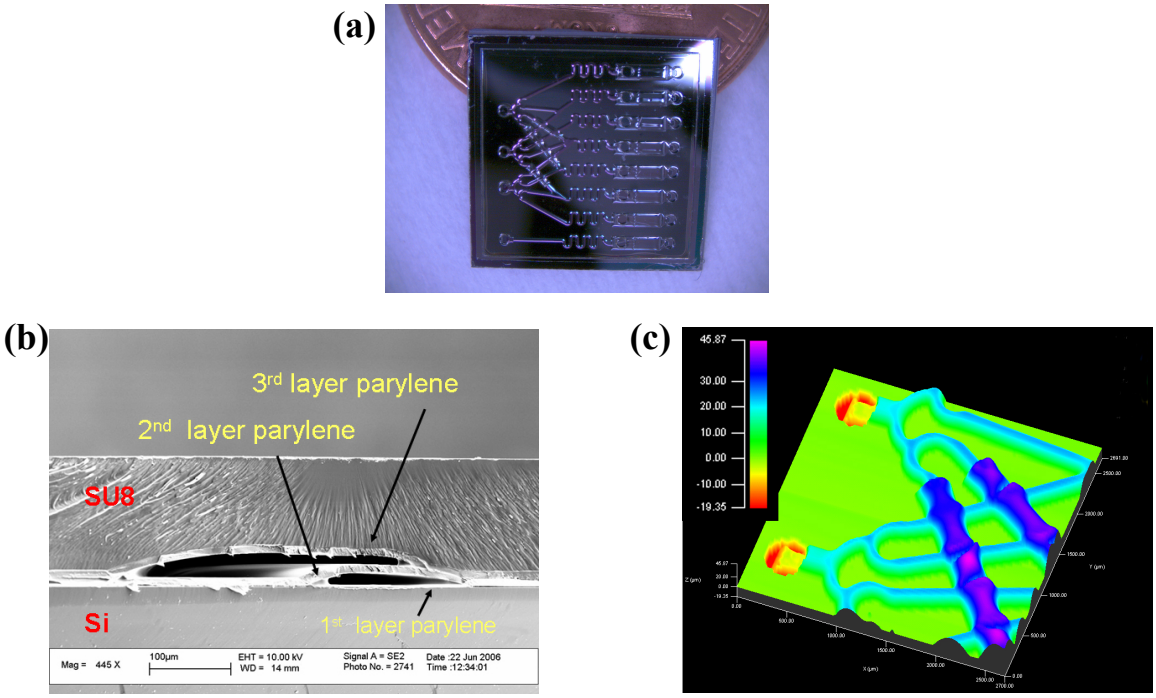

Figure 3-7. Monolithically fabricated microfluidic cell culture array with an integrated combinatorial mixer. (a) Fabricated 1 cm × 1 cm chip. (b) SEM image of the cross section of the microfluidic overpass. The overpass has two-level microfluidic channels and such structures will allow two fluidic streams to be separated spatially at the overpass. (c) Surface height profile scan of the overpass region before SU8 planarization. The overpass structure is about 15–20 µm higher than the first-level microfluidic channels.

Figure 3-7(a) shows the fabricated chip having a dimension of 1 cm × 1 cm with a thickness of approximately 672 µm. One characteristic of monolithic fabrication is that it yields devices which are typically thinner than devices fabricated using multilayer bonding process. Both Parylene and SU8 are transparent and experiment can be easily observed with a microscope from the top side of the chip. It is also possible to release the device from substrate by either adding a sacrificial photoresist before the first layer Parylene deposition or skipping the A-174 adhesion promotion step and the chip will

separate from the substrate after soaking in acetone [84]. This will result in a thin and flexible microfluidic device and the flexibility can be useful for implanting devices into animal or human bodies.

By using the bi-level sacrificial photoresist process, channels of different heights (15 and 32 μm) were successfully created. This enables overpass to be created and allows the higher microfluidic channel to cross over the shallower microfluidic channel. We examined the fabricated microfluidic overpass by taking SEM images of the cross section of the overpass structures. Figure 3-7(b) shows the two-level microfluidic channels and such a structure could allow two fluidic streams to be separated spatially at the overpass region. The microfluidic channels are semi-circular in shape because the sacrificial photoresist was hard baked. The adhesion promoter, silane-based A-174, led to a strong adhesion of the first layer Parylene to the substrate. The subsequent Parylene adhesion was strengthened by roughening the surface using oxygen plasma to increase the effective bonding area and a thorough cleaning with HF to ensure a contaminating-free surface. The SU8 further strengthened the bonding of the underlying Parylene layers to the substrate. As a result, the chip was able to withstand release in isopropyl alcohol without delamination. The SU8 also planarized the surface so sealing material such as PDMS gasket layer or o-rings can be placed directly onto the chip surface without destroying the delicate microchannels. Figure 3-7(c) shows the surface profile scan (P-15 stylus profilometer from KLA-Tencor, San Jose, CA) of the overpass structure before SU8 planarization, and it shows that the overpass structure is about 15 μm higher than the first-level microfluidic channels. This monolithic fabrication has allowed us to fabricate our chips without additional multilayer bonding. It is possible to create combinatorial

mixer with even more inputs and outputs by following the same fabrication steps. Additional overpasses can be placed in to accommodate the routing of the microchannels. This is similar to laying down all the wires in a basic circuit diagram that numerous wires can be drawn on a 2-D space by using the cross over symbols. The successful development of this method lays the foundation to build more complicated 3-D microfluidic devices.

Our proof-of-concept combinatorial mixer was able to take in the three input streams of food colorings (red, green, and blue) and generated the seven possible combinations, as shown in Figure 3-8. The input flow rate of the food coloring injection was controlled by syringe pumps and experiments at two different flow rates were shown. The control channel received only the yellow food coloring that was not mixed with any other solutions. Figure 3-8(a) shows the assembled device with appropriate tubes plugged in, and our scheme of packaging has worked without any fluid leakage. This packaging method is uncomplicated as the PDMS slab can be quickly prepared in-house and holes be readily punched in. Only a simple rectangular pattern has to be machined on the acrylic to provide access spaces for the tubes. Plugging Teflon tubes into PDMS ports has been standard in various PDMS microfluidic devices. This packaging scheme is suitable for cell-based application as no high pressure environment will be required. If high operating pressure is required (>100 psi), plugging tubes into the PDMS will not hold at such pressure, and other packaging scheme has to be used. One packaging method is to use o-rings or gaskets and machined manifold to connect to high pressure fittings [44]. Figure 3-8(b) and Figure 3-8(c) show that the overpass structures enable one fluidic stream to flow over several other microchannels. In microfluidic devices, the

Reynolds number is usually low so the fluid flows at micro scale are laminar. As a result, mixing occurs by diffusion alone and flow rate becomes an important factor that affects the homogeneity of the mixture.

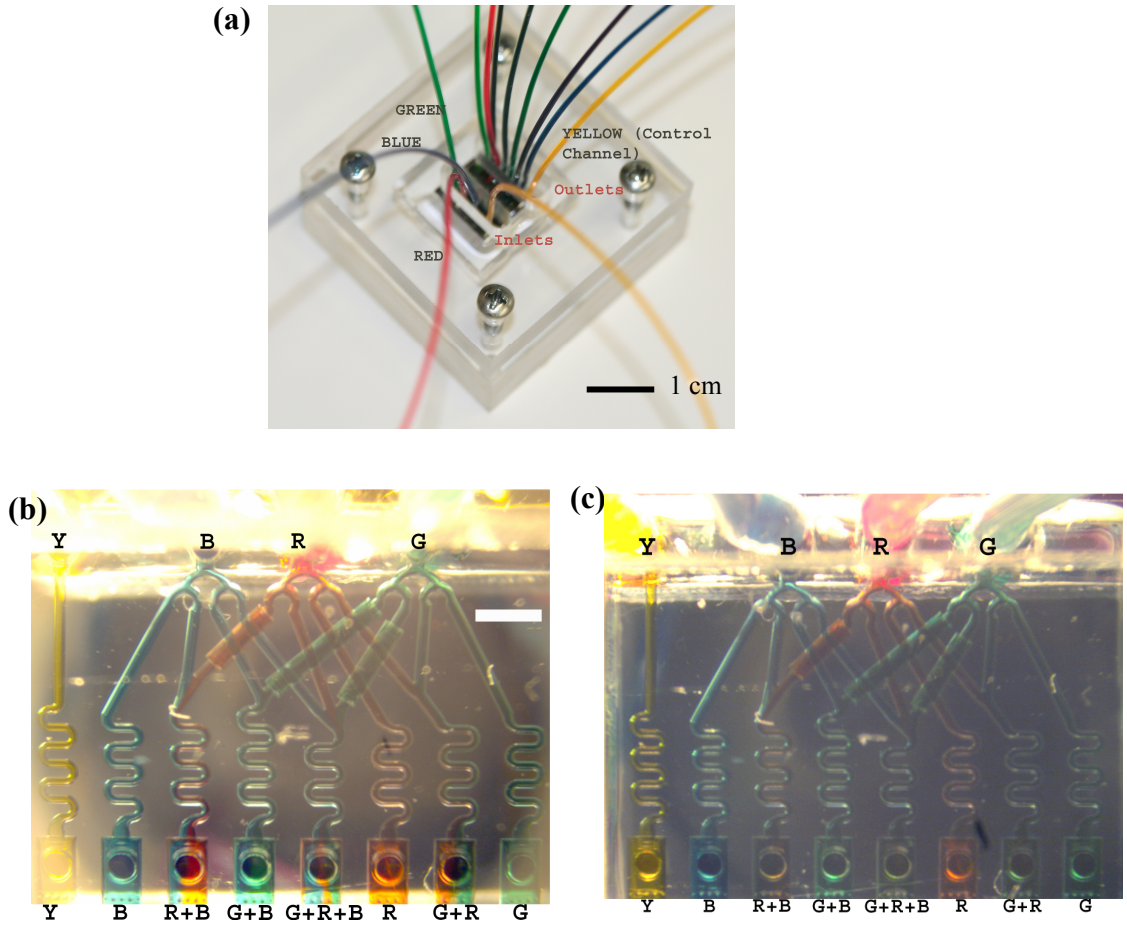

Figure 3-8. Combinatorial mixer demonstration. (a) Assembled device with food coloring being injected. Green (G), red (R) and blue (B) food coloring solutions are injected into the combinatorial mixer inlets, while the yellow (Y) food coloring solution is injected into the control channel. Combinatorial mixer operated at two flow rates: (b) 10 μL min^{-1}, (c) 0.1 μL min^{-1}. The scale bar represents 1 mm.

Figure 3-8(b) shows the combinatorial mixer at an input flow rate of 10 μL min^{-1}, and the stripes from the input streams of food coloring solutions are still visible at the end of the serpentine channels. However, even though the mixture is not homogeneous, the correct combinations of fluid streams are still generated. Figure 3-8(c) shows the

combinatorial mixer at lower flow rate, 0.1 μL min^{-1}, and as flow rate goes down, molecules have more time to diffuse across the channel for better mixing. At the flow rate of 0.1 μL min^{-1}, the stripes of the input fluid streams are no longer visible at the end of the serpentine channel. One can understand this effect conceptually by considering a T-junction mixer with two fluid streams flowing alongside each other. The time, t, for a molecule with diffusion coefficient, D, to diffuse across a channel with width w, can be estimated as $t \sim w^2/D$. With a fluid velocity of U, the molecule will travel down the channel with a distance Z during that time period, and $Z \sim Uw^2/D$ [74]. This expression indicates that as flow rate increases, the stripes will travel longer distances before they are completely mixed with each others. The serpentine channel helps mixing by giving the molecules more time to diffuse across the channel before they reach the outlet.

Our fabrication method offers the opportunity for scaling up the number of inputs for the combinatorial mixer. More inputs can be incorporated using the same method of first laying down the first-level channels, followed by the making of the overpasses. As a result, even when the number of inputs and outputs increase, the complexity of fabrication does not increase substantially. In addition, a combinatorial mixer with a diluter can be fabricated using the same fabrication process. Typical biological assays often include multiple dilutions of compounds to assess the concentration-dependent cellular responses to certain compounds. To realize such a device, we can incorporate a concentration gradient generator into each of the inputs, and each of the input streams will be diluted into sub-streams with different concentrations. Those streams of dilutions can be recombined in 3-D microfluidic networks, which can be constructed using the same method as our current fabrication process.

3.3.2 Parylene C as a Substrate for Cell Culture

The cell chamber of the chip is composed of Parylene C and we performed a biocompatibility testing to verify that cells can grow properly on Parylene C surfaces. B35 rat neuroblastoma cells were grown on three different substrates: (1) unmodified standard polystyrene petri dish, (2) petri dish coated with Parylene C, and (3) petri dish coated with Parylene C and pretreated with 0.05% polyethyleneimine (PEI) solution. The cell growth rates on the prepared substrates are plotted in Figure 3-9. The result shows that the growth rates on all three substrates are similar. The growth rate on untreated Parylene appeared to be slightly lower and this can be due to the lack of proper cell anchoring to the substrate. PEI is consisted of many positively charged amine groups and can help attract the negative charged surface molecules on the cell membrane. These results show that Parylene C is a biocompatible substrate for cell culturing and is a suitable material for constructing micro culture chambers. Other types of cells such as hippocampal CA1 and CA3 pyramidal cells, NIH-3T3 fibroblasts and AML-12 hepatocytes have also been shown to grow on Parylene C substrate [81, 85].

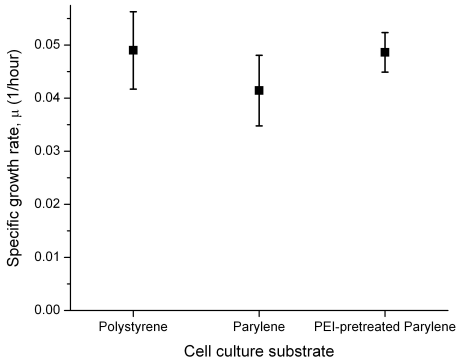

Figure 3-9. B35 cell growth rates on three different substrates: (1) unmodified standard polystyrene petri dish, (2) petri dish coated with Parylene C, (3) petri dish coated with Parylene C and pretreated with 0.05% polyethyleneimine (PEI) in borate buffer solution before cell seeding. Results are the means ± standard deviation (SD). (n = 3).

3.3.3 Microfluidic Cell Culture

Cell culture inside the micro culture chamber was performed using B35 rat neuroblastoma cells to test that the microfluidic chip could sustain cell growth. The culture chamber was treated with PEI solution to enhance cell adhesion before cell seeding. Cell suspension was delivered into the chip with a syringe and a static condition was followed to allow the cells to adhere to the surface. This step is important that without proper cell adhesion to be made to the surface, the cells would flow away when a flowing condition is introduced. The cells were grown with a continuous perfusion of media at 33 nL min^{-1} inside a 37^{o}C incubator. At this flow rate, the content of the culture chamber was turned over at approximately once every minute so cells would not be deprived of nutrients. Gas can pass through the PDMS, which is highly permeable to oxygen (diffusion constant, $D = 3.4 \times 10^{-9}$ m^2 s^{-1}) and enter the chip via any of the access holes on-chip. Figure 3-10 shows finite element analysis of oxygen transport using the combined transient diffusion/convection model and incompressible Navier-Stokes model in Comsol Multiphysics (Comsol, Burlington, MA). The culture media flows in through the inlet at 2×10^{-6} m/s and the oxygen can enter through the PDMS. The fluid velocity profile was solved first and the stored solution was used to solve for the concentration profile in the diffusion/convection module. The diffusion constant of oxygen in water is 2.1×10^{-9} m^2 s^{-1}. Result shows that oxygen can readily pass through the PDMS and enter the culture chamber.

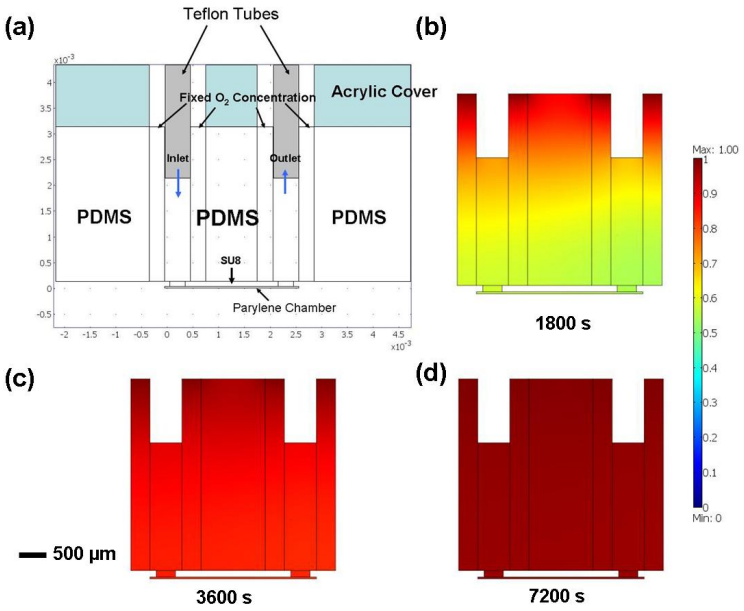

Figure 3-10. Simulation of oxygen transport through the PDMS into the chamber. (a) Configuration used for the simulation. Fluid is delivered from the inlet and the oxygen can enter through the PDMS. Oxygen concentration at various times: (b) 1800 s, (c) 3600 s, and (d) 7200 s.

Figure 3-11 shows that cells proliferated inside the micro culture chambers and eventually reached confluency after 42 hours of culturing. The calculated cell growth rate was 0.018 hr^{-1}. This study shows that cells can be sustained inside the Parylene C microfluidic cell culture chambers.

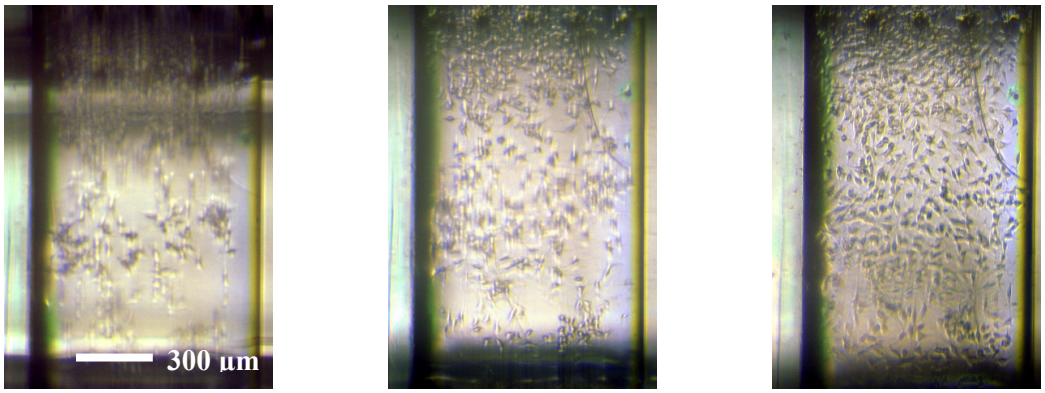

Figure 3-11. Cell culture inside Parylene C micro culture chamber.

3.3.4 Integrated Combinatorial Mixer for Cell Treatment

The combinatorial mixer was used to perform a cell treatment and the result is shown in Figure 3-12. The chip was first packaged with all of the access holes open, and the device was operated as shown in Figure 3-6. B35 cells were seeded by injecting them through the cell loading inlets of individual chambers, and the cells attached to the culture chamber surface after four hours. Following cell adhesion, three cell stains, crystal violet, methylene blue and neutral red were injected through the combinatorial mixer inlets, while no solution was injected into the control channel. The combinatorial mixer recombined the input streams and simultaneously delivered the various combinatorial streams into the cell culture chambers. Cells in different culture chambers received different combinations of the stains and were stained with different color patterns, while the cells in the control chamber were unstained. This experiment shows that we can use the on-chip combinatorial mixer to simultaneously interrogate individual culture chambers, and each group of cells inside the different culture chamber received different inputs and showed distinct responses. Eight different combinatorial conditions were created simultaneously, saving the extra pipetting steps. This preliminary study lays the foundation to perform experiments with longer duration and enhanced complexity involving cell growth under continuous perfusion of different combinatorial culturing solutions. Besides monitoring cell growth, more complicated cellular response or signal pathways such as gene expression can be studied on the current chip by integrating existing biological technologies. Real-time monitoring of gene expression on microfluidic chips has been demonstrated using a fluorescent transcription reporter, and

we can monitor the cellular response using similar methods by loading transfected cells into the culture chamber [70].

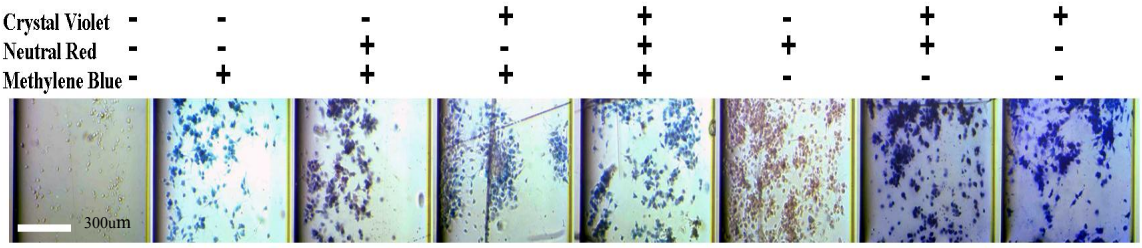

Figure 3-12. Cell treatment using the integrated combinatorial mixer.

3.4 Conclusion

In this chapter, we presented a monolithic fabrication technology of an integrated combinatorial mixer for cell assay, and showed the ability to simultaneously treat arrays of cells with different combinations of compounds. Our fabrication method enables devices to be conveniently fabricated at the wafer scale. Fabricated using a scalable five-mask process with Parylene C as the structural material, the device can simultaneously provide eight combinatorial medium outputs to study cell cultures. The microfluidic overpass structure allows one microfluidic channels to cross over other microfluidic channels, and using similar fabrication process, the number of inputs and outputs of the combinatorial mixer can be scaled up for high-throughput cell-based assay. Such device can efficiently collect large quantities of information pertaining to cyto-regulation and elucidate combinatorial effects of multiple compounds on cells. Furthermore, our fabrication technology can enhance the functionalities of current lab-on-a-chip devices by integrating the devices with complex 3-D microfluidic networks. The fruition of such

system will enable lab-on-a-chip devices to perform highly parallel and combinatorial chemical or biochemical reactions with reduced labor, reagents, and time.

Chapter 4: Combinatorial Cell Assay Device on Glass with Membrane-Based Cell Culture Chamber

4.1 Introduction

With the successful development of the monolithic fabrication of 3-D microfluidic networks, the next step is to improve device design to facilitate cell-based assay on-chip. One of the improvements is to simplify the experimental procedure and make the device more user-friendly. Microfluidic devices are often complicated to fabricate and it is important to make them easy to use for end users. Also, most modern cell culture and assay platforms such as multi-well plates are based on transparent substrates such as glass or polystyrene plastics, and it would be ideal to construct microfluidic devices based on glass. Finally, it would be advantageous to improve the cell culture chamber design to mimic the *in vivo* cellular microenvironment.

While there have been a plethora of microfluidic cell culture and assay devices being created, many of them did not take full advantages of microfluidic-based systems. One advantage that microfluidic offers over traditional culture container such as petri dish is the ability to control the cellular microenvironment. Micro scale devices have characteristic length scale of 0.1–100 μm, which is the same as the microenvironment that the cells reside in. Therefore, microfluidic device has the ability to create culture environment that mimics the *in vivo* microenvironment and provide assay results that can be more biologically relevant than tradition culture platforms. The cell microenvironment is comprised of several complex factors. One important parameter in cell microenvironment is fluid flow as it provides a way to transport important factors

such as nutrients, wastes, oxygen, and various soluble factors to and from cells. Depending on the cell locations, different cells are exposed to different range of flow rate inside our body. Endothelial cells lining the wall of aorta can experience flow rate up to as much as 300,00 μm/s, while interstitial flow at the capillary level is at 0.1–1 μm/s range [86]. Microfluidic devices have been created to study the influence of shear stress on cells and the laminar nature of the microfluidic flow and the ability to easily control flow and monitor cell behavior simultaneously have made microfluidic device very suitable for such studies. While certain cells require constant shear stress to prosper, it is important to note that high shear stress level can be detrimental to certain cell types [68]. This is an especially important aspect to be considered during microfluidic cell culture design as perfusion will inevitably introduce shear stress to cells and most microfluidic cell culture devices utilize perfusion to deliver nutrients and other soluble factors to the cells.

While cells such as endothelial cells that line the wall of blood vessel are directly exposed to fluid flow and share stress, most cells inside the tissues are residing in a space that is shielded from convective flow. Fluid flow inside such environment is minimized while transport is dominated by diffusion [69]. The Peclet number, *Pe*, is the ratio that indicates the relative importance of convection to diffusion and is defined as

$$Pe = \frac{vl}{D}, \tag{4.1}$$

where v is the fluid velocity, l is the characteristic length and D is the diffusion constant. Inside the tissue, the Peclet number is about 0.1 and the shear stress is about 0-2 Pa [69]. While traditional cell culture on flat petri dish or well plate substrate provides a low shear environment for the cells, the cells are subject to very different condition than cellular

microenvironment inside the tissue. The longer length scale and larger volume of the macro scale cultures allow for chaotic flow. While this allows for better mixing, it can disturb soluble factor patterns that can only be established with laminar flow. Another significant difference is that cells inside the tissue reside in a 3-D environment and can receive fluid from both top and bottom sides of the cells. Cells cultured on a flat substrate are limited to only receive extracellular factors from one side. Microfluidic technology can address those problems and create culture space that has precisely controlled flow conditions and better mimics the *in vivo* microenvironment.

While the potential utility of microfluidic devices is clear, there are various barriers that can present challenges for microfluidic devices to be adopted by biologists. Some issues that have to be addressed are the ease of use and integration with current laboratory equipments and techniques. It is important that the device design does not involve excess complexity and be suitable for the end users to operate. Our first-generation chip described in the pervious chapter has some improvements that can be made. The device was fabricated on silicon substrate and this can make it difficult for observation under microscopy. Such setup requires light to be illuminated from the same side as the objective for imaging the device, but many microscopes have light source on the opposite side of the objective. Also, the fluids are delivered from the top side because using patterned SU8 and etched Parylene as open ports is simpler for fabrication than performing through-wafer etching for ports from the bottom side. However, because such setup requires tubes to be plugged in from the top side, the overall device thickness is increased and a long working distance objective has to be used. This also limits the resolution of the objectives that can be used as high resolution objectives generally have

short working distance. Therefore, using a glass substrate for the device would be more ideal and imaging can be performed with minimal fluorescence interference. Proper cell-based assay can be designed so the readout can be done directly on-chip to simplify the experiments.

Another possible area for improvement is the cell loading procedure. The first-generation chip required channel walls to be treated with adhesion promoting factors before cell loading. Also, the cell loading was not very efficient as many cells were flushed through the channel before enough cells were captured inside the culture chamber. Furthermore, the previous design required that cells be loaded into each chamber separately. While doing so only required relatively short amount of time because only eight chambers were included on that chip, this can be a significant problem when the device is scaled up to include more chambers. It would be ideal to design a chip that incorporates an efficient and user-friendly cell loading process.

In this chapter, the development of 3-D microfluidic networks on glass substrate for cell-based assays with multiple combinations of compounds is presented. The final assembled device is composed of a porous membrane integrated in between a multilayer Parylene 3-D microfluidic chip and a PDMS microfluidic chip. The methods to improve cell loading efficiency and to simplify the cell loading procedure are demonstrated. The culture chamber incorporates a bi-level design to mimic the cellular microenvironment *in vivo* where the cells reside in a diffusion dominated space separated from convection dominated blood vessels. In our previous chapter, we have discussed the method to monolithically fabricate three-dimensional (3-D) microfluidic networks on silicon substrate. The developed fabrication process was based on the surface micromachining

of Parylene C (poly(chloro-p-xylylene)) and eliminated the need for the bonding steps as in many other multilayer microfluidic devices. The device presented in this chapter is fabricated based on the extension of such procedure. We have characterized concentration distribution of each output from the combinatorial mixer by using a fluorescence method. Two quantitative cell-based assays were performed using this device. We cultured rat neuronal cells, B-35, on this device and screened for the ability of three chemicals to attenuate cell death caused by cytotoxic hydrogen peroxide. We also assayed for the combinatorial effects of three chemotherapeutic compound exposures on human breast cancer carcinoma, MDA-MB-231.

4.2 Experimental

4.2.1 Device Design

The schematic of the assembled microfluidic device is shown in Figure 4-1. The device is composed of a porous PET (polyethylene terephthalate) membrane sandwiched in between the two microfluidic chips: a 3-D microfluidic Parylene C (poly(chloro-p-xylylene)) chip with integrated combinatorial mixer, and a PDMS (polydimethylsiloxane) chip with one-to-eight manifold and cell culture chambers.

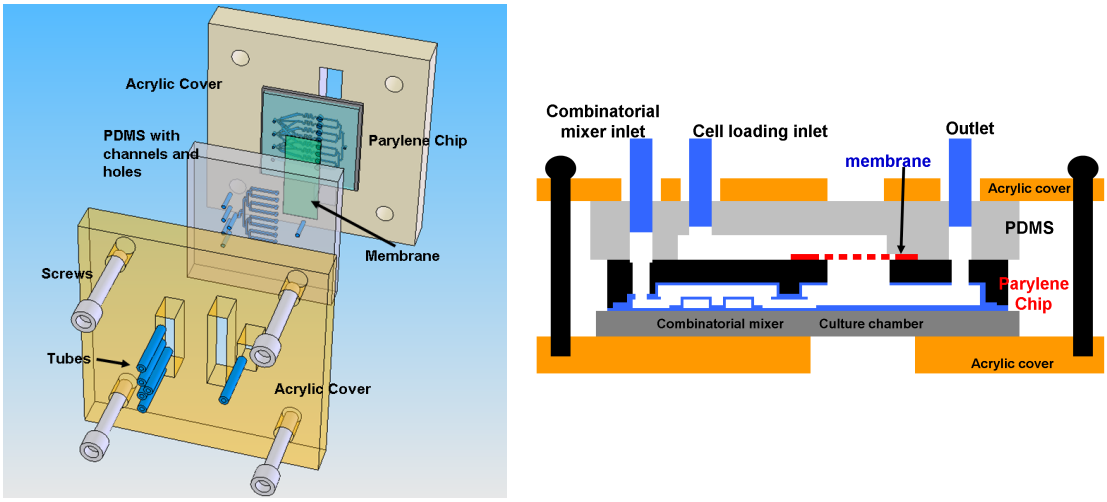

Figure 4-1. Schematics of the microfluidic device. (Left) 3-D rendition of the device before assembly. (Right) Side view of the device.

Figure 4-2 shows the layout of the 1.7 cm × 1.7 cm 3-D microfluidic Parylene-based chip with integrated combinatorial mixer. The combinatorial mixer has three inputs, which are recombined into the seven possible outputs. An unmixed control channel is also included. Like the chip described in the previous chapter, the overpass structure allows one microfluidic stream to cross over other microchannels, and a control channel that receives none of the three inputs is included. Unlike the previous chip, glass wafer will be used as the substrate instead of silicon. The chamber diameter is 1 millimeter. The 3-D microfluidic Parylene chip is consisted of two different layers of microfluidic network, with the bottom 14 µm height channels making up the basic combinatorial mixer channels and the top 25 µm height channels making up the overpasses and the outlet channels.

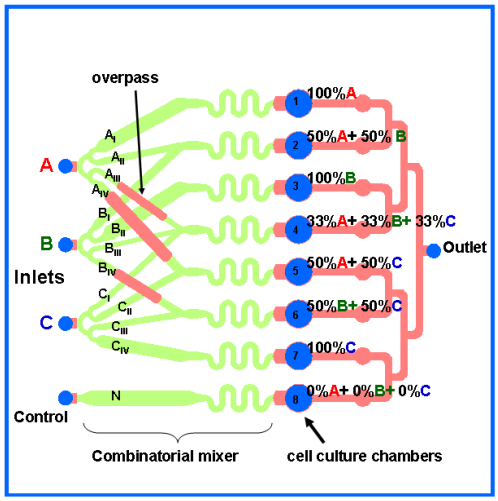

Figure 4-2. Layout of the 3-D microfluidic Parylene-based chip.

Compounds A, B, and C are delivered into eight chambers with different combinations and concentrations, and the concentration of each compound inside the chamber is determined by the fluidic resistance of the channels. As the channel width is much larger than the channel height, the resistance can be modeled using the simplified formula for rectangular channel:

$$R = \frac{12\mu L}{wh^3}. \tag{4.2}$$

R is the resistance, μ is the fluid viscosity, and L, w, and h are the length, width and height of the channel, respectively. Chambers receiving multiple compounds are designed to have equal dilution of the input compounds. For example, chamber 2 is designed to be 50% of input A and 50% of input B so the channel connecting input A and chamber 2 (channel A_{II}) and the channel connecting input B and chamber 2 (channel B_I) would have the same fluid resistance. As the channel heights are the same for all the channels in the combinatorial mixer, the channel widths and lengths are tuned to achieve

the desired flow resistance. The fluidic channels can be represented as network of fluidic resistors and the schematic is shown in Figure 4-3.

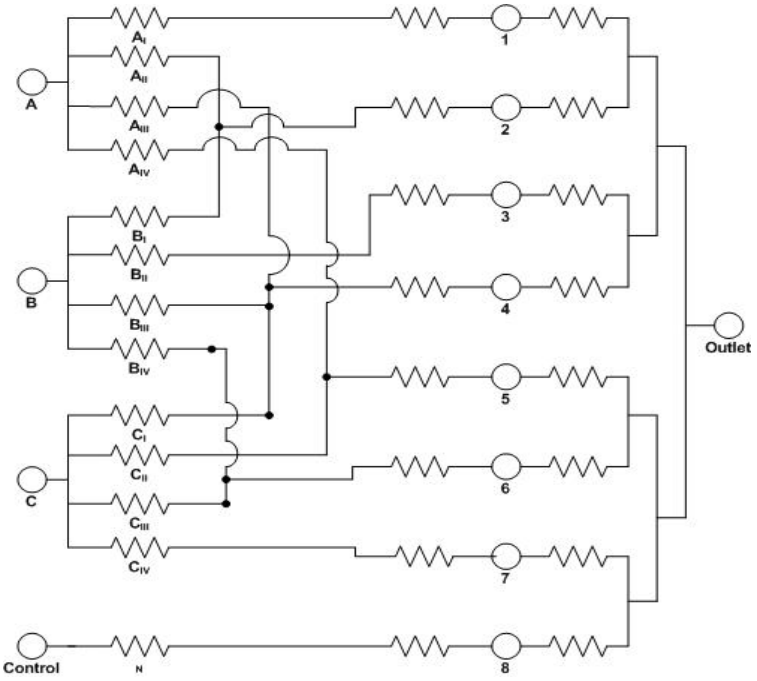

Figure 4-3. Equivalent fluidic resistance network of the chip.

In addition, the fluidic networks are designed so the flow rate into each chamber is the same to prevent variation in shear stress that can affect the cells. This is done by making the combined fluid resistances leading up to each chamber to be the same. Thus, the fluidic resistances of channels, A_I, B_{II}, C_{IV}, and N, which lead to chambers with single compounds, would be the same. The fluidic resistances of channels leading to chambers with two compounds are twice of the fluid resistances of channels leading to chambers with single compounds. For example, channels A_{II} and B_I, which connect input A to chamber 2 and input B to chamber 2, respectively, would have twice the fluidic resistance of channel A_I. The fluidic resistances of channels leading to chambers with three compounds are three times of the fluid resistances of channels leading to chambers with

single compounds. The flow rate, Q is related to the pressure drop, ΔP, and fluidic resistance, R, by the following equation,

$$Q = \frac{\Delta P}{R}. \tag{4.3}$$

With a constant flow rate source (syringe pump) delivering a flow rate, Q_O, into each input, Q_1, the flow rate into chamber 1, which receives a single compound, would be

$$Q_1 = Q_O\left(\frac{1/R[A_I]}{1/R[A_{TOTAL}]}\right). \tag{4.4}$$

$R[A_{TOTAL}]$ is defined by the following equation:

$$\frac{1}{R[A_{TOTAL}]} = \frac{1}{R[A_I]} + \frac{1}{R[A_{II}]} + \frac{1}{R[A_{III}]} + \frac{1}{R[A_{IV}]}. \tag{4.5}$$

R represents the resistance and the name inside the square bracket indicates the specific channel. For example, $R[A_I]$ is the fluidic resistance for channel A_I. The expressions for $R[B_{TOTAL}]$ and $R[C_{TOTAL}]$ follow same expression as equation 4.5.

Q_2, the flow rate into chamber 2, would be the combined flow rate of flow through channel A_{II} and channel B_I:

$$Q_2 = Q_O\left(\frac{1/R[A_{II}]}{1/R[A_{TOTAL}]}\right) + Q_O\left(\frac{1/R[B_I]}{1/R[B_{TOTAL}]}\right). \tag{4.6}$$

As stated above,

$$R[A_I] = \frac{1}{2}R[A_{II}] = \frac{1}{2}R[B_I] = \frac{1}{2}R[A_{IV}] = \frac{1}{3}R[A_{III}]$$

$$R[A_I] = R[B_{II}] = R[C_{IV}] = R[N]$$

$$R[A_{II}] = R[A_{IV}] = R[B_I] = R[B_{IV}] = R[C_{II}] = R[C_{III}]$$

$$R[A_{III}] = R[B_{III}] = R[C_I]$$

$$\frac{1}{R[A_{TOTAL}]} = \frac{1}{R[B_{TOTAL}]} = \frac{1}{R[C_{TOTAL}]}$$

Thus, the two chambers, chamber 1 and chamber 2 would receive the same flow rate of $3/7Q_O$. The designs for all the other channels follow the same principle so the flow rates into all the chambers would be equal and the chambers receiving two or more inputs would have equal flow rate from each of the connecting channels.

Figure 4-4 shows the layout of the 2.5 cm × 2.5 cm PDMS microfluidic chip with 100 μm height channels. It has punched holes that match the locations of the ports on the Parylene microfluidic chip. The PDMS piece also has a cell loading inlet and a one-to-eight manifold that distributes cells or reagents into eight chambers simultaneously. In addition, the chamber locations of the PDMS chip align to the locations of the culture chambers of the Parylene microfluidic chip. At the cell culture chamber area, a 0.5 cm × 1.5 cm transparent PET (polyethylene terephthalate) membrane with 0.4 or 1.0 μm diameter pores is sandwiched in between those two chips, and the membrane separates the culture chamber into two levels. During the device operation, the cells will be loaded via the PDMS channels, and the membrane allows cells to be efficiently collected, eliminating the need to coat the microfluidic channels with cell attachment factors. During the cell assay experiments, cells will be maintained at the cell culture level, on top of the membrane and treatment solution will be delivered via the fluid delivery level, at the bottom of the membrane. To expose all chambers to a common fluid solution such as during washing or staining the cells, fluid can be injected via the cell loading inlet or the outlet ports. For treating cells under combinatorial conditions, the fluids will be injected into combinatorial mixer inlets. The chamber for cell culture on the PDMS chip is 100

μm height and 600 μm in diameter and the chamber on the Parylene chip is 90 μm height and 1,000 μm in diameter. This results in a total volume of 100 nL. As typical cell culture has cell density range from 10^4 to 10^7 cells/mL, this would translate to about 1 to 1,000 cells per chamber. Typical cell culture procedure calls for changing of media every two to three days, so cells within the chambers under that density range should have sufficient nutrients to grow in two to three days without culture media change.

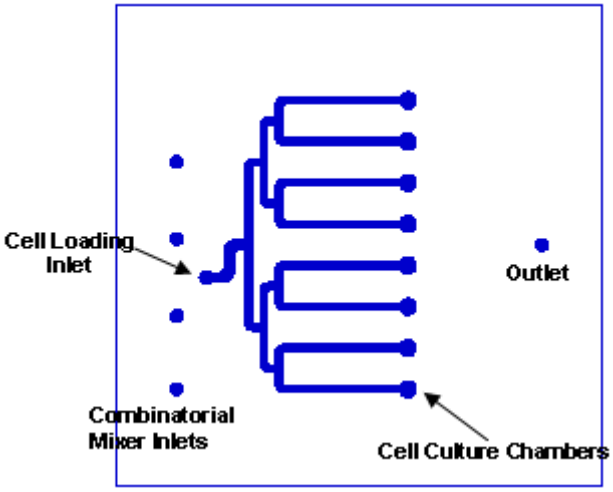

Figure 4-4. Layout of the PDMS microfluidic chip.

4.2.2 Device Fabrication

The fabrication process for constructing 3-D microfluidic Parylene chip is based on the developed fabrication method for monolithically constructing 3-D microfluidic networks as described in the previous chapter. The process flow for the surface micromachining process is shown in Figure 4-5. Soda lime glass wafer (thickness of 500 μm) was cleaned with Piranha solution (H_2SO_4: H_2O_2, H_2O; 5:1:1) at 120^{o}C for 5 minutes. The wafer was then soaked in 0.5% silane A-174 (Specialty Coating Systems, Indianapolis, IN) solution (DI water: IPA: A-174, 100:100:1) for 15 minutes to promote

the adhesion between the substrate and Parylene C. A first thin adhesion layer of Parylene C was deposited (3 μm) on the wafer. The first sacrificial photoresist layer (AZ4620 from Clariant, Charlotte, NC) was spin-coated (14 μm) and patterned to define the first-level channels. A second layer of Parylene C (10 μm) was then deposited to cover the sacrificial photoresist, forming the first-level channels. Parylene C was patterned using oxygen plasma so the areas where the overpass structures would be joined were exposed. This Parylene patterning also opened the area where the mixer and the culture chamber would be connected. A second sacrificial photoresist was spin-coated (25 μm) and patterned to define the overpass structures and the culture chambers. This second sacrificial photoresist covered the areas that were etched open, and the overpasses spanned several of the first-level microfluidic channels. A third layer of Parylene C (2 μm) was deposited. The whole chip was planarized with thick SU8 (90 μm) and Parylene C was patterned to define the access holes. To improve SU8 strength and adhesion to the bottom layers, after SU8 developing, the SU8 was subject to flood exposure under an UV canon for 3 minutes to further crosslink all SU8 molecules before hard baking the SU8 at 100^{o}C for 90 minutes. As a result, acetone was able to be used to dissolve the sacrificial photoresist. Acetone can dissolve photoresist quicker than isopropyl alcohol, which was used in the previous processes. However, acetone can also cause delamination and device failure while isopropyl alcohol causes such process at slower rate. Using the extra step to further harden the SU8, we were able to dissolve the sacrificial photoresist in heated (35^{o}C) acetone without device failure and the chip release process can be done in three days instead of one week. After sacrificial photoresist

dissolution, the remaining hollow Parylene structures become the fluidic networks of the chip.

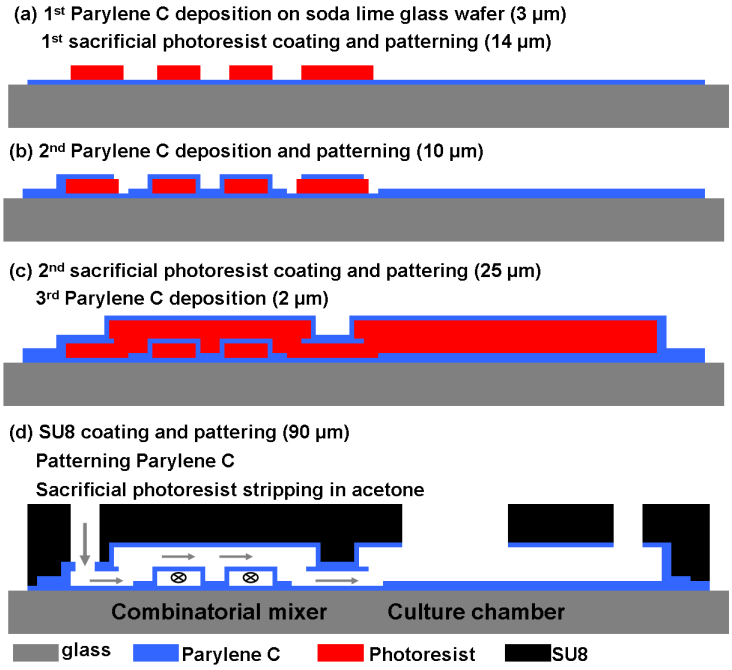

Figure 4-5. The monolithic fabrication process for making the 3-D microfluidic Parylene-based chip.

The PDMS microfluidic chip (4 mm thickness) was fabricated using the micro-molding process as shown in Figure 4-6. A 100 µm SU-8 was spin-coated on silicon wafer and patterned by photolithography. Then, the SU-8 mold was coated with 2 µm Parylene C to prevent PDMS from sticking to the mold. Polydimethylsiloxane (PDMS) (Sylgard 184, Dow Corning, Midland, MI) was prepared with a 10:1 ratio of silicone base and curing agent and poured onto the mold. The PDMS was cured in oven at 80^{o}C for 30 minutes. The PDMS was peeled off and trimmed to size of 2.5 cm × 2.5 cm and the fluidic ports were punched with a 23 gauge flat tip needle.

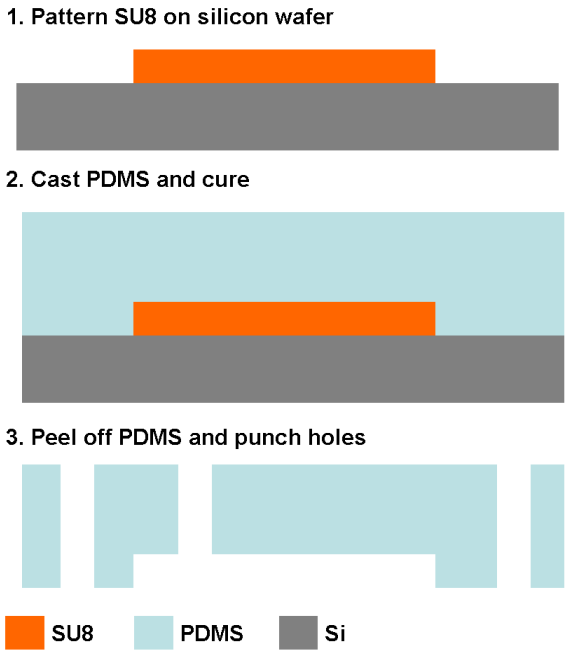

Figure 4-6. The process for making the PDMS chip.

Track-etched porous PET (polyethylene terephthalate) membranes with size of 0.5 cm × 1.5 cm were cut off from cell culture inserts. Membranes with 0.4 μm pore diameter have pore density of 4×10^6 pores cm^{-2} and were cut off from Corning Transwell 24 mm diameter inserts (Corning, Corning, NY). Membranes with 1 μm pore diameter have pore density of 1.6×10^6 pores cm^{-2} and were cut off from BD Falcon 24 mm diameter inserts (BD Biosciences, Bedford, MA).

4.2.3 Device Packaging and Operation

For device packaging, the porous membrane was placed onto the chamber area of the PDMS chip and the PDMS chip with the membrane was aligned onto the 3-D microfluidic Parylene chip. The PDMS and the Parylene chip were clamped together by two pieces of transparent acrylic that were milled with a computer-numerical-controlled (CNC) machine. With the membrane, the culture chamber turns into a two-level

configuration (Figure 4-1(b)). The PDMS also provided proper sealing and acted as an adapter to connect the tubes. Metal hollow tubes (0.025 inch OD × 0.013 inch ID × 0.25 inch length) were inserted into one end of Teflon tubes. The Teflon tubes were connected with syringes and plugged into the ports of the piece of PDMS. This packaging method allows other PDMS microfluidic chips to be integrated and provides the opportunity to construct more complicated device by adding components such as check valves, active valves and pumps.

4.2.4 Microfluidic Simulation

The mass and momentum transfer at the two-level culture chamber area was modeled in 2-D using finite element analysis with Comsol Multiphysics (Comsol, Burlington, MA). The configuration in Figure 4-7 was used. For the velocity profile simulation, the steady state incompressible Navier-Stokes application mode was implemented. The density and viscosity of water, 1 g cm^{-3} and 10^{-3} Pa·s, respectively, were used. The fluid flows into the inlet at a flow rate of 10^{-2} m s^{-1} and flows out via the outlet. In addition, simulation was done to ensure that molecules entering the inlet can reach the cell culture level in a sufficiently short amount of time. The multiphysics application mode with the combined incompressible Navier-Stokes model and transient diffusion/convection model was used. Both types of membranes that were used in this work were simulated; the membrane with 0.4 μm pore size has a pore density of 4×10^6 pores cm^{-2} and the membrane with 1 μm pore diameter has a pore density of 1.6×10^6 pores cm^{-2}. The diffusion constant of a small protein in water, $D = 10^{-6}$ cm^2 s^{-1} was used. Initially, the unsteady state flow profile was solved from 0 to 780 seconds with a time step of 30 seconds, and the solution at each time step was saved. Then, the

diffusion/convection module was applied and the concentration profile at each time step was solved using the saved fluid velocity profile. The two models were not solved together to save computation power.

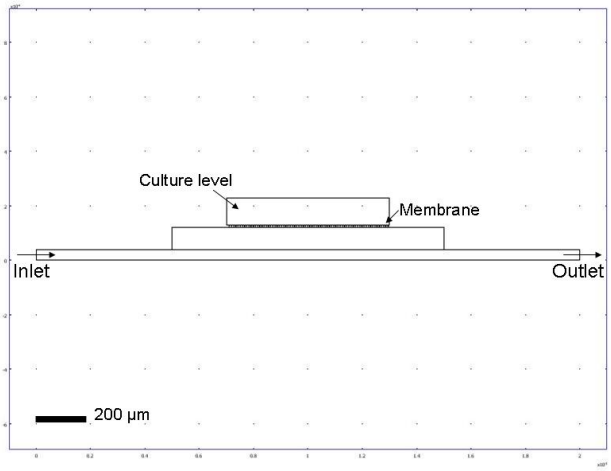

Figure 4-7. The configuration used for fluid simulation at the two-level culture chamber area.

4.2.5 Combinatorial Mixer Characterization

To characterize the concentration of the three input compounds inside each chamber, we packaged the device with a piece of PDMS with only the combinatorial mixer inlet and outlet ports. A red fluorescent molecule, sulforhodamine 101 (Sigma-Aldrich, St. Louis, MO), was used. We first tested if the fluorescence intensity would vary linearly with concentration. Background intensity was first measured by injecting DI water into the chamber. The fluorescence image of the chamber was captured with a Nikon E800 upright fluorescence microscope with a G-2E/C filter (Nikon Instruments, Melville, NY) and fluorescence intensity was measured using ImageJ. Stock solution of sulforhodamine 101 was prepared at 3.3 mM by dissolving it in dimethyl sulfoxide (DMSO), and working solution was obtained by diluting in DI water. Then,

sulforhodamine 101 solutions at different concentrations, 2.0625, 4.125, 6.1875, and 8.25 μM, were injected into the chamber. The fluorescence image of the chamber was captured and fluorescence intensity was measured using ImageJ. Background intensity was subtracted from the measured fluorescence intensity.

To characterize the combinatorial mixer, we first injected a red fluorescence solution, 8.25 μM sulforhodamine 101, into input A, while injecting DI water into input B, input C, and control. The injection was controlled by syringe pumps and was set at 5 μL min^{-1} for duration of 20 minutes. After ten minutes, the fluorescence image of each chamber was captured with an upright fluorescence microscope with a G-2E/C filter. The fluorescence intensity was measured using ImageJ and background intensity was subtracted. The fluorescent concentration at each chamber was normalized against the input concentration. Fluorescence solution was then switched to input B, while injecting DI water into other inlets. The same procedure was repeated for input C. The device was flipped over during imaging so the backside (the glass wafer side) was facing the objective. The backside acrylic had a milled slot so the excitation light and emission light can directly reach the glass side without interference from the acrylic.

4.2.6 Device Operation for Cell-Based Assay On-Chip

The device operation of a typical cell assay experiment is shown in Figure 4-8.

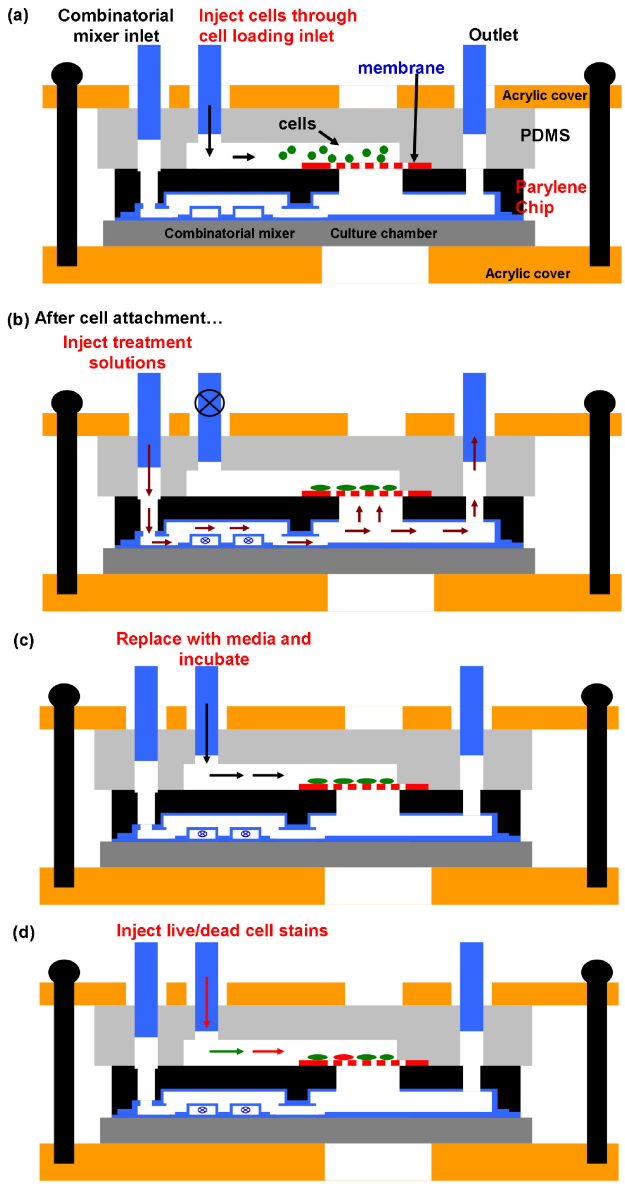

Figure 4-8. Typical device operation for cell-based assay using this device. (a) Suspension of cells was injected into the chip via the cell loading port, and cells were efficiently collected by and grown on the membrane. (b) Following incubation at static condition for cell attachment, the compounds for treatment can be injected via the combinatorial mixer inlets, while keeping the cell loading port sealed with a solid stainless steel pin. (c) Reagents for washing the cells can be injected either via the outlet or the cell loading inlet. (d) Live/dead cell stains can be injected at the end to assess the viability.

Before the device assembly, the PDMS chips and 3-D Parylene chips were sterilized with UV and ultrasonicated in ethanol for 10 minutes followed by

ultrasonication in water for 5 minutes. After the devices were assembled, the devices were rinsed with DI water and filled with media prior to use. The porous membranes were sterilized by the manufactures, and a new piece of membrane was used for every experiment. The microfluidic channels were primed with water followed by cell culture media. Suspension of cells was loaded into syringe and was injected into the chip via the cell loading port. Cells were efficiently collected by and grown on the membrane, which was cell culture treated by the manufactures. Following incubation at static condition for cell attachment, the compounds for treatment can be injected via the combinatorial mixer inlets, while keeping the cell loading port sealed with a solid stainless steel pin. Reagents for washing the cells and staining cells can be injected either via the outlet or the cell loading inlet to replace the treatment compound solutions. After certain period of incubation, live/dead cell stains can be injected to assess the viability of the cells on-chip.

Two cell-based assays were performed using this device and the general device operation follows the procedure described previously. The details of both experiments are described in the following sections.

4.2.7 Assay for Compounds' Ability to Reduce Cytotoxicity of Hydrogen Peroxide

This microfluidic device was used to assay for the ability of 1,5-dihydroxyisoquinoline (ISO), deferoxamine (DFO), and 3-aminobenzoic acid (ABA) to alleviate cytotoxicity of hydrogen peroxide, which is generated during brain ischemia and reperfusion injury and various neuropathological conditions [87]. B35 rat neuroblastoma cells were cultured in 100 mm × 15 mm polystyrene petri dishes and passaged every two to three days. All culture reagents were purchased from Invitrogen (Carlsbad, CA) unless otherwise stated. The cells were maintained in Dulbecco's Modified Eagle's Medium

(DMEM) with 10% fetal bovine serum and 1% penicillin/streptomycin/amphotericin B, and incubated in 5% CO_2 at 37^{o}C. The three compounds, 1,5-dihydroxyisoquinoline (ISO), deferoxamine (DFO), and 3-aminobenzoic acid (ABA) were all purchased from Sigma-Aldrich (St. Louis, MO). Stock solution of 1,5-dihydroxyisoquinoline was prepared by dissolving it in dimethyl sulfoxide (DMSO) at a final concentration of 60 mM. Stock solution of deferoxamine was prepared by dissolving it in Dulbecco's phosphate buffered saline (DPBS) at a final concentration of 76 mM. Stock solution of 3-aminobenzoic acid was prepared by dissolving it in dimethyl sulfoxide (DMSO) at a final concentration of 800 mM. The device was packaged with the porous membrane with 0.4 μm pore diameter. Cells were suspended using 0.25% trypsin (0.25% (w/v) trypsin, 0.53 mM EDTA solution) and suspension of B35 cells was injected into the cell loading port. The cells were collected by and grown on the membrane. Following three hours of incubation inside the incubator after cell seeding, each compound (300 μM ISO, 1 mM DFO, 1 mM ABA) was mixed in DMEM media containing 1.5 mM hydrogen peroxide and injected into the combinatorial mixer inlets at 5 μL min^{-1} for 30 minutes, followed by static condition inside the incubator for five minutes, while keeping the cell loading inlet sealed with a solid stainless steel pin. Then, fresh DMEM solution was injected into the cell loading inlet to replace the treatment solutions, and the cells were rinsed again by injecting DMEM via the outlet, while keeping the cell loading inlet sealed. The cells were incubated under static condition inside the incubator for three hours. Live/dead cell stains (2 μM calcein AM/2 μM propidium iodide) were injected via the cell loading inlet and the cells were incubated for 10 minutes. Calcein AM can permeate the cell membrane and the lipophilic blocking groups are cleaved

nonspecifically by intracellular esterases. The hydrolyzed form, calcein, results in a charged green fluorescent compound that is retained very well inside the cells. Therefore, green fluorescence is an indicator of live cells. Propidium iodide is a red fluorescent molecule that can only pass through cells with compromised membranes and bind to the nucleic acids. Thus, propidium iodide indicates dead cells. Often, there would be cells that are stained by both dyes and they are counted as dead cells because their membranes are already compromised while some intracellular esterases are still present. The visualization and fluorescence image capturing of the cells were carried out using a fluorescence microscope with a G-2E/C and B-2E/C filters, and cytotoxicity was determined by the ratio of dead cells to total cells. Four experiments were done for this assay.

4.2.8 Assay for Exposing Breast Cancer Cells to Chemotherapeutic Agents

The device was used to assay for the cytotoxic activity of three chemotherapeutic agents, vinorelbine (VIN), paclitaxel (PAC), and γ-linolenic acid (GLA), on human breast cancer carcinoma, MDA-MB-231 cells (American Type Culture Collection, Manassas, VA). The cells were maintained in Dulbecco's Modified Eagle's Medium with 10% fetal bovine serum and 1% penicillin/streptomycin/amphotericin B, and incubated in 5% CO_2 at 37^{o}C. The three compounds, vinorelbine (VIN), paclitaxel (PAC), and γ-linolenic acid (GLA), were all purchased from Sigma-Aldrich (St. Louis, MO). Stock solution of vinorelbine was prepared by dissolving it in Dulbecco's phosphate buffered saline (DPBS) at a final concentration of 10 mM and stored at 4^{o}C. Stock solution of paclitaxel was prepared by dissolving paclitaxel in dimethyl sulfoxide (DMSO) at a final concentration of 10 mM and stored at 4^{o}C. Stock solution of γ-

linolenic acid was prepared by dissolving γ-linolenic acid in ethanol at a final concentration of 120 mM and stored in the dark at −20°C. The device was packaged with the membrane with 1 μm pores. Suspension of cells was injected into the cell loading port and trapped and cultured on the membrane surface. Following three hours of incubation after cell seeding, each compound (8 μM VIN, 2 μM PAC, 50 μM GLA) was mixed in complete culture media and injected into the combinatorial mixer inlet at 10 μL min^{-1} for 5 minutes, while keeping the cell loading inlet sealed with a solid stainless steel pin. Then, the cells were incubated with the treatment solutions for another 25 minutes inside the incubator. Afterwards, normal culture media was injected through the cell loading port to replace the treatment solutions, and the rinsing was done again by injection through the outlet, while keeping the cell loading inlet sealed. The cells were then incubated for another 24 hours. Live/dead stains (2 μM calcein AM/2 μM propidium iodide) were injected and incubated for ten minutes, and the cells were visualized with a fluorescence microscope. The cytotoxicity was determined by the ratio of dead cells to total cells. Six experiments were done for this assay.

4.3 Results and Discussion

4.3.1 Combinatorial Mixer Characterization

A fabricated Parylene chip and a packaged device with three different colors of food coloring solutions injected are shown in Figure 4-9. The chip was able to withstand releasing in warm (35°C) acetone without any delamination of the SU8 or Parylene layers. In contrast to the previous chip built on silicon, this version is based on glass substrate and is more compatible with microscopy. Both SU8 and Parylene C are transparent and

will allow the experiments to be observed from either side of the chip. The tubes will no longer obstruct the microscope objectives as the objectives can be used on the different side from the tubes. Fluid delivery follows the same straightforward procedure as previously described, using syringes and syringe pumps.

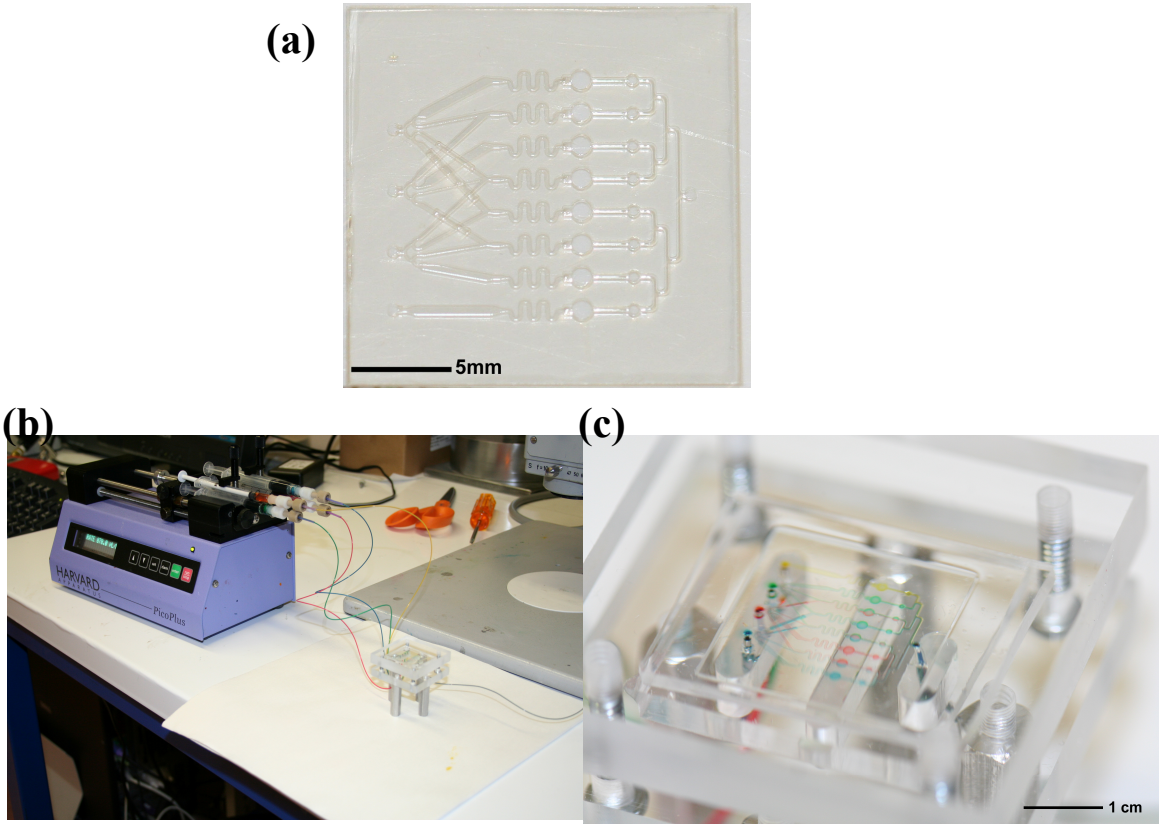

Figure 4-9. (a) Fabricated Parylene chip after sacrificial photoresist dissolution. (b) Experiment setup to deliver food coloring solutions into the chip. (c) Packaged device with various food coloring solutions injected.

Figure 4-10 shows the serial dilution experiment with sulforhodamine 101 by measuring the fluorescence intensity of sulforhodamine 101 at various concentrations on-chip. The linear fit of that data is included and has a coefficient of determination, r^2, value of 0.9995. The result shows that sulforhodamine 101 has fluorescence intensity

that varies linearly with the concentration at the concentration range we will work in and is suitable for our experiment.

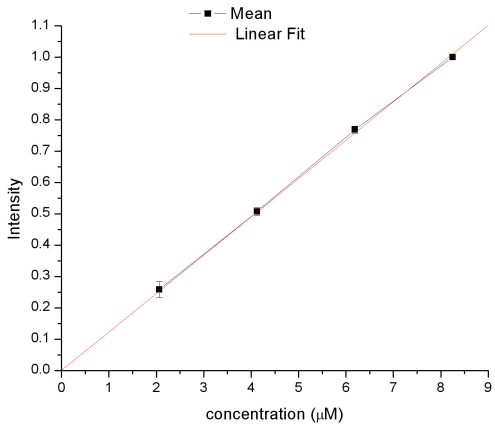

Figure 4-10. Serial dilution of sulforhodamine 101 on-chip.

Figure 4-11 shows the concentration of the three input compounds at each chamber. The combinatorial mixer was able to generate the correct combinations of the compound solutions. The experiment was done by injecting red fluorescent sulforhodamine 101 solution into one of the combinatorial inlet while injecting DI water into the other inlets. Fluorescence image of each chamber was taken and the fluorescence level was measured with ImageJ. The same procedure was repeated for the other two combinatorial mixer inlets. While it is possible to use three fluorescent compounds with different excitation/emission spectra and injecting one compound into one separate inlet simultaneously, we avoided such procedure to prevent possible fluorescence crossover among the three fluorescent molecules. The concentration of the compounds can deviate from the design value because of dimensional inaccuracy in processing. Also, the sacrificial photoresist was baked during fabrication and this resulted in the edge of channel to be rounded and deviated from the rectangular profile

that was used when calculating fluidic resistance. A more precise control during the fabrication process can result in the concentration profile better matching the design values. This characterization allows us to know the concentrations of the input compounds at each chamber. Such information will assist us in deciding the input treatment compound concentration and let us know the treatment compound concentration at each chamber for the cell assay experiments. This method can be adopted for characterizing combinatorial mixer with higher inputs as choosing four or more fluorescent molecules with non-overlapping emission/excitation spectra can be difficult and add to the cost because four or more optical filters for the fluorophores have to be obtained.

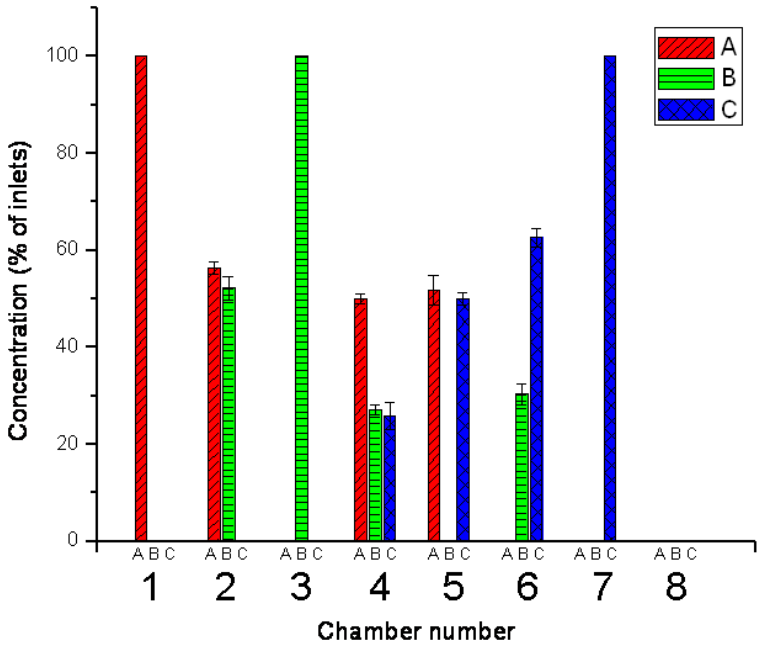

Figure 4-11. Fluorescence characterization of the combinatorial mixer showing the concentration of the three input compounds at each chamber. Error bars are one standard deviation (SD). Number of experiments = 3.

The combinatorial mixing can be treated as matrix operation, shown as a linear equation, Ex = O. E represents the components of each input, x represents the

combinatorial function of the chip and O is the output components. For the current device with three-input combinatorial mixer (with one unmixed control), the matrix operation is

$$\begin{bmatrix} A_x & B_x & C_x \\ A_y & B_y & C_y \\ A_z & B_z & C_z \end{bmatrix} \begin{bmatrix} a_i & b_i & c_i & d_i & e_i & f_i & g_i & h_i \\ a_j & b_j & c_j & d_j & e_j & f_j & g_j & h_j \\ a_k & b_k & c_k & d_k & e_k & f_k & g_k & h_k \end{bmatrix} = \begin{bmatrix} a_x & b_x & c_x & d_x & e_x & f_x & g_x & h_x \\ a_y & b_y & c_y & d_y & e_y & f_y & g_y & h_y \\ a_z & b_z & c_z & d_z & e_z & f_z & g_z & h_z \end{bmatrix}. \quad (4.7)$$

For the input matrix E, the components, A, B, and C represent the individual inputs and the component in each column represents the concentration of the individual input compounds in input A, input B, and input C. For example, if we inject solution I_1 into input A, I_2 into input B and I_3 into input C, the input matrix E would be

$$\mathrm{E} = \begin{bmatrix} I_1 & 0 & 0 \\ 0 & I_2 & 0 \\ 0 & 0 & I_3 \end{bmatrix}. \quad (4.8)$$

The combinatorial mixer operator, x, governs how the inputs will be combined into the outputs. With the original combinatorial mixer design, the matrix operation is represented as

$$\begin{bmatrix} I_1 & 0 & 0 \\ 0 & I_2 & 0 \\ 0 & 0 & I_3 \end{bmatrix} \begin{bmatrix} 1 & \frac{1}{2} & 0 & \frac{1}{3} & \frac{1}{2} & 0 & 0 & 0 \\ 0 & \frac{1}{2} & 1 & \frac{1}{3} & 0 & \frac{1}{2} & 0 & 0 \\ 0 & 0 & 0 & \frac{1}{3} & \frac{1}{2} & \frac{1}{2} & 1 & 0 \end{bmatrix} = \begin{bmatrix} 1I_1 & \frac{1}{2}I_1 & 0 & \frac{1}{3}I_1 & \frac{1}{2}I_1 & 0 & 0 & 0 \\ 0 & \frac{1}{2}I_2 & 1I_2 & \frac{1}{3}I_2 & 0 & \frac{1}{2}I_2 & 0 & 0 \\ 0 & 0 & 0 & \frac{1}{3}I_3 & \frac{1}{2}I_3 & \frac{1}{2}I_3 & 1I_3 & 0 \end{bmatrix}. \quad (4.9)$$

Each column in the output matrix, O, represents the compounds and concentrations in each chamber. Characterizing the combinatorial mixer allows us to know the values for the combinatorial mixer operation of the device and the equation becomes

$$\begin{bmatrix} I_1 & 0 & 0 \\ 0 & I_2 & 0 \\ 0 & 0 & I_3 \end{bmatrix} \begin{bmatrix} 1 & 0.55 & 0 & 0.5 & 0.54 & 0 & 0 & 0 \\ 0 & 0.5 & 1 & 0.26 & 0 & 0.32 & 0 & 0 \\ 0 & 0 & 0 & 0.25 & 0.49 & 0.64 & 1 & 0 \end{bmatrix} = \begin{bmatrix} 1I_1 & 0.55I_1 & 0 & 0.5I_1 & 0.54I_1 & 0 & 0 & 0 \\ 0 & 0.5I_2 & 1I_2 & 0.26I_2 & 0 & 0.32I_2 & 0 & 0 \\ 0 & 0 & 0 & 0.25I_3 & 0.49I_3 & 0.64I_3 & 1I_3 & 0 \end{bmatrix}. \quad (4.10)$$

Knowing the values in the combinatorial mixer operator allows other output combinations to be designed using the same chip. As the values in the matrix x have been determined, one can choose the desired output and solved for E in the matrix operation, Ex = O.

For example, if the output $\begin{bmatrix} 0.4I_1 & 0.37I_1 & 0.3I_1 & 0.278I_1 & 0.216I_1 & 0.096I_1 & 0 & 0 \\ 0.6I_2 & 0.58I_2 & 0.5I_2 & 0.43I_2 & 0.324I_2 & 0.16I_2 & 0 & 0 \\ 0.3I_3 & 0.465I_3 & 0.6I_3 & 0.556I_3 & 0.652I_3 & 0.832I_3 & 1I_3 & 0 \end{bmatrix}$ is desired, one can solve for the necessary input matrix to generate such output. The input would be $\begin{bmatrix} 0.4I_1 & 0.3I_1 & 0 \\ 0.6I_2 & 0.5I_2 & 0 \\ 0.3I_3 & 0.6I_3 & I_3 \end{bmatrix}$, and the whole matrix operation is

$$\begin{bmatrix} 0.4I_1 & 0.3I_1 & 0 \\ 0.6I_2 & 0.5I_2 & 0 \\ 0.3I_3 & 0.6I_3 & I_3 \end{bmatrix} \begin{bmatrix} 1 & 0.55 & 0 & 0.5 & 0.54 & 0 & 0 & 0 \\ 0 & 0.5 & 1 & 0.26 & 0 & 0.32 & 0 & 0 \\ 0 & 0 & 0 & 0.25 & 0.49 & 0.64 & 1 & 0 \end{bmatrix}$$

$$= \begin{bmatrix} 0.4I_1 & 0.37I_1 & 0.3I_1 & 0.278I_1 & 0.216I_1 & 0.096I_1 & 0 & 0 \\ 0.6I_2 & 0.58I_2 & 0.5I_2 & 0.43I_2 & 0.324I_2 & 0.16I_2 & 0 & 0 \\ 0.3I_3 & 0.465I_3 & 0.6I_3 & 0.556I_3 & 0.652I_3 & 0.832I_3 & 1I_3 & 0 \end{bmatrix}. \quad (4.11)$$

It is noted that not all possible output can be generated because certain output combination would require inputs to have negative concentration. By characterizing the combinatorial mixer and transforming the combinatorial mixing into a matrix operation, we can expand the possible combinations of experiments that can be done using the current chip and also lay the foundation for easily designing and characterizing future devices with more inputs and outputs.

4.3.2 Device Packaging with Integrated Membrane and Microfluidic Simulation

For the cell assay experiments, porous PET (polyethylene terephthalate) membranes were incorporated into the device packaging and the culture chamber area was turned into a two-level configuration. Figure 4-12 shows a cell culture experiment on this chip. The B35 rat neuroblastoma cells were loaded and captured by the membrane and grown at a continuous perfusion of culture media that was injected through the outlet at 80 nL min^{-1}, while keeping the cell loading inlet sealed with a stainless steel pin. The cells eventually reached confluency after 70 hours.

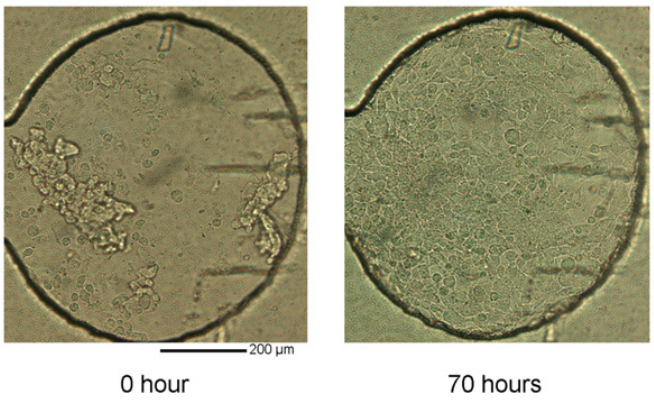

Figure 4-12. Cell culture inside the culture chamber with integrated membrane. (Left) Cells loaded into the chamber. (Right) Cell population reached confluency after 70 hours.

The integrated membrane served several purposes and greatly facilitated the on-chip cell assay experiment. Cell seeding in many other microfluidic cell culture devices was done by flowing cell suspension through channels that were coated with attachment factors such as collagen or fibronectin. Many cells can be lost in this process and the pretreating of the channel surface with attachment factor can take 4 hours to 24 hours. In our previous chip, the channel walls were pretreated with 0.05% polyethyleneimine (PEI) solution for 24 hours for cell to adhere during cell loading and proper cell spreading after incubation. With the porous membrane, cells were injected into the cell loading port of

the PDMS chip and cells were efficiently trapped on the porous membrane at the culture chamber area. The membrane also provided a proper surface for cell growth because the membrane was cell culture treated by the manufactures with oxygen or nitrogen plasma. The need to pretreat the channel surfaces was eliminated. The membrane is inexpensive and disposable so a new sterile membrane can be used for each experiment. In addition, studies have shown that growing cells on porous membrane allows cells to access media from both apical and basolateral sides and results in an *in vivo*-like environment and improved cell morphology [88]. Our packaging method to allow membrane to be incorporated into microfluidic devices is straightforward and the method allows PDMS microfluidic chip to be integrated. Integrating various components can extend the versatility of the devices. Different types of membrane can be used depending on the applications, and other PDMS microfluidic chips such as concentration diluter can be integrated. This method of incorporating membrane into microfluidic devices can be extended to other devices as the use of membrane in microfluidics has increased in recent years for process such as concentration, filtration or other cell studies.

In addition, the two-level configuration allows the cells to be kept in the cell culture level and be separated from the fluid delivery level during cell assay experiments. This setup minimizes the exposure of cells to direct fluid flow and the resultant shear stresses, which can cause adverse effect to cells. Finite element analysis of the fluid velocity modeling was done using Comsol Multiphysics, and Figure 4-13 shows the simulated fluid velocity profile.

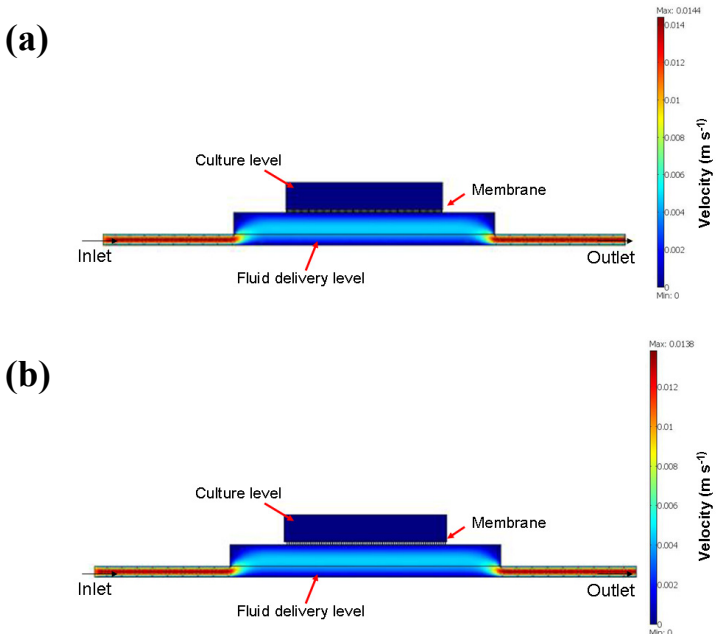

Figure 4-13. Fluid velocity profile at the two-level culture chamber for (a) 0.4 μm porous membrane and (b) 1 μm porous membrane.

For both membrane pore sizes, the majority of the fluid flow occurs inside the fluid delivery level and the fluid flow inside the culture level is minimal. Also, the fluid velocity inside culture level is very uniform, resulting in a uniform growth environment for the cells. For microfluidic perfusion system, the 2-D Poiseuille flow results in an estimated shear stress at the wall,

$$\tau = \frac{6\mu Q}{h^2 w}, \tag{4.12}$$

where τ is the shear stress, μ is the viscosity, Q is the flow rate, h is the channel height and w is the channel width. As the flow rate inside the culture chamber level is reduced, the shear stress at the wall is reduced as well.

Finite element analysis using the combined Navier-Stokes and diffusion/convection model was done to simulate the solute transport during cell assay and results show that the transport of treatment molecules from the fluid delivery level

into the cell culture level is dominated by diffusion. The membrane is thin (10 µm) with high porosity (4×10^6 pores cm^{-2} and 1.6×10^6 pores cm^{-2} for the 0.4 µm and 1 µm pore size membranes, respectively) and this allows the treatment compounds to quickly reach the cell culture area. Figure 4-14 shows that for the membrane with 0.4 m pore diameter, molecules ($D = 10^{-6}$ cm^2 s^{-1}) can reach the cell culture surface in a short time, 270 seconds, and fill the entire chamber within 660 seconds. The membrane with 1 µm pore diameter allows even faster transport of molecules, filling the entire chamber in less than 450 seconds. It is noted that cells are residing on top of the membrane and as soon as the molecules cross the 10 µm membrane, the molecules can start affecting the cells and it is not required for the molecules to fill the entire chamber for them to take effect. The simulation results show that our device setup is appropriate for exposing cells to different compounds and those compounds can be delivered to the cells efficiently without disturbance from convection.

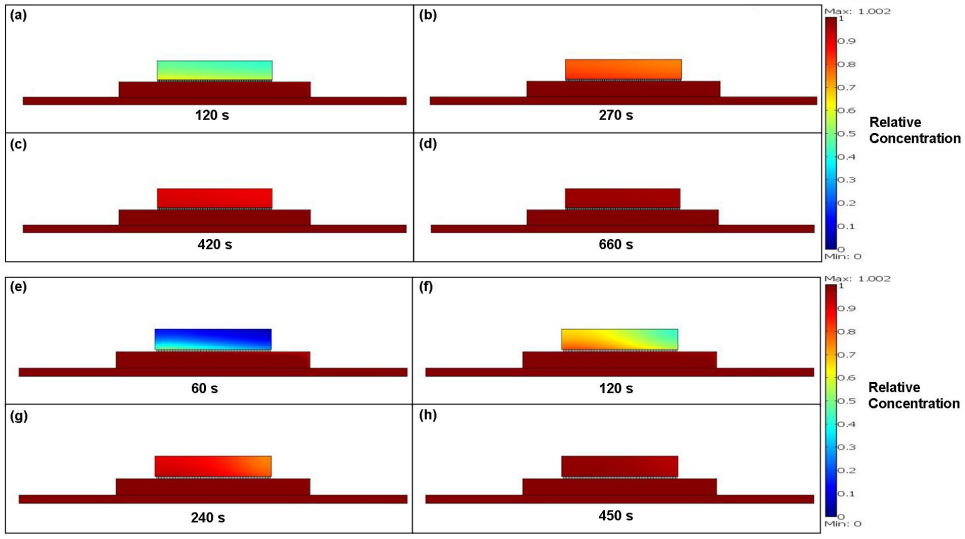

Figure 4-14. Simulation of the solute transport at the two-level culture chamber area. Concentration profile was shown for 0.4 µm pore membrane (a–d) and 1 µm pore membrane (e–h). $D = 10^{-6}$ cm^2 s^{-1}.

In addition, this configuration mimics the *in vivo* interstitial environment as fast convective flow dominates the fluid delivery level that resembles blood flow in tissue and diffusion dominates the cell culture level with low shear stress. The Peclet number extracted from the simulation model at the height of cell (10 μm) is around 0.1, which is similar to the value inside the tissue. The effect of such culturing environment on the cells will be investigated in future works. Such ability to create a physiologically relevant condition is one unique advantage for microfluidic devices and is unavailable for conventional culturing containers such as flasks or well plates. Further additions can be made such as culturing cells in gel or co-culturing with other cell types to further simulate the various characteristics of the *in vivo* cellular microenvironment. As cell-based assays use cells as model for studies such as drug response, it is important that cells be kept in an environment as close to the *in vivo* environment as possible so the cells would behave similarly as they would in human body and test results would be more validated. The integrated membrane serves several beneficial purposes as it simplifies the cell loading process and also allows cells to be maintained in an *in vivo*-like environment during the cell assay experiment.

4.3.3 Oxygen Supply for the Cell Culture Chamber

The chamber was designed so the cells would have sufficient oxygen during the experiment. PDMS has been known to be a permeable material to gases and would allow oxygen to freely pass through. The oxygen transport through the cell culture chamber can be modeled using the configuration shown in Figure 4-15.

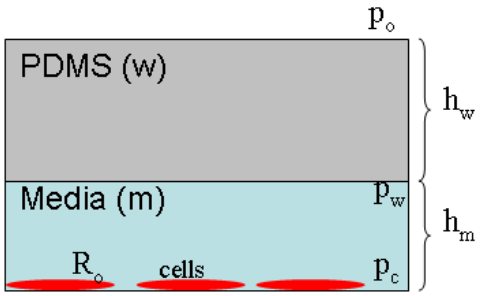

Figure 4-15. Side view of the culture chamber for oxygen transport modeling.

The cells have an oxygen utilization rate per cell, R_O [mol min^{-1} cell^{-1}], and a total consumption rate, O_T,

$$O_T = \frac{R_O N}{A}, \tag{4.13}$$

where N is the total number of cells per chamber, and A is the surface area of the chamber. Flux of oxygen would be constantly transferred from the surface of the chamber into the chamber at rate, J, and at steady state, flux of oxygen transferred from surface to the chamber equals the consumption rate by the cells.

$$J = \frac{R_O N}{A}. \tag{4.14}$$

J can be expressed by Flick's first law:

$$J = \frac{D_w \alpha_w}{h_w}(p_o - p_w) = \frac{D_m \alpha_m}{h_m}(p_w - p_c). \tag{4.15}$$

The first part denotes the flux of oxygen through the wall (w), PDMS, with thickness h_w and the second part denotes the flux of oxygen through the media (m) to the cell surface, with thickness h_m. D_w is the diffusion coefficient of oxygen in the wall, α_w is the solubility of oxygen into the wall, p_o is the partial pressure of oxygen at the outer surface, p_w is the partial pressure of oxygen at the inner surface, D_m is the diffusion coefficient of

oxygen in the media, α_m is the solubility of oxygen into the media, and p_c is the partial pressure of oxygen at the cell surface.

The expression can be rewritten and eliminate the term p_w, to become

$$J = \frac{(p_o - p_c)}{((h_w / \alpha_w D_w) + (h_m / \alpha_m D_m))}. \tag{4.16}$$

This can be equated to the gas consumption equation and an expression is derived:

$$\frac{N}{A} = \frac{p_o - p_c}{R_O(\frac{h_m}{\alpha_m D_m} + \frac{h_w}{\alpha_w D_w})}. \tag{4.17}$$

The maximum cell density, $N/A_{(\max)}$, that can be supported by the system can be found by plugging in the lowest allowable value of p_c, the partial pressure of oxygen at cell surface. That value is denoted as p_c*, the limiting oxygen concentration below which proliferation is not supported, and the value of p_c* for hepatocyte, one of most oxygen-demanding cells, is 40 mmHg [89].

$$\frac{N}{A}_{(\max)} = \frac{p_o - p_c^*}{R_O(\frac{h_m}{\alpha_m D_m} + \frac{h_w}{\alpha_w D_w})}, \tag{4.18}$$

The oxygen utilization rate, R_O, for hepatocyte cell is around 12 fmol min^{-1} $cell^{-1}$ [90]. As PDMS is used as the wall material, the values for D_w and α_w are 3.4×10^{-9} m^2 s^{-1} and 0.34 g m^{-3} $mmHg^{-1}$, respectively. The oxygen inside the media has similar property to that of inside the water as the media is a dilute aqueous solution and the values for D_m and α_m are 2.1×10^{-9} m^2 s^{-1} and 4.32×10^{-2} g m^{-3} $mmHg^{-1}$, respectively [89]. The partial pressure of oxygen inside the incubator, p_o, is around 148 mmHg. As a result, the maximum number of cell density, $N/A_{(\max)}$ that this chamber can support is 3.7

$\times 10^3$ cells mm^{-2}. As our chamber has a culture area of 2.8×10^{-1} mm^2, this would translate to be about 10^3 cells per chamber. Typical cell culture experiments have a density of 10^4–10^7 cells mL^{-1}. The cell culture chamber has a volume of 100 nL, and this would translate to 1 to 1,000 cells per chamber. Thus, our cell culture chamber, which can sustain cell density of 10^3 cells per chamber with enough oxygen, is sufficient for the typical cell density range. It is noted that the value used for oxygen utilization rate and limiting oxygen concentration at cell surface, p_c^*, is that for hepatocyte, which is more oxygen demanding than other cell types. The cells used in our experiments are immortalized mammalian cells and they can use oxygen at rate 10 to 20 times slower. For example, CHO, Chinese hamster ovary cell, has a oxygen utilization rate of only 0.5 fmol min^{-1} $cell^{-1}$ [90]. Therefore, the chamber should be able to support more than 10^3 cells per chamber for most of the cell types unless oxygen demanding cells such as hepatocytes are used.

4.3.4 Assay for Compounds' Ability to Reduce Cytotoxicity of Hydrogen Peroxide

The device was used to assay for the ability of three compounds on reducing the cytotoxicity of hydrogen peroxide. Hydrogen peroxide is generated during brain ischemia and reperfusion injury and various neuropathological conditions, and leads to significant DNA damage and cell death [87]. B-35 rat neuroblastoma cells were used as a model system. After cell seeding and static incubation for cell adherence, solutions containing the individual compounds in DMEM media with hydrogen peroxide were delivered into the combinatorial mixer to treat the cells. After incubation with the treatment molecules, the solutions were replaced with normal DMEM media. Cells were incubated and stained with calcein AM (live) and propidium iodide (dead) stains. Figure

4-16(a) shows the result of the cytotoxicity experiment, and Figure 4-16(b) shows the arrays of cells after the cells were stained by live/dead stains.

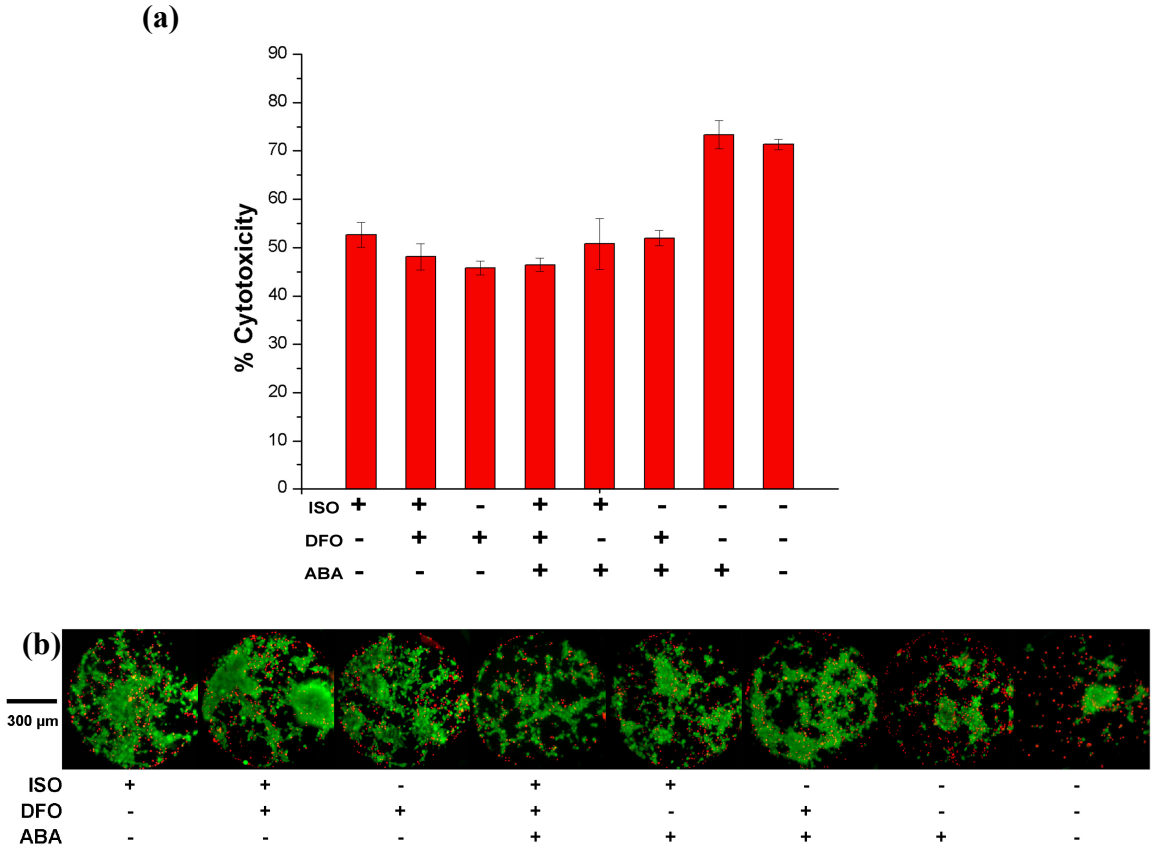

Figure 4-16. Result of the assay to test the ability of three compounds, 1,5-dihydroxyisoquinoline (ISO), deferoxamine (DFO), and 3-aminobenzoic acid (ABA), to reduce cytotoxicity of hydrogen peroxide. (a) Plot of cytotoxicity of the cells, B35 rat neuroblastoma cells, at each chamber with different compound exposure. Each compound was mixed in media containing 1.5 mM hydrogen peroxide. Results are the means ± standard deviation (SD). Number of experiments = 4. (b) Cells in each chamber after live (green)/dead (red) staining.

1,5-dihydroxyisoquinoline and deferoxamine showed cytoprotective effect against hydrogen peroxide. 1,5-dihydroxyisoquinoline reduces cell death by inhibiting Poly(ADP-Ribose) polymerase, whose over-production in response to hydrogen peroxide can cause cell death [91]. Deferoxamine reduces cell death by decreasing the conversion of hydrogen peroxide to hydroxyl radicals that damage DNA [92]. 3-aminobenzoic acid

is structurally similar to 3-aminobenzamide, which is an agent that can reduce cytotoxicity of hydrogen peroxide. However, it has been shown that 3-aminobenzoic acid has no effect on cytotoxicity of hydrogen peroxide. ISO and DFO were able to reduce the cytotoxicity when treating the cells as individual molecules or in combination. There did not appear to be synergistic interaction among the two compounds as the combination did not increase the ability to reduce cytotoxicity of hydrogen peroxide. When either ISO or DFO were combined with ABA, the ability to reduce cytotoxicity was not reduced although the concentration of each was lowered. The efficacy of ISO and DFO can start to saturate after reaching certain concentration and this is shown in some studies [92]. Separate control experiments were performed with the same cell seeding and cell treatment condition, but exposing cells to only DMEM media without hydrogen peroxide and the three chemicals. The cytotoxicity was found to be 4%.

4.3.5 Assay for Exposing Breast Cancer Cells to Chemotherapeutic Agents

MDA-MB-231 human breast cancer cells were exposed to combinations of three chemotherapeutic agents, vinorelbine (VIN), paclitaxel (PAC), and γ-linolenic acid (GLA), using this device. In this experiment, the device was packaged with a 1 μm porous membrane and suspension of cells were loaded and captured by the membrane. After incubation for cell attachment, cells were exposed to the various compounds. Following incubation with the treatment agents, the cells were washed and culture chambers were replenished with normal culture media. Cells were incubated for another 24 hours and calcein AM and propidium iodide were loaded to assess the viability of the cells. Figure 4-17(a) shows the result of the cytotoxicity experiment, and Figure 4-17(b) shows the arrays of cells after the cells were stained by live/dead stains. Paclitaxel, a

taxane, was first extracted from the bark of western yew trees Taxus brevifolia. It produces its antitumor activity by binding to microtubules of the cells, causing polymerization and stabilization. The inability for depolymerization of microtubules disables the cells from completing cell division [93]. Vinorelbine, a semisynthetic vinca alkaloid, also binds to microtubules, but disrupts microtubule functions by inducing depolymerization and loss of mitotic spindle [94]. Both drugs have been used in cancer chemotherapy with demonstrated clinical activity against breast cancer. γ-linolenic acid has been shown to suppress tumor growth and metastasis and is a potential anticancer drug. More importantly, researches have shown that γ-linolenic acid can potentiate the cytotoxicity of several anticancer drugs such as vinorelbine, paclitaxel and doxorubicin [95, 96]. Studies have also shown that paclitaxel and vinorelbine to have synergy when used in combination [97]. As seen in Figure 4-17(a), all three compounds showed antitumor activity when treating the cells as a single agent. When cell were exposed to the combination of γ-linolenic acid and vinorelbine or paclitaxel, the cytotoxicity increased even with reduced concentration of the compounds. In the control chamber, the cells were not exposed to any of the three agents and the cytotoxicity was around 4%.

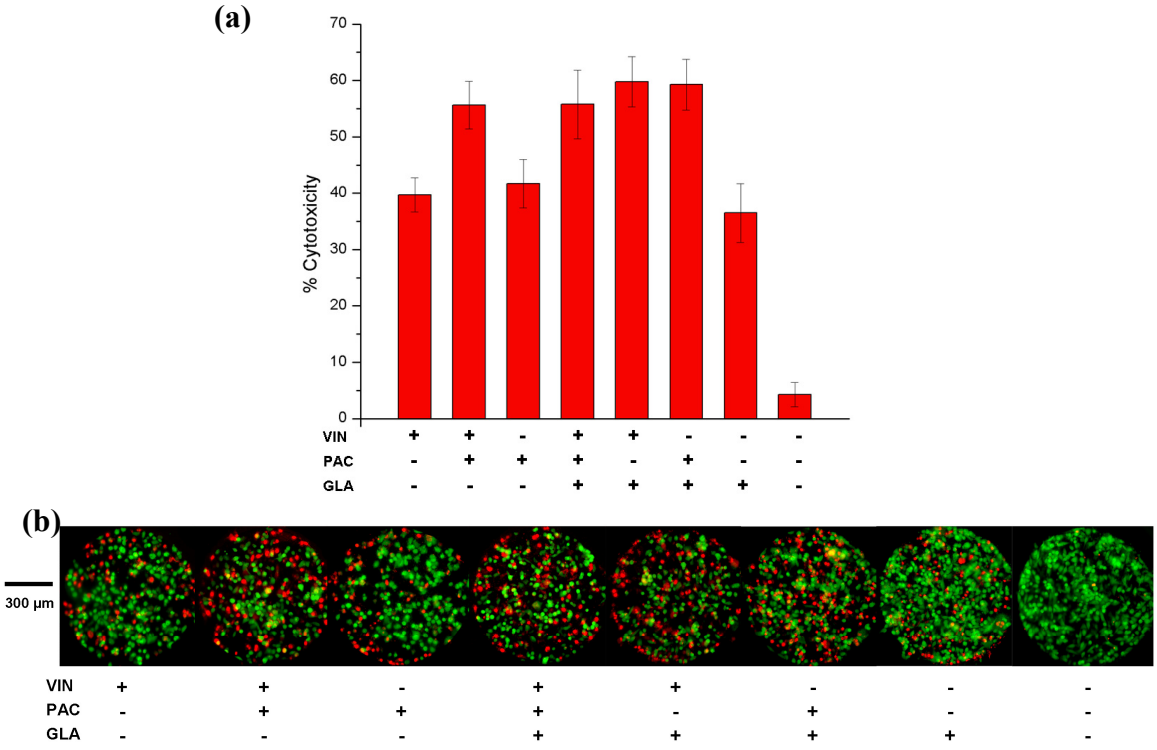

Figure 4-17. Result of the assay for exposing breast cancer cells, MDA-MB-231, to chemotherapeutic agents, vinorelbine (VIN), paclitaxel (PAC), and γ-linolenic acid (GLA). (a) Plot of cytotoxicity of the cells. Results are the means ± standard deviation (SD). Number of experiments = 6. (b) Cells in each chamber after live (green)/dead (red) staining.

This device successfully demonstrated that with just three inputs, eight distinct cell-based assay experiments were performed with different combinatorial compounds using a single chip. The cell seeding was simple and efficient as the one-to-eight splitter loaded cells to all chambers at once and the porous membrane trapped the cells at the chambers. Using the integrated combinatorial mixer saved numerous pipetting steps that have to be done to create all the possible combinations. While only three compounds were used on this chip, the chip can be scaled up using the same fabrication steps to include four, five or even more inputs by placing the overpass structure to cross over

channels. This will result in a high-density chip that is able to perform hundreds of assays at once and greatly simplify the complexity of the experiments. In addition, chip-based assays will provide a cheaper alternative to using robotics and well plates and provide finer and more sophisticated fluid control. This microfluidic device also creates culture environment that mimics interstitial environment by creating two flow levels and maintaining the cells at the diffusion dominated level with minimized fluid velocity. With this device, the experiment did not require many complicated external apparatus and setups, and only syringe pumps were used for fluid delivery and fluorescence microscope for imaging the cells. This will allow the whole systems to be simply automated with dispensing and imaging systems in the future. Besides performing viability assay, metabolites or gene expression can also be studied on-chip. Moreover, other chip components such as flow cytometer or HPLC, which have been demonstrated in our group, can be integrated to create a complete cell-based assay platform for quantitative cell biology experiments.

4.4 Conclusion

In this chapter, the development of an integrated 3-D microfluidic device on glass for cell-based screening of combinatorial compounds on-chip was discussed. The Parylene-based chip was fabricated using multilayer surface micromachining technology and integrated with a PDMS chip and porous PET (polyethylene terephthalate) membrane. The combinatorial mixer correctly delivered the distinct combinations of input compounds into the chambers and the concentration of each input compound at the chamber was characterized. The incorporated membrane created a cell culture space

with minimized flow velocity and simplified the cell loading and assaying procedure. The fabricated chip had three inputs for combinatorial mixer with one control, and output eight combinatorial streams to the culture arrays. We have demonstrated quantitative cell-based assay for screening three different compounds' ability to reduce cytotoxicity of hydrogen peroxide and assaying combinatorial exposures of three chemotherapeutic agents on breast cancer cells. Based on the capabilities demonstrated in this chapter, devices with high-density cell array and integrated high-input combinatorial mixer can be constructed. Such chip will enable inexpensive high-throughput cell-based assay and significantly benefit research in many different fields including drug screening and systems biology.

Chapter 5: Monolithic Multilevel Microfluidic Networks with Integrated Membrane

5.1 Introduction

In the previous chapter, a microfluidic device that incorporated a membrane structure was presented. The membrane facilitated the cell culture and assay process while creating a cell culture space that can mimic *in vivo* conditions. The straightforward method to incorporate the membrane only required clamping a piece of commercially available membrane in between a PDMS piece and the Parylene-based chip. Such incorporation method was simple but required a membrane to be placed manually every time before experiment. It is advantageous to devise a process that integrates the membrane structure during the 3-D microfluidic fabrication. As the use of membrane with microfluidic device is gaining popularity, such fabrication technique can benefit research in that area and improve the ease of use of microfluidic devices. 3-D microfluidic devices have already broadened the range of possible applications from 2-D microfluidic devices and adding a membrane feature can further add to the versatility of the microfluidic devices. The use of membrane with microfluidic will be introduced and several fabrication strategies will be presented.

The use of membrane as a mean of transport control in microfluidic has grown in the past 15 years [98]. One popular use of membrane is in sample preparation. Song et al. used a laser-patterned nanoporous membrane at the junction of a cross channel to concentrate the proteins with a concentration factor of 2 to 4 [99]. Samples were moved by electrophoretic injection and buffer can pass through membrane while proteins were

maintained. Timmer et al. fabricated a device to increase electrolyte concentration by evaporation [100]. A microchannel was covered with Teflon membrane and nitrogen was flowed over the channel. Samples were concentrated as the water vapor can pass through the membrane. Furthermore, membrane has been used for sample filtration on-chip such as demonstrated by Moorthy et al. to filter blood cells [101]. Researchers have integrated membrane on chemical reactor devices on-chip. Cui et al. fabricated a membrane microreactor for the dehydrogenation of cyclohexane to benzene [102]. In addition, membranes can function as a surface for gas molecule absorption in gas sensors. PDMS has a high permeability for gases and has been used in oxygen sensors as demonstrated by Vollmer et al. [103]. Also, PDMS has been used as the material for constructing microfluidic cell culture device because oxygen can easily transport across the PDMS. Besides cell culturing, devices have also be made to study oxygen consumption by organisms such as E. coli [104].

Various fabrication technologies have been developed to incorporate membrane into microfluidic devices to fulfill different applications. One of the most straightforward methods is by direct incorporation such as our clamping method described in the previous chapter. Besides clamping, membranes can also be incorporated by lamination [105]. The membrane can be prepared in-house or bought from commercial sources, and can be modified by functionalization such as coating with bovine serum albumin [106]. One major advantage of using the direct incorporation method is the range of different membranes that can be obtained. Membrane with different materials and morphologies can be chosen to suit the need of the particular experiment. The downsides of such method are that 1) care must be taken to ensure that leaking would not occur and 2) such

fabrication technique will be challenging to scale up for large-scale production. Membranes can be integrated as part of the device fabrication process. For example, free-standing porous silicon as membrane on top of microchannel can be fabricated by electrochemically forming the porous silicon and undercutting the silicon substrate to release the channel and membrane [107]. Other materials, such as alumina, can be formed as free-standing membrane [108]. Silicon wafer was coated with SiN from both sides and the backside SiN was etched away, followed by Si etching. Al was sputtered and turned into porous structure by anodization. While using cleanroom process is more expensive and complex than direct incorporation, such technology has other advantages. It has precise control over the features to the nanometer range, and more chemical and thermal resistant materials are often used for microfabrication. Furthermore, sealing of the device is more reliable using this method. Another way of integrating membrane is by fabricating the membrane *in situ* after the microfluidic chip is fabricated. Artificial lipid bilayers, which is useful for studying transport of materials across cell walls can be prepared at an aperture of a chip by contacting lipid solution with buffers [109]. An UV laser beam has been used to induce phase separation of acrylate monomers to form membrane in between two pillars [110]. While this method offers the possibility to build in membrane on existing chip, the process is very complex and has a very limited range of materials to choose from. Finally, the material used to build channel walls can be used as membrane as well. For example, PDMS channels are permeable to gases. Hydrogel such as calcium alginate has also been used to construct microfluidic channel walls and are permeable to solutes such as dextran [111]. This method of integration is simple and no extra fabrication steps are required.

The fabrication process to construct monolithic 3-D microfluidic networks presented in previous chapters can be modified to integrate a membrane structure inside the devices. Here, we expand this technology to create an integrated membrane at the interface of the microfluidic channels. Surface micromachining enables chips to be conveniently batch fabricated and the integrated method avoids sealing problems when incorporating membrane into devices. In addition, integration with 3-D microfluidic networks expands the complexity of applications for membrane devices. The channels are made up of biocompatible Parylene C and are suitable for biological experiments. The device has two-layer microfluidic channels with a porous membrane in between. In this chapter, the fabrication techniques are discussed and the applications of such fabrication process are demonstrated. The membrane-based microfluidic device can be used for constructing *in vivo*-like culture chamber and can be used for cell co-culture.

5.2 Experimental

5.2.1 Design

Our device is composed of two-level microfluidic networks and a membrane structure that is positioned in between the two microfluidic channels (Figure 5-1). Each microfluidic level has its own inlet and outlet ports for sample introduction. Parylene C is chosen as the structural material because of its compatibility with surface micromachining processes, which enables 3-D microfluidic networks to be fabricated monolithically. Other advantageous properties of Parylene C include its biocompatibility, optical transparency and chemical inertness. The device is built on a glass substrate for ease of observation by microscopy.

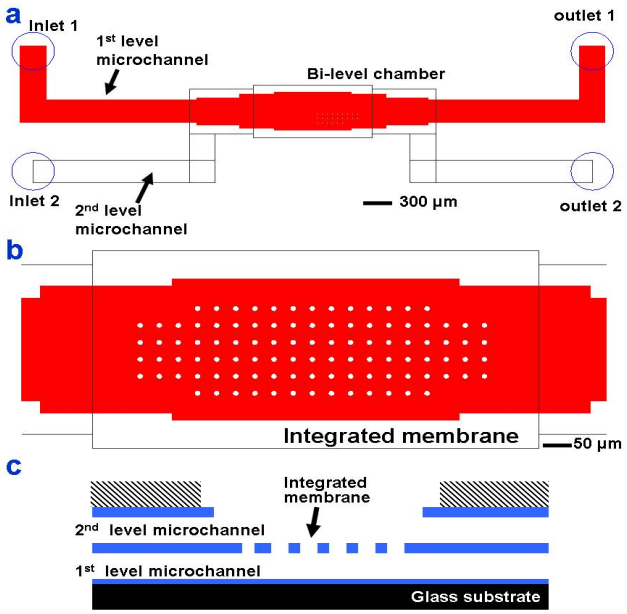

Figure 5-1. Design layout of the monolithic multilevel microfluidic device with integrated membrane. (a) Top view. (b) Bi-level chamber with integrated membrane in between the two fluidic levels. (c) Cross section view of the device.

5.2.2 Fabrication

The fabrication process is shown in Figure 5-2. Soda Lime glass wafer was cleaned with Piranha solution (H_2SO_4: H_2O_2, H_2O, 5:1:1) at 120°C for 5 minutes and treated with A-174 silane adhesion promoter for 15 minutes. Then, the entire wafer was coated with Parylene C (2 µm). A first sacrificial photoresist (15 µm) was spin-coated and patterned with photolithography. A second layer of Parylene (10 µm) was deposited to cover the sacrificial photoresist. Parylene was patterned using oxygen plasma at the chamber area to create pores in the membrane. By modifying the mask of this pattering step, membranes with different pore sizes can be created, and membranes with 10, 20, and 40 µm pores were made. A second sacrificial photoresist (30 µm) was defined for the second-level channels. A third layer Parylene was deposited and patterned, followed by chip planarization with SU8 (100 µm). The chips were soaked in isopropyl alcohol

(IPA) to dissolve the sacrificial photoresist, and the remaining hollow Parylene structures became the fluidic networks.

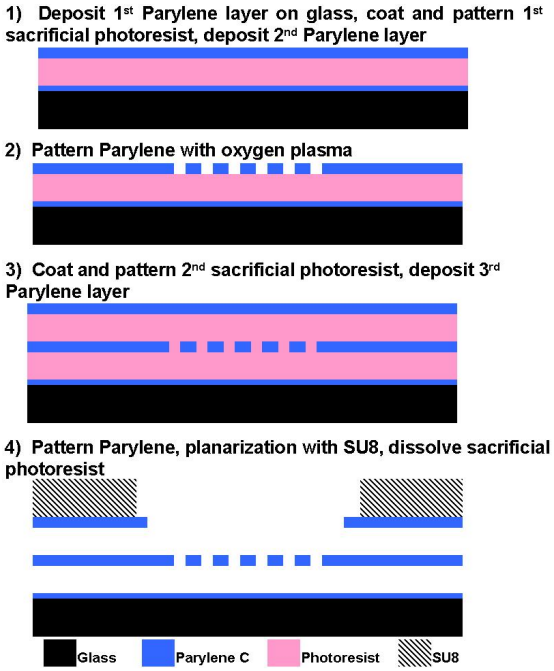

Figure 5-2. Fabrication process flow for the monolithic multilevel microfluidic device with integrated membrane.

Similar packaging method as described in the previous chapter was used. A piece of PDMS with punched holes was aligned onto the chip. The chip and PDMS were clamped together by two pieces of transparent acrylic. Tubes were plugged into the holes of the PDMS and on-chip experiments can be observed with a microscope (Figure 5-3).

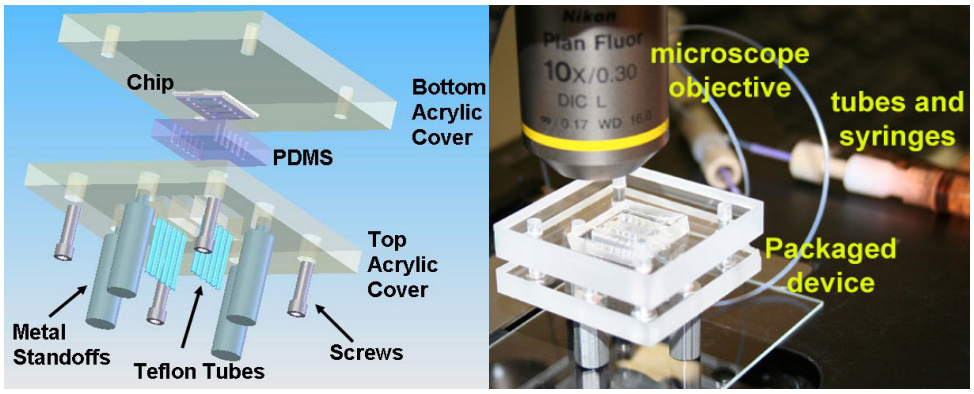

Figure 5-3. Device packaging and testing setup for the monolithic multilevel microfluidic device with integrated membrane.

5.3 Results and Discussion

Figure 5-4 shows the fabricated chip after the sacrificial photoresist was dissolved. Chips with different sizes of pore diameter (10, 20, and 40 μm) were created. Pore sizes can be conveniently adjusted by changing the design of the photolithography mask and smaller size of pores down to 4 μm can be created [112]. Asides from oxygen plasma, laser has also been used to etch Parylene to create pores [113]. To create submicron pores, techniques such as e-beam photolithography can be used. Using our fabrication technique, membranes were conveniently created in 3-D microfluidic network during fabrication. As a result, sealing of the membrane to prevent leaking would not be a concern as in direct incorporation methods. At the bi-level chamber area, the roof of the channel was etched open, but that part can remain if that is desirable for certain applications. Also, more levels of channels can be made by repeating the process of patterning sacrificial photoresist, covering with Parylene, etching Parylene to create pores, patterning sacrificial photoresist, covering with Parylene, etching Parylene and so on. Device packaging followed the straightforward method that was presented in earlier

chapters. Food coloring was injected into the first-level channel and was shown to readily enter the second-level channel (Figure 5-4 (c)).

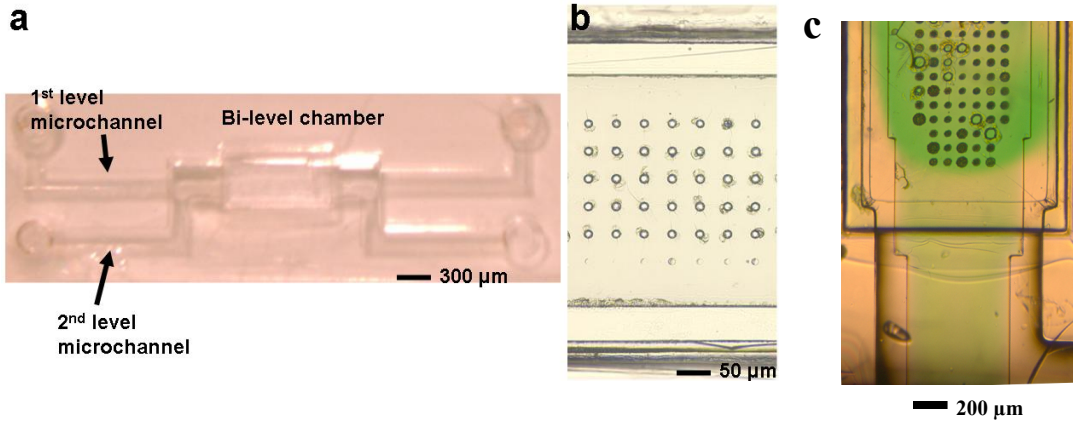

Figure 5-4. Fabricated monolithic multilevel microfluidic device with integrated membrane. (a) Chip after channel release. (b) Integrated membrane with 10 µm pores. (c) Green solution injected into the first-level channel can enter the second-level channel through the membrane.

As discussed in the previous chapter, integrating a membrane in between multilevel microfluidic networks can be used to create a culture chamber that mimics the *in vivo* tissue environment, where transport of molecules to the cells is dominated by diffusion (Figure 5-5). The cells can be loaded into the cell culture level, while fluid is delivered into the other level. As the cell culture chamber is separated from the fluid delivery channel, shear stress, which can be detrimental to many types of cells, is minimized. A fluid velocity profile simulation was done using COMSOL Multiphysics incompressible Navier-Stokes model and the result shows that the flow velocity inside the culture chamber is minimal (Figure 5-5). In addition, with this configuration, culture media components delivered into the chamber during perfusion can achieve a uniform distribution as the fluid velocity inside the chamber is uniform. Also, in conventional culture containers such as culture flasks, secreted molecules by cells are swept away in

random direction by convection as the large air/liquid surface results in significant convection. Such secreted molecules can play an important signaling role in governing cellular behaviors such as cancer cell development *in vivo* [114]. While those molecules are randomly distributed in tradition culture vessels, microfluidic device can recreate the condition where those molecules remain close by the cells. Our device presents the opportunities for studies to be done to examine how soluble factors from one cell can influence the surrounding cells. The diffusion dominated cell culture space allows secreted factors be remained inside the chamber without getting swept away by convection.

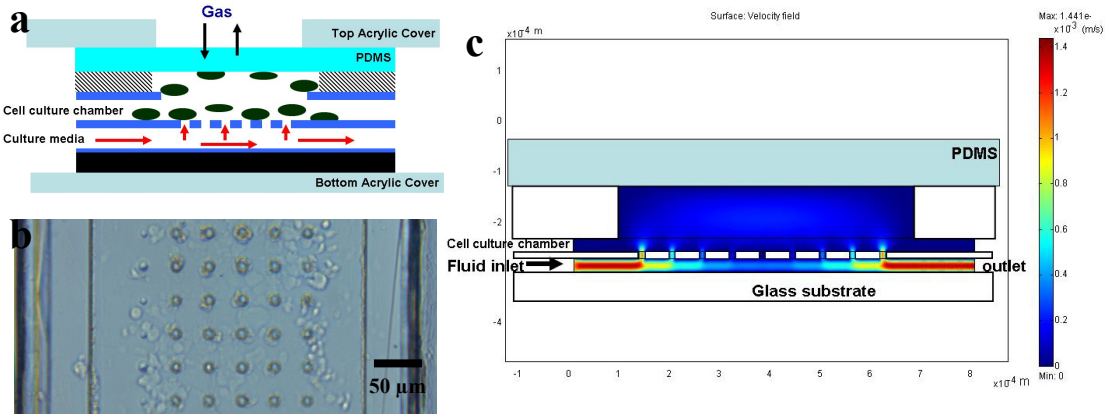

Figure 5-5. Bi-level cell culture chamber. (a) Device operation. (b) Cells inside the second-level chamber. (c) Fluid velocity simulation.

Another application for the device is for use in on-chip cell co-culture. Co-culture has been a common method to maintain cell phenotype *in vitro*, such as co-culture of embryonic stem cells with murine embryonic fibroblasts [115], or in studying cell-cell interactions [116]. Using a microfluidic device can simplify the process to create the co-culture configuration, reduce the cells needed for the experiment and recreate a more *in vivo*-like condition. In our device, different cells can be loaded into different levels of chamber, and the membrane allows communication between the two levels (Figure 5-6).

For the proof-of-concept experiment, rat neuroblastoma cells, B35, were stained with green fluorescent calcein AM or orange fluorescent molecule, CellTracker Orange CMTMR (5-(and-6)-(((4-chloromethyl)benzoyl)amino)tetramethylrhodamine) from Invitrogen (Carlsbad, Ca). The cells were loaded into the different level of channels. More levels of channels can be constructed to simulate complex *in vivo* microstructures such as the three-layer structure (adventitia, media, and intima) of a blood vessel [117].

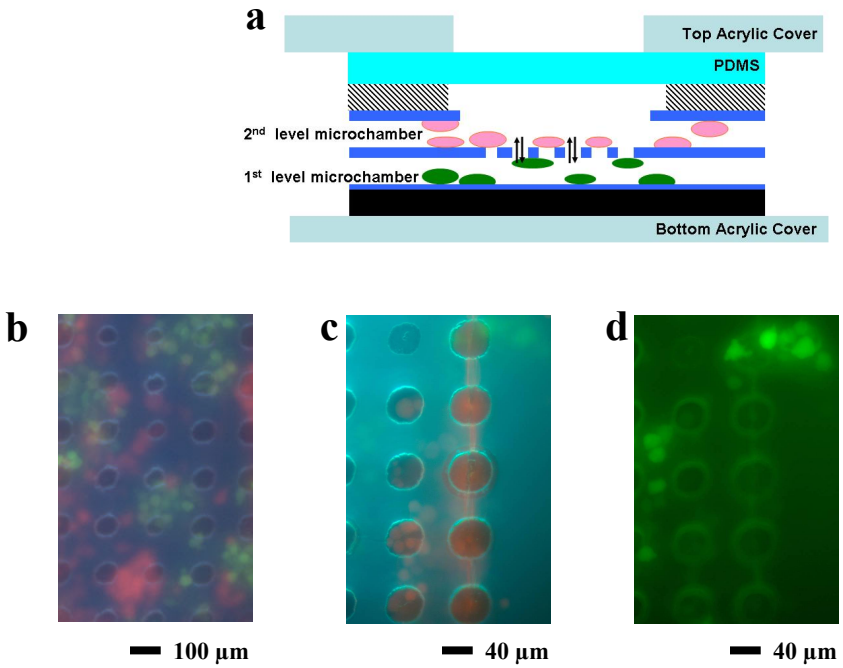

Figure 5-6. Device for on-chip cell co-culture. (a) Schematic of device operation for co-culture. (b) Different cells were loaded into the different levels of channels. (c) Cells fluorescing orange are underneath the membrane. (d) Cells fluorescing green are on top of the membrane.

5.4 Conclusion

In this chapter, we demonstrated a new method of fabricating monolithic 3-D microfluidic devices with an integrated Parylene membrane. Our fabrication method enables devices to be conveniently fabricated at the wafer scale, and our device can be integrated with other microfluidic components to build complete lab-on-a-chip systems.

Using this method, membranes no longer need to be placed into the device assembly manually before each experiment, and pore sizes can be varied by changing the mask design. Two possible applications for this device were proposed and preliminary results were shown. This device can have other applications beyond the field of cell biology, such as performing experiments in analytical chemistry for sample filtration or concentration.

Chapter 6: Applications of Microfluidics in Marine Microbiology

6.1 Introduction

The uses of microfluidic devices are not limited to cell culture and cell-based assay for mammalian cells as discussed in previous chapters. Any other types of cells can take advantage of the benefits that microfluidic devices offer: high-throughput screening, portability, inexpensive platform, and reduced sample volume and reagents. Under the collaboration with Dr. David Caron's group at University of Southern California's Department of Biological Sciences, one area that our group has applied microfluidic devices to is in the field of marine biology, specifically in studying algal bloom and toxin production by algae. Algal bloom and toxins produced by different algae have always caused problems to the environment and marine ecology. Due to certain favorable changes in environmental conditions, some algae can increase to a large density in a short period of time. For example, many studies have shown a strong correlation between phosphorus loading and phytoplankton production in freshwater [118]. Some produced toxin and can directly cause sickness or death of organisms such as shellfishes that feed on the algae. The phosphorus can originate from excess nutrients in fertilizers that enter the river or sea during water runoff. More importantly, when large quantity of those contaminated shellfishes was consumed by organisms in higher order of the food chain, fatalities often resulted. For example, *Alexandrium tamarense*, can produce saxitoxin and cause paralytic shellfish poisoning [119]. Non-toxic algal bloom can lead to harmful effects by disrupting food chains.

Pseudo-nitzschia is one type of algae that produces a neural toxin called domoic acid, which when transferred through the food chain causes sickness and mortality in marine mammals, seabirds and even humans [120]. Perl et al. reported an outbreak of domoic acid intoxication in Canada in late 1987 that led to illness of 107 adults and death of three elderly people [121]. Mussels were contaminated and resulted in amnesic shellfish poisoning with symptoms of gastrointestinal and neurological disorders. Also, domoic acid has been linked to the death of numerous sea lions along the California coastline in 1998 [122].

Domoic acid is a neural toxin that affects animals with complex central nervous systems. Domoic acid is structurally analogous to neural transmitter glutamic acid, which is present in nearly 40% of all neuronal synaptic sites, and upon binding to receptors, domoic acid prolongs receptor activation and excessive cation influx. This uncontrolled influx can cause nerve cells to degenerate. During *Pseudo-nitzschia* bloom, domoic acid is not always produced. In another word, growth of algae does not equal domoic acid production. Studies done by other groups have suggested that many factors might induce or suppress algae to produce toxin. Maldonado el al. reported that deficiency in iron and copper can induce domoic acid production [123]. Silicate depletion has been shown to cause increase in domoic acid production [124]. It has been suggested that high phosphate level can lead to increased domoic acid production [125]. Bacteria strains have also been shown to increase domoic acid production by as much as 95-fold [126]. Yet, exact causes are unclear and there are numerous possible factors that can cause toxin production. To completely elucidate the causes of toxin production,

many potential compounds will have to be screened. This leads to an enormous number of experiments to be performed and large quantity of reagents and cells to be used.

To facilitate progress in marine biology research and speed up the process of screening for possible factors inducing toxin production, we would like to make a chip to culture *Pseudo-nitzschia* under different growing conditions. The toxin will be detected using ELISA method or an ultra sensitive optical sensor being developed at Dr. Chih-Ming Ho's lab at University of California at Los Angeles. The current state-of-the-art detection technology indicates that per cell toxin load may range over 2 or 3 orders of magnitude but its sensitivity is limited since a sample size of at least 100 cells/mL is required. The new optical sensor will be able to push the sensitivity to 10 cells/mL or to even single molecule of domoic acid. The algal cells will be trapped and cultured on-chip and combinatorial mixer discussed in chapter 3 and 4 will be used to expose algal cells to different conditions. Cellular contents will be extracted for detection of toxin from lysates.

In this chapter, the development of the applications of microfluidic cell-based assaying device for studying toxin production by algae is discussed. As most algal cells are not adherent like the mammalian cells used in previous experiments, on-chip traps were needed to contain floating cells like algal cells inside the micro chambers. Various trapping designs will be presented and the developed trapping protocol will be discussed. The method to maintain algae in a healthy state and to culture algae on-chip has been developed. As the presence of the intracellular toxin, domoic acid, cannot be directly monitored on-chip, a method to lyse the cells on-chip is presented.

6.2 Trapping Algal Cells On-Chip

6.2.1 Trapping Cells with Parylene Posts Inside Micro Culture Chamber

The first-generation cell culture chip with combinatorial mixer on silicon substrate described in chapter 3 was equipped with filter structure designed to contain floating cells. The trap is consisted of two rows of rectangular post structures with gap in between and the configuration is shown in Figure 6-1. Each post has a length of 20 μm and width of 10 μm. The gap in between each post is 12 μm and is designed to trap cells larger than that dimension. To fabricate the chamber with traps, photoresist (AZ 4620) was first spin-coated on silicon wafer at thickness of 32 μm and soft-baked at 100°C for 30 minutes. Then, the post areas were exposed and developed, leaving an array of holes on the photoresist. Those holes were then filled with Parylene C during the subsequent Parylene deposition (10 μm). After the sacrificial photoresist was dissolved with isopropyl alcohol, the Parylene posts remained.

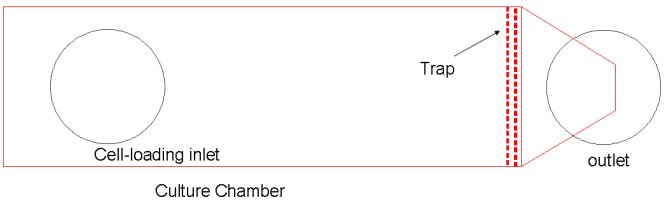

Figure 6-1. Configuration of the trap inside the culture chamber of the first-generation cell culture chip with combinatorial mixer.

Figure 6-2 shows the SEM image of the cross section of the culture chamber with filter. We were able to integrate filter into the chip without adding extra fabrication steps as the sacrificial photoresist patterning and Parylene deposition was already part of the fabrication process to construct the culture chambers.

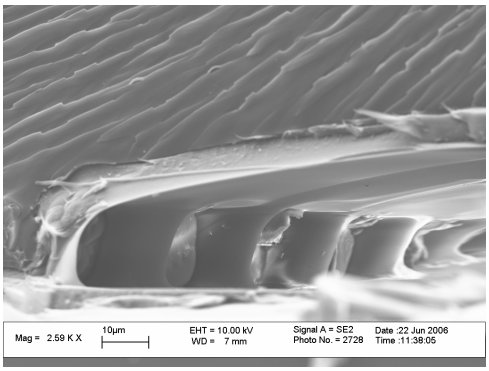

Figure 6-2. SEM image of the Parylene post filter structure.

We tested the filter by first using the algae *Prorocentrum gracile* as a model. *Prorocentrum gracile* was chosen because it constantly swims around the space it resides in and such high mobility is a good indication of healthy cells. Solution containing the cells was injected into the cell loading inlet and image of the chamber was taken with a stereoscope equipped with a CCD camera. Results show that the chamber was able to contain algal cells as shown in Figure 6-3. However, the *Prorocentrum gracile* cells appeared to be stationary and not constantly moving around as in typical healthy cells. Some possible reasons might be that the cells dislike the loading conditions such as the material of the tubes or culture chamber or the loading pressure. Another reason might be that the culture chamber height of 32 µm was too low and some cells were in contact with the walls which impede the cells from moving around. A cell culture chamber with higher ceiling might improve this situation.

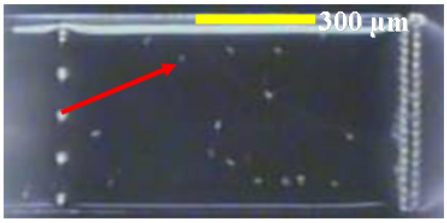

Figure 6-3. *Prorocentrum gracile* inside the Parylene culture chamber. Arrow indicates one of the cells.

6.2.2 Trapping Cells with PDMS Structures

To investigate whether chamber height can affect compatibility for algal cell culture, culture chamber with higher ceiling (100 µm) was fabricated using PDMS. PDMS was used because it involved very short fabrication steps so different prototypes can be made quickly and various designs can be tested in a short period of time. The PDMS pieces were made following the same protocol as described in chapter 4. To make the post structures, holes were made during patterning of the SU8 for the mold fabrication. When PDMS was casted onto the mold, it filled the holes and became the post structures after PDMS was cured. The cured PDMS was peeled off from the mold and cut into pieces. The PDMS pieces were cleaned with acetone, then isopropyl alcohol, followed by water. The PDMS pieces were reversibly bonded to glass slides by treating both glass slides and PDMS pieces with oxygen plasma (50 Watts, 400 mTorr), and pressing the PDMS pieces onto the glass slides. The assembly was baked in oven at 70^{o}C for three hours. Figure 6-4 shows a fabricated device. The posts consisted of square PDMS structure with dimension of 120 µm × 120 µm and the gaps between each post are 10–20 µm.

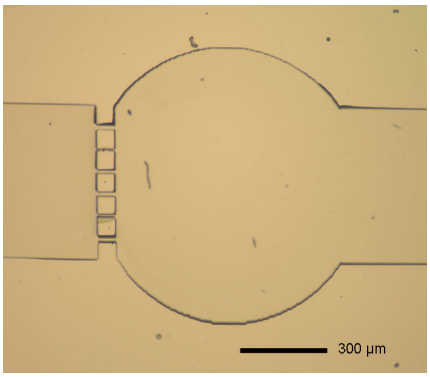

Figure 6-4. PDMS chamber with 100 µm height ceiling.

Prorocentrum gracile cells were loaded into the chamber. As shown in Figure 6-5, series of pictures were taken at different times and the result showed that the cells appeared to be healthy as they moved around constantly. Chamber height of 100 µm was suitable for culturing this type of algae and cells were not stuck by the channel walls and had room to float around.

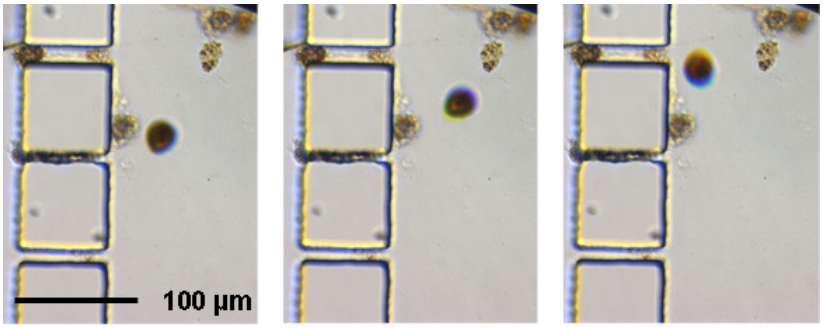

Figure 6-5. Images of *Prorocentrum gracile* inside the culture chamber at different times.

Following the creation of the trap that can successfully contain algal cells in a healthy state, the next step was to create trap to contain *Pseudo-nitzschia*. Unlike *Prorocentrum gracil*e and typical mammalian cells, *Pseudo-nitzschia* has a long, slender, rod shape. The width of the cell is around 2–10 µm while the length is 50–150 µm [127, 128]. In addition, this type of cell can form into a chain with one cell attaching to the other and can reach a total length of 1 mm. One possible trap configuration that has been explored utilizes an array of posts to trap the slender cells and the schematic is shown in Figure 6-6. While the gaps in between the trapping posts are wider than the cell width, because the cells are long, they are not able to make the turn to escape the array of posts.

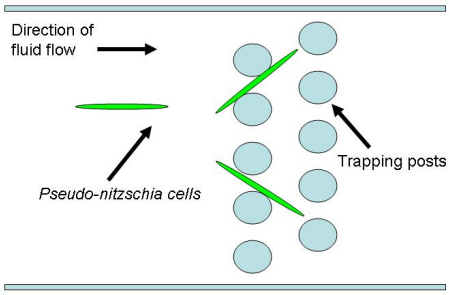

Figure 6-6. Schematic of the trap geometry used to contain *Pseudo-nitzschia.*

The trap fabrication was based on the same PDMS micro-molding process as described previously. The chamber height was 100 µm. Each circular post had a diameter of 30 µm and a gap between posts of 30 µm. Four arrays were included with each array shifted by 30 µm horizontally and by 30 µm vertically. *Pseudo-nitzschia pungens* were loaded into syringe and injected into the chamber at high and low concentration. Figure 6-7 shows *Pseudo-nitzschia pungens* inside the chamber at low concentration and Figure 6-8 shows the cells loaded at high concentration. The trapping geometry was able to trap the long and slender *Pseudo-nitzschia* and the number of cells inside the chamber can be adjusted by changing the cell concentration for loading.

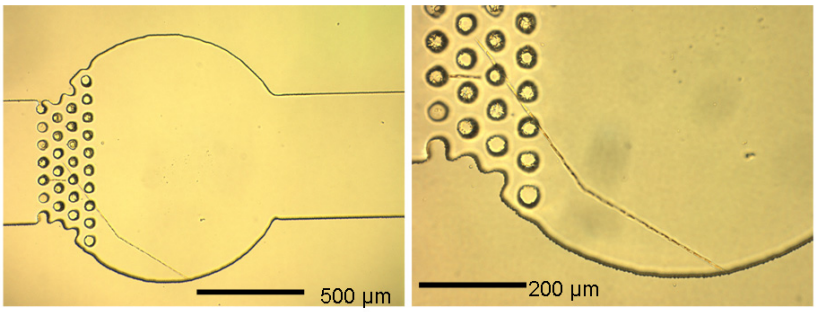

Figure 6-7. *Pseudo-nitzschia pungens* loaded inside the chamber at low concentration. Images taken at different magnification.

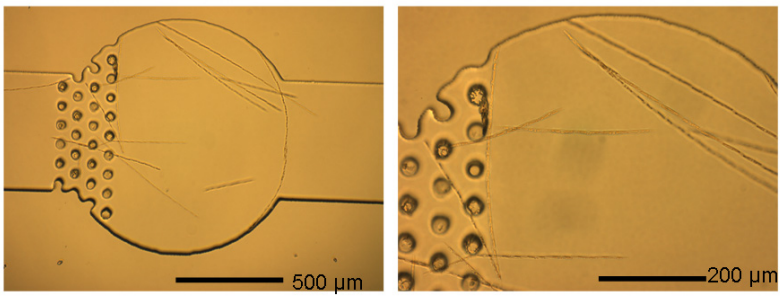

Figure 6-8. *Pseudo-nitzschia pungens* loaded inside the chamber at high concentration. Images taken at different magnification.

6.2.3 Trapping Algal Cells with Membrane-Based Systems

With the successful development of a membrane-based cell culture system as described in chapter 4, it became also possible to trap algae using that system. The membrane with pore size of 1 µm was used and the device was packaged with PDMS microfluidic chip and Parylene-based chip as described in chapter 4. *Chattonella marina* and *Pseudo-nitzschia pungens* were loaded into the chamber. As seen in Figure 6-9, both types of cells were successfully trapped inside the culture chamber. *Chattonella marina* cells were mobile like *Prorocentrum gracile* and they appeared to be moving around constantly inside the chamber, indicating that they were in a healthy state. The membrane-based systems offer a simple and reliable method to maintain algal cells on-chip and the wide selection of membranes can make trapping cell of any sizes possible. After each experiment, the membrane can be disposed and new membrane can be used for the new experiment to prevent any contamination from previous experiment and possible clogging of the membranes by the cells.

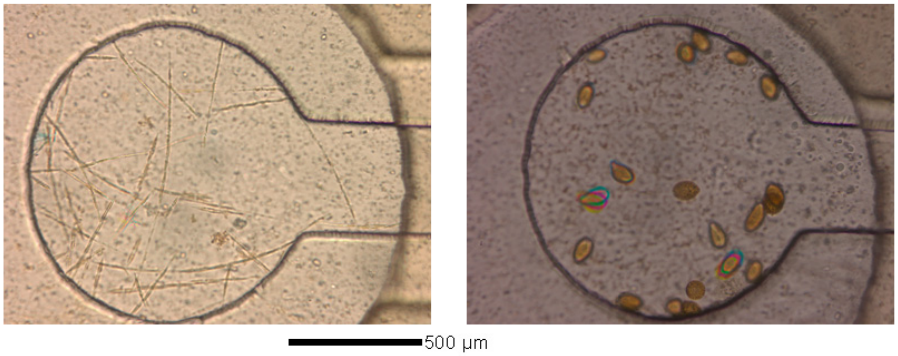

Figure 6-9. *Pseudo-nitzschia pungens* (left) and *Chattonella marina* (right) loaded into membrane-based chamber.

6.3 Culturing of Algae On-Chip

Experiment was done to test if algal cells can be sustained on-chip. Membrane-based device was used with the 1 µm pore size membrane and packaged in the same method as described in chapter 4. The device was then primed with DI water followed by culture media, F/2 + Si. Device operation is shown in Figure 6-10. *Chattonella marina* and *Pseudo-nitzschia pungens* were loaded into the culture chamber, and culture media, F/2 + Si, was injected via the cell loading inlet at flow rate of 80 nL min^{-1}. The chip was placed inside a refrigerator with temperature set at 15–20^{o}C. The refrigerator was fitted with a fluorescent light bulb (580 lumens, 10 watts, 4100K) and a controller to set a 12 hour light and 12 hour dark cycle.

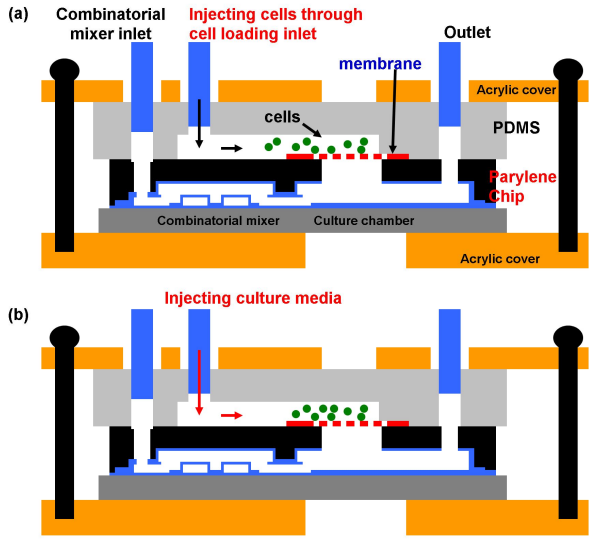

Figure 6-10. Device operation schematic for the culture of algal cells on-chip.

Figure 6-11 shows the image of *Pseudo-nitzschia pungens* inside the culture chamber at different times. The cells were able to proliferate inside the culture chamber under constant perfusion condition as seen in the increase in number of cells. Figure 6-12 shows the *Chattonella marina* inside the culture chamber at different times. The cells proliferated from 0 to 24 hour, but the number remained static afterwards. The cells were still moving around constantly and appeared to be in a healthy state.

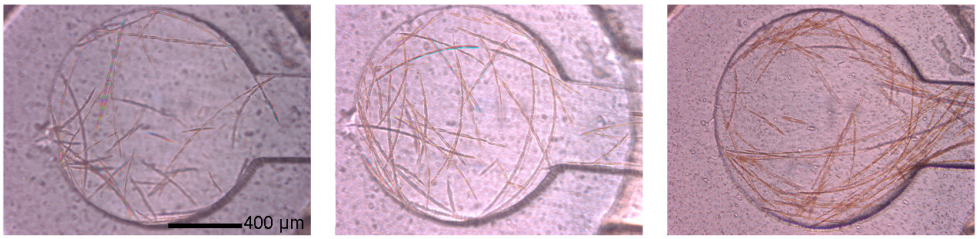

Figure 6-11. *Pseudo-nitzschia pungens* inside the culture chamber at different times.

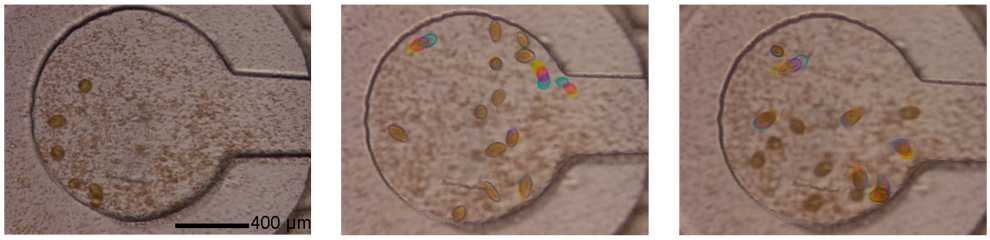

Figure 6-12. *Chattonella marina* inside the culture chamber at different times.

6.4 Lysis of Algae On-Chip

The algal cells loaded on the chip will be cultured and exposed to variation of culture media. Then, their intracellular contents such as toxin would be analyzed. To analyze the intracellular content, the cells will have to be lysed and the lysate will be transported out of the chip for analysis. A straightforward way to lyse the cells on-chip using external ultrasonicator is presented in this section.

The membrane-based device was used with the 1 µm pore size membrane and the fluidic networks were primed with DI water, followed by culture media, F/2 + Si. *Pseudo-nitzschia pungens* were loaded into the chip and the whole packaged device was put into an ultrasonicator, PC3 by L&R (Kearny, NJ), with power of 70 watts and frequency of 55 kHz. The water level inside the ultrasonicator bath is approximately 1 cm, or almost covering the whole thickness of the bottom acrylic piece. The ultrasonicator was turned on and image of the culture chamber was taken at 0, 10, 30 and 50 seconds.

Figure 6-13 shows the result of the ultrasonication. The algal cells gradually lost their color as the cell membranes and cell walls were disrupted by the ultrasonication and the chlorophyll came out from the cells. One can still see some shell-like structures with

very faint color at 30 second, but they all eventually disappeared after 50 seconds, indicating complete lysis of the cells. The lysate can then be delivered out of the cells by injecting air through the inlet and collecting the liquids at the outlet.

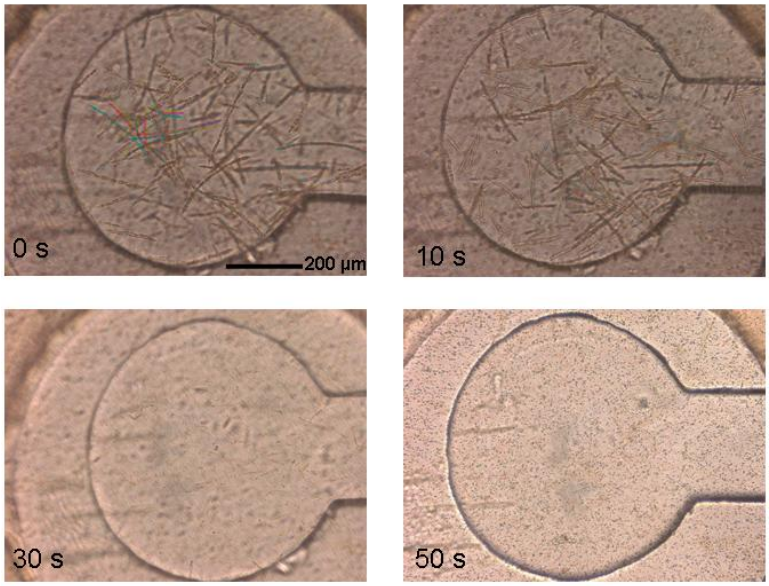

Figure 6-13. Results of the ultrasonication for cell lysis at different times.

6.5 Conclusion

Applications of microfluidic devices for marine microbiology have been demonstrated. Various schemes for trapping cells have been developed and the method to maintain algal cells inside the micro culture chamber in healthy states has been presented. Culture of algal cells has also been performed. On-chip lysis of the cells has been done using an ultrasonicator. Integration of this device with toxin detector in the future will enable high-throughput screening of factors that induce toxin production by algae.

Chapter 7: Conclusion

Cell culture and cell-based assay have been key techniques in different fields including pharmaceutical industry, cell biology and tissue engineering. Cell culture was a method invented over a century ago and has undergone continuous refinements and several breakthroughs. Various advancements were made to use cells for performing assays, and development of sophisticated call-based assays revealed a wealth of information from cellular studies. The complex behavior of cell-cell interactions and molecular components of the cells were discovered, making cell-based assay an invaluable tool. As the demand for high-throughput screening rises, conventional techniques such as well plates and robotics have been continuously engineered and improved to meet the demand. However, these techniques suffered from drawbacks such as limited liquid handling ability, inability to scale up well plate density past 1,536 wells per plate, and high costs of equipments and operations.

Microfluidic emerges as a promising platform to perform cell culture and cell-based assay in a high-throughput manner. Microfluidic devices hold several distinct advantageous properties including high-throughput, mass fabrication capability, and reduction of reagents, cells and cost. For cell culture use, microfluidic devices have the ability to build culturing environment mimicking the microenvironment that cells reside *in vivo*. Microfluidic, with immense potential, is still a young field with some commercialized products. It was derived from MEMS, which itself was originated from silicon semiconductor fabrication technology, but eventually became a major research area of its own. Dramatic increases in publications and new start-up companies showed

the burgeoning of the field and growing interest. The application of microfluidic has expanded and demonstrated uses in analytical chemistry, biology, forensics and diagnostics. In this thesis, a novel cell-based assay on-chip is presented.

Microfluidic cell culture devices have been created and are still part of ongoing researches in different groups in academia. Many of the other devices being developed can only expose cells to a single compound at once. However, cells are sustained in complex environments and received multiple environmental cues simultaneously. Also, combined drugs for treatment of diseases such as cancer and HIV have been promising. To screen for the combined effects of multiple compounds at once, an integrated combinatorial mixer is necessary. Such structure would require fabrication of three-dimensional (3-D) microfluidic networks. In this work, an integrated method is presented to monolithically fabricate 3-D microfluidic networks without performing bonding process as in many other methods for 3-D microfluidic fabrication. The fabrication is based on the surface micromachining of biocompatible Parylene C. Such fabrication process presented here can be adopted to create microfluidic chips with complex networks and combinatorial mixer with large number of inlets and outlets. We first developed a chip on silicon with a three-input combinatorial mixer plus one unmixed control and eight outputs to the cell culture arrays. Fluidic packaging scheme was developed and combinatorial mixing was demonstrated. Cell culture was successfully done using this device and cell treatment with the combinatorial mixer was performed. To improve ease of use of the device for cell-based assay, another device based on glass substrate was fabricated, and a method to integrate a membrane into the device was used. The membrane created a cell culture environment similar to that of *in vivo* cell culture

conditions and also facilitated the cell loading and cell assaying process. Cell-based assays were performed using this device by screening for the ability of compounds to reduce cytotoxicity of hydrogen peroxide and combinatorial exposure of chemotherapeutic agents.

Our 3-D microfluidic fabrication method was extended to make multilayer microfluidic networks with an integrated membrane. Our method offers the ability to create a monolithic device, and integrating membrane with 3-D microfluidic also expands the functionality of membrane-based microfluidic devices. Besides mammalian cells, microfluidic devices can be used for marine biology. Algal cell trapping, culturing and lysis were demonstrated in microfluidic devices with the eventual goal of making an integrated system to screen for the factors that induce toxin production.

Our microfluidic devices were designed for cellular studies, but it is possible to extend its use to other areas such as combinatorial chemistry or in clinics for testing the combination of drugs to treat bacteria infection. Integrated system with detection and fluidic control for sample delivery is also possible. The development of this platform with integration of other components would very likely create devices that can bring major impact to drug screening, life science companies and biological researches.

References

[1] R. I. Freshney, *Culture of Animal Cells: A Manual of Basic Technique*, 5th ed. Hoboken, NJ: John Wiley & Sons, 2005.

[2] D. L. Earnshaw, T. H. Bacon, S. J. Darlison, K. Edmonds, R. M. Perkins, and R. A. Vere Hodge, "Mode of antiviral action of penciclovir in MRC-5 cells infected with herpes simplex virus type 1 (HSV-1), HSV-2, and varicella-zoster virus," *Antimicrobial Agents and Chemotherapy,* vol. 36, pp. 2747–2757, 1992.

[3] T. Takenouchi, Y. Iwamaru, M. Sato, T. Yokoyama, M. Shinagawa, and H. Kitani, "Establishment and characterization of SV40 large T antigen-immortalized cell lines derived from fetal bovine brain tissues after prolonged cryopreservation," *Cell Biology International,* vol. 31, pp. 57–64, 2007.

[4] B. P. McSharry, C. J. Jones, J. W. Skinner, D. Kipling, and G. W. G. Wilkinson, "Human telomerase reverse transcriptase-immortalized MRC-5 and HCA2 human fibroblasts are fully permissive for human cytomegalovirus," *Journal of General Virology,* vol. 82, pp. 855–863, 2001.

[5] J. E. González and P. A. Negulescu, "Intracellular detection assays for high-throughput screening," *Current Opinion in Biotechnology,* vol. 9, pp. 624–631, 1998.

[6] M. C. Alley, D. A. Scudiero, A. Monks, M. L. Hursey, M. J. Czerwinski, D. L. Fine, B. J. Abbott, J. G. Mayo, R. H. Shoemaker, and M. R. Boyd, "Feasibility of drug screening with panels of human tumor cell lines using a microculture tetrazolium assay," *Cancer Research,* vol. 48, pp. 589–601, 1988.

[7] P. L. Myers, "Will combinatorial chemistry deliver real medicines?," *Current Opinion in Biotechnology,* vol. 8, pp. 701–707, 1997.

[8] J. Drews, "Drug discovery: A historical perspective," *Science,* vol. 287, pp. 1960–1964, 2000.

[9] L. Chen, "Combinatorial gene regulation by eukaryotic transcription factors," *Current Opinion in Structural Biology,* vol. 9, pp. 48–55, 1999.

[10] R. A. Wagner, R. Tabibiazar, A. Liao, and T. Quertermous, "Genome-wide expression dynamics during mouse embryonic development reveal similarities to *Drosophila* development," *Developmental Biology,* vol. 288, pp. 595–611, 2005.

[11] S. J. Morrison, N. M. Shah, and D. J. Anderson, "Regulatory mechanisms in stem cell biology," *Cell,* vol. 88, pp. 287–298, 1997.

[12] C. L. Sawyers, "Cancer: Mixing cocktails," *Nature,* vol. 449, pp. 993–996, 2007.

[13] J. E. Dancey and H. X. Chen, "Strategies for optimizing combinations of molecularly targeted anticancer agents," *Nature Reviews Drug Discovery,* vol. 5, pp. 649–659, 2006.

[14] S. Decker and E. A. Sausville, "Preclinical modeling of combination treatments: Fantasy or requirement?," *Annals of the New York Academy of Sciences,* vol. 1059, pp. 61–69, 2005.

[15] R. J. Pomerantz and D. L. Horn, "Twenty years of therapy for HIV-1 infection," *Nature Medicine,* vol. 9, pp. 867–873, 2003.

[16] A. M. Maffia, III, I. Kariv, and K. R. Oldenburg, "Miniaturization of a mammalian cell-based assay: Luciferase reporter gene readout in a 3 microliter 1536-well plate," *Journal of Biomolecular Screening,* vol. 4, pp. 137–142, 1999.

[17] A. Dove, "Drug screening—beyond the bottleneck," *Nature Biotechnology,* vol. 17, pp. 859–863 1999.

[18] S. C. Terry, J. H. Jerman, and J. B. Angell, "A gas chromatographic air analyzer fabricated on a silicon wafer," *IEEE Transactions on Electron Devices,* vol. 26, pp. 1880–1886, 1979.

[19] F. C. M. Van de Pol, H. T. G. Van Lintel, M. Elwenspoek, and J. H. J. Fluitman, "A thermopneumatic micropump based on micro-engineering techniques," *Sensors and Actuators A: Physical,* vol. 21, pp. 198–202, 1990.

[20] S. Shoji, M. Esashi, and T. Matsuo, "Prototype miniature blood gas analyzer fabricated on a silicon wafer," *Sensors and Actuators,* vol. 14, pp. 101–107, 1988.

[21] M. Esashi, S. Shoji, and A. Nakano, "Normally close microvalve and micropump fabricated on a silicon wafer," in *Micro Electro Mechanical Systems, 1989, Proceedings, An Investigation of Micro Structures, Sensors, Actuators, Machines and Robots. IEEE*, pp. 29–34, Feb. 20–22, 1989.

[22] A. Manz, N. Graber, and H. M. Widmer, "Miniaturized total chemical analysis systems: A novel concept for chemical sensing," *Sensors and Actuators B: Chemical,* vol. 1, pp. 244–248, 1990.

[23] D. R. Reyes, D. Iossifidis, P.-A. Auroux, and A. Manz, "Micro total analysis systems. 1. Introduction, theory, and technology," *Analytical Chemistry,* vol. 74, pp. 2623–2636, 2002.

[24] A. T. Woolley, D. Hadley, P. Landre, A. J. deMello, R. A. Mathies, and M. A. Northrup, "Functional integration of PCR amplification and capillary

electrophoresis in a microfabricated DNA analysis device," *Analytical Chemistry,* vol. 68, pp. 4081–4086, 1996.

[25] C. Haber, "Microfluidics in commercial applications; an industry perspective," *Lab on a Chip,* vol. 6, pp. 1118–1121, 2006.

[26] G. T. A. Kovacs, *Micromachined Transducers Sourcebook*, 1st ed. New York, NY: McGraw-Hill 1998.

[27] S. Bhattacharya, A. Datta, J. M. Berg, and S. Gangopadhyay, "Studies on surface wettability of poly(dimethyl) siloxane (PDMS) and glass under oxygen-plasma treatment and correlation with bond strength," *Journal of Microelectromechanical Systems,* vol. 14, pp. 590–597, 2005.

[28] M. A. Eddings, M. A. Johnson, and B. K. Gale, "Determining the optimal PDMS-PDMS bonding technique for microfluidic devices," *Journal of Micromechanics and Microengineering,* vol. 18, p. 067001, 2008.

[29] Y. Xia and G. M. Whitesides, "Soft lithography," *Annual Review of Materials Science,* vol. 28, pp. 153–184, 1998.

[30] Y. S. Heo, L. M. Cabrera, J. W. Song, N. Futai, Y.-C. Tung, G. D. Smith, and S. Takayama, "Characterization and resolution of evaporation-mediated osmolality shifts that constrain microfluidic cell culture in poly(dimethylsiloxane) devices," *Analytical Chemistry,* vol. 79, pp. 1126–1134, 2007.

[31] M. W. Toepke and D. J. Beebe, "PDMS absorption of small molecules and consequences in microfluidic applications," *Lab on a Chip,* vol. 6, pp. 1484–1486, 2006.

[32] H. Becker and C. Gärtner, "Polymer microfabrication methods for microfluidic analytical applications," *Electrophoresis,* vol. 21, pp. 12–26, 2000.

[33] "Specialty Coating Systems Parylene knowledge > discovery/history," 2009. [Online]. Available from http://www.scscoatings.com/parylene_knowledge/history.aspx [Accessed: Sept. 17, 2009].

[34] W. F. Beach, C. Lee, D. R. Bassett, T. M. Austin, and R. Olson, "Xylene polymers," in *Encyclopedia of Polymer Science and Engineering*. vol. 17, J. I. Kroschwitz, Ed. Hoboken, New Jersey: John Wiley & Sons, 1985, pp. 990–1025.

[35] N. Stark, "Literature review: Biological safety of Parylene C " *Medical Plastics and Biomaterials* vol. 3, 1996.

[36] E. M. Schmidt, J. S. Mcintosh, and M. J. Bak, "Long-term implants of Parylene-C coated microelectrodes," *Medical and Biological Engineering and Computing,* vol. 26, pp. 96–101, 1988.

[37] K. M. Vaeth and K. F. Jensen, "Transition metals for selective chemical vapor deposition of Parylene-based polymers," *Chemistry of Materials,* vol. 12, pp. 1305–1313, 2000.

[38] D. C. Rodger, "Development of flexible Parylene-based microtechnologies for retinal and spinal cord stimulation and recording," Ph.D. Thesis in Bioengineering, California Institute of Technology, Pasadena, CA, 2007.

[39] E. Meng, P.-Y. Li, and Y.-C. Tai, "Plasma removal of Parylene C," *Journal of Micromechanics and Microengineering,* vol. 18, p. 045004, 2008.

[40] H.-Y. Chen, Y. Elkasabi, and J. Lahann, "Surface modification of confined microgeometries via vapor-deposited polymer coatings," *Journal of the American Chemical Society,* vol. 128, pp. 374–380, 2006.

[41] J. Xie, J. Shih, Q. Lin, B. Yang, and Y.-C. Tai, "Surface micromachined electrostatically actuated micro peristaltic pump," *Lab on a Chip,* vol. 4, pp. 495–501, 2004.

[42] S. Zheng, M. Liu, and Y.-C. Tai, "Micro coulter counters with platinum black electroplated electrodes for human blood cell sensing," *Biomedical Microdevices,* vol. 10, pp. 221–231, 2007.

[43] J. Xie, Y. Miao, J. Shih, Y.-C. Tai, and T. D. Lee, "Microfluidic platform for liquid chromatography−tandem mass spectrometry analyses of complex peptide mixtures," *Analytical Chemistry,* vol. 77, pp. 6947–6953, 2005.

[44] S. Miserendino and Y.-C. Tai, "Modular microfluidic interconnects using photodefinable silicone microgaskets and MEMS O-rings," *Sensors and Actuators A: Physical,* vol. 143, pp. 7–13, 2008.

[45] D. C. Rodger, J. D. Weiland, M. S. Humayun, and Y.-C. Tai, "Scalable high lead-count parylene package for retinal prostheses," *Sensors and Actuators B: Chemical,* vol. 117, pp. 107–114, 2006.

[46] P.-J. Chen, D. C. Rodger, S. Saati, M. S. Humayun, and Y.-C. Tai, "Microfabricated implantable Parylene-based wireless passive intraocular pressure sensors," *Journal of Microelectromechanical Systems,* vol. 17, pp. 1342–1351, 2008.

[47] N. L. Jeon, S. K. W. Dertinger, D. T. Chiu, I. S. Choi, A. D. Stroock, and G. M. Whitesides, "Generation of solution and surface gradients using microfluidic systems," *Langmuir,* vol. 16, pp. 8311–8316, 2000.

[48] N. L. Jeon, H. Baskaran, S. K. W. Dertinger, G. M. Whitesides, L. V. D. Water, and M. Toner, "Neutrophil chemotaxis in linear and complex gradients of interleukin-8 formed in a microfabricated device," *Nature Biotechnology,* vol. 20, pp. 826–830, 2002.

[49] W. Saadi, S.-J. Wang, F. Lin, and N. L. Jeon, "A parallel-gradient microfluidic chamber for quantitative analysis of breast cancer cell chemotaxis," *Biomedical Microdevices,* vol. 8, pp. 109–118, 2006.

[50] B. G. Chung, L. A. Flanagan, S. W. Rhee, P. H. Schwartz, A. P. Lee, E. S. Monuki, and N. L. Jeon, "Human neural stem cell growth and differentiation in a gradient-generating microfluidic device," *Lab on a Chip,* vol. 5, pp. 401–406, 2005.

[51] S. Takayama, E. Ostuni, P. LeDuc, K. Naruse, D. E. Ingber, and G. M. Whitesides, "Laminar flows: Subcellular positioning of small molecules," *Nature,* vol. 411, p. 1016, 2001.

[52] E. M. Lucchetta, J. H. Lee, L. A. Fu, N. H. Patel, and R. F. Ismagilov, "Dynamics of *Drosophila* embryonic patterning network perturbed in space and time using microfluidics," *Nature,* vol. 434, pp. 1134–1138, 2005.

[53] S. W. Rhee, A. M. Taylor, C. H. Tu, D. H. Cribbs, C. W. Cotman, and N. L. Jeon, "Patterned cell culture inside microfluidic devices," *Lab on a Chip,* vol. 5, pp. 102–107, 2005.

[54] S. Takayama, J. C. McDonald, E. Ostuni, M. N. Liang, P. J. A. Kenis, R. F. Ismagilov, and G. M. Whitesides, "Patterning cells and their environments using multiple laminar fluid flows in capillary networks," *Proceedings of the National Academy of Sciences of the United States of America,* vol. 96, pp. 5545–5548, 1999.

[55] H. Lu, L. Y. Koo, W. M. Wang, D. A. Lauffenburger, L. G. Griffith, and K. F. Jensen, "Microfluidic shear devices for quantitative analysis of cell adhesion," *Analytical Chemistry,* vol. 76, pp. 5257–5264, 2004.

[56] P. J. Lee, P. J. Hung, R. Shaw, L. Jan, and L. P. Lee, "Microfluidic application-specific integrated device for monitoring direct cell-cell communication via gap junctions between individual cell pairs," *Applied Physics Letters,* vol. 86, p. 223902, 2005.

[57] S. Fiedler, S. G. Shirley, T. Schnelle, and G. Fuhr, "Dielectrophoretic sorting of particles and cells in a microsystem," *Analytical Chemistry,* vol. 70, pp. 1909–1915, 1998.

[58] J. A. Davis, D. W. Inglis, K. J. Morton, D. A. Lawrence, L. R. Huang, S. Y. Chou, J. C. Sturm, and R. H. Austin, "Deterministic hydrodynamics: Taking blood apart," *Proceedings of the National Academy of Sciences of the United States of America,* vol. 103, pp. 14779–14784, 2006.

[59] Y.-C. Tung, M. Zhang, C.-T. Lin, K. Kurabayashi, and S. J. Skerlos, "PDMS-based opto-fluidic micro flow cytometer with two-color, multi-angle fluorescence detection capability using PIN photodiodes," *Sensors and Actuators B: Chemical,* vol. 98, pp. 356–367, 2004.

[60] D. D. Carlo, K.-H. Jeong, and L. P. Lee, "Reagentless mechanical cell lysis by nanoscale barbs in microchannels for sample preparation," *Lab on a Chip,* vol. 3, pp. 287–291, 2003.

[61] D. W. Lee and Y.-H. Cho, "A continuous electrical cell lysis device using a low dc voltage for a cell transport and rupture," *Sensors and Actuators B: Chemical,* vol. 124, pp. 84–89, 2007.

[62] J. Khandurina, T. E. McKnight, S. C. Jacobson, L. C. Waters, R. S. Foote, and J. M. Ramsey, "Integrated system for rapid PCR-based DNA analysis in microfluidic devices," *Analytical Chemistry,* vol. 72, pp. 2995–3000, 2000.

[63] D. J. Harrison, K. Fluri, K. Seiler, Z. Fan, C. S. Effenhauser, and A. Manz, "Micromachining a miniaturized capillary electrophoresis-based chemical analysis system on a chip," *Science,* vol. 261, pp. 895–897, 1993.

[64] O. Hofmann, D. Che, K. A. Cruickshank, and U. R. Muller, "Adaptation of capillary isoelectric focusing to microchannels on a glass chip," *Analytical Chemistry,* vol. 71, pp. 678–686, 1999.

[65] D. D. Carlo, L. Y. Wu, and L. P. Lee, "Dynamic single cell culture array," *Lab on a Chip,* vol. 6, pp. 1445–1449, 2006.

[66] A. Prokop, Z. Prokop, D. Schaffer, E. Kozlov, J. Wikswo, D. Cliffel, and F. Baudenbacher, "NanoLiterBioReactor: Long-term mammalian cell culture at nanofabricated scale," *Biomedical Microdevices,* vol. 6, pp. 325–339, 2004.

[67] P. J. Hung, P. J. Lee, P. Sabounchi, R. Lin, and L. P. Lee, "Continuous perfusion microfluidic cell culture array for high-throughput cell-based assays," *Biotechnology and Bioengineering,* vol. 89, pp. 1–8, 2005.

[68] L. Kim, Y.-C. Toh, J. Voldman, and H. Yu, "A practical guide to microfluidic perfusion culture of adherent mammalian cells," *Lab on a Chip,* vol. 7, pp. 681–694, 2007.

[69] P. J. Lee, P. J. Hung, V. M. Rao, and L. P. Lee, "Nanoliter scale microbioreactor array for quantitative cell biology," *Biotechnology and Bioengineering,* vol. 94, pp. 5–14, 2006.

[70] K. R. King, S. Wang, D. Irimia, A. Jayaraman, M. Toner, and M. L. Yarmush, "A high-throughput microfluidic real-time gene expression living cell array," *Lab on a Chip,* vol. 7, pp. 77–85, 2007.

[71] L. Kim, M. D. Vahey, H.-Y. Lee, and J. Voldman, "Microfluidic arrays for logarithmically perfused embryonic stem cell culture," *Lab on a Chip,* vol. 6, pp. 394–406, 2006.

[72] A. Tourovskaia, X. Figueroa-Masot, and A. Folch, "Differentiation-on-a-chip: A microfluidic platform for long-term cell culture studies," *Lab on a Chip,* vol. 5, pp. 14–19, 2005.

[73] D. J. Beebe, G. A. Mensing, and G. M. Walker, "Physics and applications of microfluidics in biology," *Annual Review of Biomedical Engineering,* vol. 4, pp. 261–286, 2002.

[74] T. M. Squires and S. R. Quake, "Microfluidics: Fluid physics at the nanoliter scale," *Reviews of Modern Physics,* vol. 77, pp. 977–1026, 2005.

[75] H. Bruus, *Theoretical Microfluidics* vol. 1. New York, NY: Oxford University Press, 2008.

[76] B. Wojciak-Stothard and A. J. Ridley, "Shear stress-induced endothelial cell polarization is mediated by Rho and Rac but not Cdc42 or PI 3-kinases," *The Journal of Cell Biology,* vol. 161, pp. 429–439, 2003.

[77] K. M. Reich, C. V. Gay, and J. A. Frangos, "Fluid shear stress as a mediator of osteoblast cyclic adenosine monophosphate production," *Journal of Cellular Physiology,* vol. 143, pp. 100–104, 1990.

[78] Y. Kikutani, T. Horiuchi, K. Uchiyama, H. Hisamoto, M. Tokeshia, and T. Kitamori, "Glass microchip with three-dimensional microchannel network for 2 x 2 parallel synthesis," *Lab on a Chip,* vol. 2, pp. 188–192, 2002.

[79] C. Neils, Z. Tyree, B. Finlayson, and A. Folch, "Combinatorial mixing of microfluidic streams," *Lab on a Chip,* vol. 4, pp. 342–350, 2004.

[80] B. H. Jo, L. M. Van Lerberghe, K. M. Motsegood, and D. J. Beebe, "Three-dimensional micro-channel fabrication in polydimethylsiloxane (PDMS) elastomer," *Journal of Microelectromechanical Systems,* vol. 9, pp. 76–81, 2000.

[81] J. Erickson, A. Tooker, Y. C. Tai, and J. Pine, "Caged neuron MEA: A system for long-term investigation of cultured neural network connectivity," *Journal of Neuroscience Methods,* vol. 175, pp. 1–16, 2008.

[82] G. L. Witucki, "A silane primer: Chemistry and applications of alkoxy silanes," in *57th Annual Meeting of the Federation of Societies for Coatings Technology*, Chicago, IL, October 21, 1992.

[83] A. Vancha, S. Govindaraju, K. Parsa, M. Jasti, M. Gonzalez-Garcia, and R. Ballestero, "Use of polyethyleneimine polymer in cell culture as attachment factor and lipofection enhancer," *BMC Biotechnology,* vol. 4, p. 23, 2004.

[84] D. C. Rodger, A. J. Fong, W. Li, H. Ameri, A. K. Ahuja, C. Gutierrez, I. Lavrov, H. Zhong, P. R. Menon, E. Meng, J. W. Burdick, R. R. Roy, V. R. Edgerton, J. D. Weiland, M. S. Humayun, and Y.-C. Tai, "Flexible parylene-based multielectrode array technology for high-density neural stimulation and recording," *Sensors and Actuators B: Chemical,* vol. 132, pp. 449–460, 2008.

[85] T. Y. Chang, V. G. Yadav, S. De Leo, A. Mohedas, B. Rajalingam, C.-L. Chen, S. Selvarasah, M. R. Dokmeci, and A. Khademhosseini, "Cell and protein compatibility of Parylene-C surfaces," *Langmuir,* vol. 23, pp. 11718–11725, 2007.

[86] I. Meyvantsson and D. J. Beebe, "Cell culture models in microfluidic systems," *Annual Review of Analytical Chemistry,* vol. 1, pp. 423–449, 2008.

[87] D. S. Warner, H. Sheng, and I. Batinic-Haberle, "Oxidants, antioxidants and the ischemic brain," *Journal of Experimental Biology* vol. 207, pp. 3221–3231, 2004.

[88] S. D. Sheridan, M. Wilgo, J. Park, and S. Gil, "Membrane based cardiomyocyte differentiation from embryonic stem cells," 2006, [Online]. Available from http://www.millipore.com/publications.nsf/a73664f9f981af8c852569b9005b4eee/9f08f0b1493919ca852574a60048bb24/$FILE/ps1081enus.pdf [Accessed: Sept. 05, 2009].

[89] K. Sumaru, S. Sugiura, and T. Kanamori, "Optimal design of cell culture chip on the basis of oxygen and glucose supply to cultivated cells in the chip," *Biochemical Engineering Journal,* vol. 36, pp. 304–309, 2007.

[90] R. D. Guarino, L. E. Dike, T. A. Haq, J. A. Rowley, J. B. Pitner, and M. R. Timmins, "Method for determining oxygen consumption rates of static cultures

from microplate measurements of pericellular dissolved oxygen concentration," *Biotechnology and Bioengineering,* vol. 86, pp. 775–787, 2004.

[91] J. A. Walisser and R. L. Thies, "Poly(ADP-Ribose) polymerase inhibition in oxidant-stressed endothelial cells prevents oncosis and permits caspase activation and apoptosis," *Experimental Cell Research,* vol. 251, pp. 401–413, 1999.

[92] J. Bowes, J. Piper, and C. Thiemermann, "Inhibitors of the activity of poly (ADP-ribose) synthetase reduce the cell death caused by hydrogen peroxide in human cardiac myoblasts," *British Journal of Pharmacology,* vol. 124, pp. 1760–1766, 1998.

[93] E. K. Rowinsky and R. C. Donehower, "Paclitaxel (Taxol)," *The New England Journal of Medicine,* vol. 332, pp. 1004–1014, 1995.

[94] R. K. Gregory and I. E. Smith, "Vinorelbine - a clinical review," *British Journal of Cancer,* vol. 82, pp. 1907–1913, 2000.

[95] J. A. Menéendez, S. Ropero, M. del Mar Barbacid, S. Montero, M. Solanas, E. Escrich, H. Cortés-Funes, and R. Colomer, "Synergistic interaction between vinorelbine and gamma-linolenic acid in breast cancer cells," *Breast Cancer Research and Treatment,* vol. 72, pp. 203–219, 2004.

[96] J. A. Menéndez, M. del Mar Barbacid, S. Montero, E. Sevilla, E. Escrich, M. Solanas, H. Cortés-Funes, and R. Colomer, "Effects of gamma-linolenic acid and oleic acid on paclitaxel cytotoxicity in human breast cancer cells," *European Journal of Cancer,* vol. 37, pp. 402–413, 2001.

[97] A. Y. Chang and G. C. Garrow, "Pilot study of vinorelbine (Navelbine) and paclitaxel (Taxol) in patients with refractory breast cancer and lung cancer," *Seminars in Oncology,* vol. 22, pp. 66–70, 1995.

[98] J. d. Jong, R. G. H. Lammertink, and M. Wessling, "Membranes and microfluidics: a review," *Lab on a Chip,* vol. 6, pp. 1125–1139, 2006.

[99] S. Song, A. K. Singh, and B. J. Kirby, "Electrophoretic concentration of proteins at laser-patterned nanoporous membranes in microchips," *Analytical Chemistry,* vol. 76, pp. 4589–4592, 2004.

[100] B. H. Timmer, K. M. van Delft, W. Olthuis, P. Bergveld, and A. van den Berg, "Micro-evaporation electrolyte concentrator," *Sensors and Actuators B: Chemical,* vol. 91, pp. 342–346, 2003.

[101] J. Moorthy and D. J. Beebe, "*In situ* fabricated porous filters for microsystems," *Lab on a Chip,* vol. 3, pp. 62–66, 2003.

[102] T. Cui, J. Fang, A. Zheng, F. Jones, and A. Reppond, "Fabrication of microreactors for dehydrogenation of cyclohexane to benzene," *Sensors and Actuators B: Chemical,* vol. 71, pp. 228–231, 2000.

[103] A. P. Vollmer, R. F. Probstein, R. Gilbert, and T. Thorsen, "Development of an integrated microfluidic platform for dynamic oxygen sensing and delivery in a flowing medium," *Lab on a Chip,* vol. 5, pp. 1059–1066, 2005.

[104] A. Zanzotto, N. Szita, P. Boccazzi, P. Lessard, A. J. Sinskey, and K. F. Jensen, "Membrane-aerated microbioreactor for high-throughput bioprocessing," *Biotechnology and Bioengineering,* vol. 87, pp. 243–254, 2004.

[105] Y.-C. Hsieh and J. D. Zahn, "Glucose recovery in a microfluidic microdialysis biochip," *Sensors and Actuators B: Chemical,* vol. 107, pp. 649–656, 2005.

[106] P.-C. Wang, J. Gao, and C. S. Lee, "High-resolution chiral separation using microfluidics-based membrane chromatography," *Journal of Chromatography A,* vol. 942, pp. 115–122, 2002.

[107] R. W. Tjerkstra, G. E. Gardeniers, J. J. Kelly, and A. van den Berg, "Multi-walled microchannels: free-standing porous silicon membranes for use in μTAS," *Journal of Microelectromechanical Systems,* vol. 9, pp. 495–501, 2000.

[108] C.-S. Toh, B. M. Kayes, E. J. Nemanick, and N. S. Lewis, "Fabrication of free-standing nanoscale alumina membranes with controllable pore aspect ratios," *Nano Letters,* vol. 4, pp. 767–770, 2004.

[109] H. Suzuki, K. V. Tabata, H. Noji, and S. Takeuchi, "Highly reproducible method of planar lipid bilayer reconstitution in polymethyl methacrylate microfluidic chip," *Langmuir,* vol. 22, pp. 1937–1942, 2006.

[110] S. Song, A. K. Singh, T. J. Shepodd, and B. J. Kirby, "Microchip dialysis of proteins using in situ photopatterned nanoporous polymer membranes," *Analytical Chemistry,* vol. 76, pp. 2367–2373, 2004.

[111] M. Cabodi, N. W. Choi, J. P. Gleghorn, C. S. D. Lee, L. J. Bonassar, and A. D. Stroock, "A microfluidic biomaterial," *Journal of the American Chemical Society,* vol. 127, pp. 13788–13789, 2005.

[112] S. Selvarasah, S. H. Chao, C. L. Chen, S. Sridhar, A. Busnaina, A. Khademhosseini, and M. R. Dokmeci, "A reusable high aspect ratio parylene-C

shadow mask technology for diverse micropatterning applications," *Sensors and Actuators A: Physical,* vol. 145-146, pp. 306–315, 2008.

[113] E. M. Schmidt, M. J. Bak, and P. Christensen, "Laser exposure of Parylene-C insulated microelectrodes," *Journal of Neuroscience Methods,* vol. 62, pp. 89–92, 1995.

[114] L. E. Heasley, "Autocrine and paracrine signaling through neuropeptide receptors in human cancer," *Oncogene,* vol. 20, pp. 1536–1569, 2001.

[115] B. E. Reubinoff, M. F. Pera, C.-Y. Fong, A. Trounson, and A. Bongso, "Embryonic stem cell lines from human blastocysts: somatic differentiation in vitro," *Nature Biotechnology* vol. 18, pp. 399–404, 2000.

[116] S. N. Bhatia, U. J. Balis, M. L. Yarmush, and M. Toner, "Effect of cell-cell interactions in preservation of cellular phenotype: cocultivation of hepatocytes and nonparenchymal cells," *The Journal of Federation of American Societies for Experimental Biology,* vol. 13, pp. 1883–1900, 1999.

[117] W. Tan and A. D. Tejal, "Microscale multilayer cocultures for biomimetic blood vessels," *Journal of Biomedical Materials Research Part A,* vol. 72A, pp. 146–160, 2005.

[118] D. M. Anderson, P. M. Glibert, and J. M. Burkholder, "Harmful algal blooms and eutrophication: Nutrient sources, composition, and consequences," *Estuaries and Coasts,* vol. 25, pp. 704–726, 2002.

[119] J. Deeds, J. Landsberg, S. Etheridge, G. Pitcher, and S. Longan, "Non-traditional vectors for paralytic shellfish poisoning," *Marine Drugs,* vol. 6, pp. 308–348, 2008.

[120] A. C. Bejarano, F. M. VanDola, F. M. Gulland, T. K. Rowles, and L. H. Schwacke, "Production and toxicity of the marine biotoxin domoic acid and its effects on wildlife: A review " *Human and Ecological Risk Assessment,* vol. 14, pp. 544–567 2008.

[121] T. M. Perl, L. Bedard, T. Kosatsky, J. C. Hockin, E. C. Todd, and R. S. Remis, "An outbreak of toxic encephalopathy caused by eating mussels contaminated with domoic acid," *New England Journal of Medicine,* vol. 322, pp. 1775–1780, 1990.

[122] C. A. Scholin, F. Gulland, G. J. Doucette, S. Benson, M. Busman, F. P. Chavez, J. Cordaro, R. DeLong, A. De Vogelaere, J. Harvey, M. Haulena, K. Lefebvre, T. Lipscomb, S. Loscutoff, L. J. Lowenstine, R. Marin Iii, P. E. Miller, W. A. McLellan, P. D. R. Moeller, C. L. Powell, T. Rowles, P. Silvagni, M. Silver, T. Spraker, V. Trainer, and F. M. Van Dolah, "Mortality of sea lions along the central California coast linked to a toxic diatom bloom," *Nature,* vol. 403, pp. 80–84, 2000.

[123] M. T. Maldonado, M. P. Hughes, E. L. Rue, and M. L. Wells, "The effect of Fe and Cu on growth and domoic acid production by *Pseudo-nitzschia multiseries* and *Pseudo-nitzschia australis*," *Limnology and Oceanography,* vol. 47, pp. 515–526, 2002.

[124] Y. Pan, D. V. Subba Rao, K. H. Mann, R. G. Brown, and R. Pocklington, "Effects of silicate limitation on production of domoic acid, a neurotoxin, by the diatom *Pseudo-nitzschia multiseries*. I. Batch culture studies," *Marine Ecology Progress Series,* vol. 131, pp. 225–233, 1996.

[125] Y. Pan, D. V. Subba Rao, and K. H. Mann, "Changes in domoic acid production and cellular chemical composition of the toxigenic diatom *Pseudo-nitzschia multiseries* under phosphate limitation," *Journal of Phycology,* vol. 32, pp. 371–381, 1996.

[126] S. S. Bates, D. J. Douglas, G. J. Doucette, and C. Léger, "Enhancement of domoic acid production by reintroducing bacteria to axenic cultures of the diatom *Pseudo-nitzschia multiseries*," *Natural Toxins,* vol. 3, pp. 428–435, 1995.

[127] G. R. Hasle, "*Pseudo-nitzschia pungen*s and *P. multiseries* (Bacillariophyceae): nomenclatural history, morphology, and distribution," *Journal of Phycology,* vol. 31, pp. 428–435, 1995.

[128] I. V. Stonik, T. Y. Orlova, and O. G. Shevchenko, "Morphology and Ecology of the Species of the Genus *Pseudo-nitzschia* (Bacillariophyta) from Peter the Great Bay, Sea of Japan," *Russian Journal of Marine Biology,* vol. 27, pp. 362–366, 2001.